Alma Mater Studiorum – Università di Bologna

DOTTORATO DI RICERCA IN

SCIENZE FARMACOLOGICHE, TOSSICOLOGICHE, DELLO SVILUPPE E DEL MOVIMENTO UMANO

Ciclo XXXII

Settore Concorsuale di afferenza: 05/G1

Settore Scientifico disciplinare: BIO 14

PERSONALIZATION OF ELECTRONIC NICOTINE DELIVERY SYSTEMS
Toxicological impact in *in-vivo* model

Presentata da: **Silvia Cirillo**

Coordinatore Dottorato
Prof.ssa Patrizia Hrelia

Supervisore
Prof. Moreno Paolini

Co-supervisore
Dott.ssa Donatella Canistro

Esame finale anno 2020

SUMMARY

ABSTRACT

Electronic nicotine delivery systems (ENDS) use has grown exponentially in recent years despite the related unknown health effects. It has been reported that e-cig generates many carcinogenic chemical compounds (such as formaldehyde, acetaldehyde and acrolein) and free radicals, especially reactive oxygen species (ROS). Both carbonyls and ROS are formed when the liquid comes into contact with a heating element that is housed within an e-cig's atomizer. In this study the chemical and biological effects of coil resistance (1.5 Ω and 0.25 Ω coils) applied on the same device were investigated. Moreover, a preliminary *in-vivo* study the new heat-not-burn devices (IQOS®) has been conducted to evaluate the effect of the device on antioxidant biomarkers.

By keeping constant the voltage value, the amount of carbonyls (formaldehyde, acetaldehyde, acrolein) was measured by GC-MS analysis. The two e-liquids used for carbonyls detection were base solutions of 50% propylene glycol (PG) and 50% vegetable glycerol (VG) without and with nicotine (18 mg/mL). The nicotine-free liquid was then used for the detection of ROS in the aerosol by performing 2',7'-dichlorodihydrofluorescein DCFH-DA assay. The impact of the non-nicotine vapor on cell viability in H1299 human lung carcinoma cells, as well as the biological effects in a rat model of e-cig aerosol exposure, were also evaluated. After the exposure of Sprague Dawley rats to e-cig and IQOS® aerosol, the effect of 28-day treatment was examined on enzymatic and non-enzymatic antioxidant response, lung inflammation, blood

homeostasis and tissue damage by using scanning electron microscope (SEM) technique.

The results show a significant ($p<0.05$) correlation between the low resistance coils and the generation of higher concentrations of the selected carbonyls and ROS in e-cig aerosols. Moreover, exposure to e-cig vapor reduced the viability of H1299 cells by up to 45.8%, and this effect was inversely related to coil resistance. This experimental model highlighted an impairment of the pulmonary antioxidant and detoxifying machinery, confirmed by the perturbation of the antioxidant and phase II enzymatic activities, probably related to increased ROS levels ($p<0.01$) due to the enhanced activity of xanthine oxidase (XO) ($p<0.01$). Interestingly, frames from SEM showed a marked disorganization of alveolar and bronchial epithelium in 0.25 Ω group. IQOS® exposed animals shows a significant production of ROS which is related to the unbalance of antioxidant defense and alteration of macromolecule integrity.

The present research demonstrates how several toxicological aspects, widely recognized as smoke-related injuries, can potentially occur in e-cig consumers who use low-voltage and resistance device coupled with nicotine-free liquid. Although further studies are needed to better elucidate the potential toxicity of ENDS emissions, these results suggest that these devices may expose users to hazardous compounds, which, in turn, may promote chronic obstructive pulmonary diseases (COPD) and other degenerative diseases.

INTRODUCTION

Electronic cigarette (e-cig) has been distributed on the global market for more than a decade, as both potential strategy to aid smoking cessation (Franks et al., 2018) and safe alternative to cigarette smoke. However, in 2016 the World Health Organization (WHO) presented a conspicuous number of leaks in the e-cig regulation goals, especially regarding its use among young people, the effectiveness in smoking cessation and the risk-benefit ratio for both users and non-users.

ELECTRONIC CIGARETTE: THE DEVICE

Electronic cigarettes consist of mouthpiece, a refillable cartridge, a lithium battery and a heating atomizer. Almost all the devices operate on the same basic principle: a power button allows the user to activate the heating element during inhalation, thus producing the flavored vapor. The devices have a liquid reservoir with a wicking material that draws the liquid to the atomizer. It consists of a coil made of resistance wire that an electrical current is passed through, which quickly generates intense heat used to atomize the liquid. The current is produced by the activation of the battery, and the liquid is vaporized and condenses into an aerosol, which is inhaled by the user through the mouthpiece. The wide variety of e-liquids on the market, together with the continuous evolution in the e-cig technologies, makes these devices extremely customizable. Consequently, evidences on risks related to e-cig deeply depend on the devices, liquids and the conditions used.

REGULATION OF ELECTRONIC CIGARETTES

Electronic cigarette is sold as an electronic nicotine delivery system (ENDS), which is classified as a noncombustible tobacco product. It differs from other ENDS due to the presence of a liquid (e-liquid) – generally composed by propylene glycol (PG), vegetable glycerol (VG) and different concentrations of flavors and nicotine – which is heated to create an aerosol.

The regulation of tobacco products in the United States (US) is under the control of the Family Smoking Prevention and Tobacco Control Act (TCA), signed into a law by President Barack Obama in 2009. The TCA gives the Food and Drug Administration (FDA) the power to regulate tobacco industry. In 2016, FDA extended its regulatory authority on the manufacture, import, packaging, labeling, advertising, promotion, sale, and distribution of electronic cigarette (FDA, 2016). Under this ruling, FDA declares that even though e-cigs may have the potential to be less harmful than other tobacco products, more evidences are needed. The new rule also bans e-cig access to minors, forcing vendors to require a photo ID document and prohibiting the sale in all-age vending machines. Finally, a recent rule by FDA excludes e-cigs from the definition of "medical product", pointing the attention on the close similarity between the nicotine effects derived from e-cigs and conventional cigarettes (FDA, 2017). However, in the respect of the legislation, US have not set any limit related to the nicotine content in e-liquid (FDA, 2017), which, in some brand, reaches the concentration of 59 mg/mL.

In Europe, e-cigs are regulated by the European Union Tobacco Products Directive (2014/40/EU), which administers the manufacture, presentation and sale of tobacco and products. The Directive indicates the limit of nicotine content in the refill liquid (up to 20 mg/mL) and the maximum

size of the cartridge (10 mL for refill cartridge and 2 mL for single use cartridge), the required information on the label, and the requirements for manufactures and importers not only about the product and its market, but also about the suspected adverse effects on human health. Interestingly, the text establishes the prohibition of commercial communications that promote e-cig use. This restrictive approach is supported by the idea that e-cig can represent a gateway to nicotine addiction and to traditional tobacco consumption, due to the close similarity with smoking gesture. One of the primary goals of the Directive, in fact, is to create a high base level of protection of human health. For this reason, a report on the potential risk to public health associated with the use of e-cig has to be periodically submitted to the European Parliament and Council.

Italy has transposed the Directive 2014/40/EU into its national legislation by the Legislative Decree 6/2016. The Decree obliges the manufactures to include a label in the package indicating contraindications, warning on risk groups of consumers, potentially harmful effects, and ability to induce addiction and toxicity. Moreover, the package must indicate the following advice: "*This product contains nicotine, substance which creates high addiction. Not recommended for non-smokers*". The use of e-cig is forbidden not only for minors, but also for people who are driving vehicles in presence of minors and pregnant women. The sale of liquids to people younger than 18 years old can be fined 500-3000 euros with the suspension of the license. However, this ban is restricted only to nicotine-containing cartridges, pointing the attention on the fact that the early consumption of nicotine can represent the first step towards nicotine addiction and use of tobacco cigarettes.

ELECTRONIC CIGARETTE USE AMONG ADULTS AND YOUNG PEOPLE

Electronic cigarette has been promoted as a strategy to quit conventional smoking. However, most adults who use e-cig continue smoking conventional cigarette. In 2014, 93% of e-cig users continued to smoke cigarettes in the United States (Ogunwale et al., 2017) and 60% in the United Kingdom (UK Off. Natl. Stat., 2016). A recent meta-analysis reports that e-cig is ineffective in smoking cessation and that smokers who don't use e-cig are about 1/3 more likely to quit smoking, compared to e-cig users (Glanz and Bareham, 2018). These findings are consistent with the study by Kulik et al. (2018) that suggests how e-cig use reduces the ability of quitting smoking.

In addition to smoking cessation, there are other two reasons that encourage adults to try e-cig: because it is perceived as a safer alternative to tobacco cigarettes, and because, in many Countries, it allows to get around smoke free laws (Simonavicius et al., 2017; UK Off. Natl. Stat., 2016).

As of 2016, the prevalence of e-cig use in US among youth surpassed that of traditional cigarette (Jamal et al., 2017) and represented the first phase of initiating tobacco habit. An observational study conducted on US adolescents reported that e-cig habit is often associated with cigarette smoking (Corsi et al., 2011). Estimates from the National Youth Tobacco Survey, inform that the majority of current tobacco users in middle and high school report the employ of more than one tobacco product (Apelberg et al., 2014; Nasim et al., 2012). The frequency of e-cig vaping among dual users is much higher compared to never smokers (1-2 days per month), who generally choose nicotine-free liquids (Bals et al., 2019).

This alarming increase has been attributed to several factors, including the possibility to select among a great variety of appealing flavored e-liquids

and, overall, the perception that flavored tobacco products are safer than tobacco ones (Harrel et al., 2017; Kowitt et al., 2017). In particular, several studies suggest that adolescents who had ever used e-cigs perceived them as less harmful than cigarettes, as compared to non-users (Amrock et al., 2015; Ambrose et al., 2014) and it is frequent that some of them consider e-cig as a healthy alternative to tobacco cigarette (Wills et al., 2015). Even if there are limited studies focused on the deleterious effects of e-cig and dual use in teenagers, a recent meta-analysis reports that never-smoking and adolescents who have at least tried e-cig have quadruple odds of risk starting conventional smoking compared to those who never tried e-cig (Soneji et al., 2017).

ELECTRONIC CIGARETTE FOR SMOKING CESSATION

Contrary to the nicotine replacement therapy (NRT), e-cigs are marketed as recreational products and not as drugs developed to be administered under clinical supervision. Beside this, in Europe, e-cig has been largely used both as a medical treatment provided by healthcare professionals, and as an arbitral choice of smokers, as an alternative to tobacco cigarette.

An analysis on subject from 28 European Countries estimated that 6.1 million people declared that e-cig was helpful in stop smoking (Farsalinos et al., 2016). In contrast, a meta-analysis conducted by Kalkhoran and colleagues (2016) on e-cig and smoking cessation in real-world clinical setting showed that e-cig use was associated with a significant decrease in smoking cessation. These findings were confirmed by subsequent studies that concluded that e-cig smokers were significantly less likely to stop smoking cigarettes compared to non-vapers (Gmel et al., 2016; Hirano et al., 2017; Kulik et al., 2018; Manzoli et al., 2017; Yong et al., 2017; Zawertailo qt al., 2017; Zhuang et al., 2016). Altogether, these results

suggest that e-cig is effective in attracting smokers who are trying to stop smoking but, at the same time, it reduces the success of attempt to quit.

STUDIES ON ELECTRONIC CIGARETTE

In 2014, as a consequence of a single consensus meeting of 12 people convened by D.J. Nutt, it was claimed that e-cigs are unequivocally 95% safer than tobacco cigarette (Nutt et al., 2014). Even if any specific evidence supported this conclusion, a number of studies on human health effects of e-cig promoted this settlement. However, a 2015 editorial in *Lancet,* identified financial conflict of interest associated with the publication of Nutt and coauthors (Lancet, 2015). It was then found that several individuals involved in the paper received funding from associations as EuroSwiss Health and Lega Italiana Antifumo, and from tobacco multinational companies such as British American Tobacco and Philip Morris International (PMI) (McKee et al., 2015; Spindle et al., 2017). As a consequence of this complaint, a great number of evidence has been rapidly accumulated and it is now well established that the true risk of e- cigarette use is much higher than the "95% safer" claim would indicate.
A summary of the current literature is reported below.

E-LIQUID AND AEROSOL - Although the e-liquid is generally composed by vegetable glycerol (VG), propylene glycol (PG), water and an impressive variety of flavors and nicotine at different concentrations, the personalization of the vaporization process is responsible for different emission levels of toxic and/or carcinogenic carbonyl compounds, such as formaldehyde, acetaldehyde, acrolein (Goniewicz et al., 2014; Bitzer et al., 2018; Cirillo et al., 2019) and reactive free radicals (Goel et al., 2015; Lerner et al., 2015, Sussan et al., 2015).

PG and VG are considered the main emission sources of carbonyls inhaled during the vaporization process and their relative percentage in the e-liquid seems to be related to the proportion of generated carbonyls (Wang et al., 2018) and free radicals (Bitzer et al., 2018). Bitzer et al. demonstrated that, under constant-wattage mode conditions, the radical content appears to be PG-dependent and reported higher free radical concentration in aerosol vaporized from 100% PG e-liquid compared to mixtures (Bitzer et al., 2018). In addition, it has been reported that PG/VG composition can influence the nicotine emission, which is higher after vaporization of 100% PG liquid, compared to 50/50 PG/VG and 100% VG, at low wattages (Kosmider et al., 2018). Nicotine in e-liquids is extracted from tobacco, so it may contain low levels of minor tobacco alkaloids and tobacco-specific nitrosamines, depending on the degree of purification (Lisko et al., 2015).

To date, only few studies have examined the toxicity of specific flavorants (Grana et al., 2014; Barrington-Trimis et al., 2014; Behar et al., 2014; Kosmider et al., 2016). A wide variety of volatile organic compounds has been identified in both in flavored e-cigarette liquids and their aerosols (Lim et al., 2017). It has been shown that benzene is formed as a result of the thermal decomposition of benzaldehyde, a natural fruit flavorant present in many e-liquid flavors (Pankow et al., 2017). By analyzing 49 different flavored e-liquids, it has recently been reported that flavorants in e-liquid can have a direct impact on the generation of highly reactive free radicals (Bitzer et al., 2018). Altogether, these studies suggest that flavor compounds may play an important role in the potential toxicity of e-cigarettes.

***IN VITRO* STUDIES -** E-cig effects on cell lines have been studied using a great variety of models. Existing studies suggest that the toxicological responses are qualitatively similar to smoking, and the exposure of cell lines

and cultures to the aerosols induces a pro-inflammatory effect (Misra et al., 2014; Husari et al., 2016), disruption to epithelia barriers (Schweitzer et al., 2015), oxidative stress (Scheffer et al., 2015a), cytotoxicity (Scheffer et al., 2015b), neutrophil inflammatory response (Higham et al., 2016) and DNA damage (Holliday et al., 2016; Thorne et al., 2016).

A study from British American Tobacco showed that, contrary to tobacco cigarette, exposure to e-cig vapor did not induce either cytotoxicity or a decrease in epithelial barrier function (Neilson et al., 2015). Moses et al. used a similar approach by exposing cells to aerosols generated by e-cig or smoke generated by tobacco cigarette (Moses et al., 2017). Even if no overt cytotoxicity was noted with e-cig (as compared to tobacco cigarette), both e-cig vapor and cigarette smoke caused similar changes in gene expression. In particular, alterations in expression of genes related to xenobiotic metabolism, oxidative stress, DNA damage, apoptosis, and cilia formation and function were noted. In normal human bronchial epithelial (NHBE) cells exposed to e-cig aerosols, with or without nicotine, increase IL-6 and IL-8 cytokine levels (Garcia-Arcos et al., 2016).

Other studies used human immortalized or tumor lung epithelial cells to assess cytotoxic effects, and changes in gene expression or function induced by exposure to extracts of e-cig vapor or e-liquid (Lerner et al., 2015; Cervellati et al., 2014; Husari et al., 2016).

***IN VIVO* STUDIES -** A limited number of animal studies has investigated the effect of e-cig either on lung or at systemic level.

Acute mice exposure to nebulized nicotine and e-cig vapor has evidenced alterations in the functioning of the endothelial barrier of the lung, thus reflecting an airway inflammatory response, and systemic oxidative and nitroxidative stress highlighted by 8-hydroxydeoxyguanosine (8-OHdG)

and nitrotyrosine levels in plasma (Scheffler et al., 2015). An unbalance in oxidation-reduction reactions, as a consequence of reduced glutathione levels, and an increase in inflammatory cytokine levels has also been found by Lerner et al. who exposed C57BL/6J mice to e-cig vapor for 3 days (Lerner et al., 2015). Short-term exposure was also employed to compare the consequences of cigarette smoke and e-cig vapor in a mice model (Husari et al., 2016). In this study the acute in vivo harmful effects on lung tissue, underlined by significant increase in the inflammatory mediators, IL-6 expression, was demonstrated compared to control. However, alterations in lung parenchyma and evidence of increased apoptotic activity or oxidative stress were revealed when tobacco cigarette group, but not e-cig, was compared to control (Husari et al., 2016).

Even when exposure time was enhanced to 4 weeks, the levels of inflammatory cytokines in bronco alveolar liquid fluid (BALF) in exposed mice were significantly higher compared to non-exposed mice (Hwang et al., 2016). After 4 weeks of exposure, the co-mutagenic and cancer-initiating effects of e-cig vapor were demonstrated in a rat lung model (Canistro et al., 2017). In this study, e-cig induced phase-I carcinogen-bioactivating enzymes, increased oxygen free radical production and DNA oxidation and damage at systemic level, as a consequence of strand breaks in leukocytes, micronuclei formation in reticulocytes and point mutations revealed in urine (Canistro et al., 2017).

Several studies investigated the effect of e-cig exposure on host defense. Increased susceptibility to infection with influenza A and *Streptococcus pneumonia* has been demonstrated in mice exposed to e-cig vapor for 2 weeks (Sussan et al., 2015), while decreased macrophage and neutrophil antimicrobial function and increased susceptibility in a mouse pneumonia model exposed for 4-week has been described (Hwang et al., 2016).

Only few studies have investigated the long-term effects of e-cig in animal models. 4-months exposure to nicotine e-cig vapor has shown outcomes normally associated with the development of chronic obstructive pulmonary diseases (COPD)-like tissue damage in a nicotine-dependent manner (Garcia-Arcos et al., 2016). A 7-months cigarette smoke inhalation study (sponsored by tobacco industry) in C57BL/6 mice showed nicotine-dependent lung inflammation and emphysema after e-cig exposure, that was however lower than that observed following exposure to smoke from tobacco cigarettes (Phillips et al., 2015).

HUMAN STUDIES – Only few studies have addressed the effects of e-cigs on vapers, but many of them indicate that the major adverse events related to the use of e-cigarette are pulmonary and cardiovascular diseases.

Case-control studies showed that the acute inhalation of e-cig vapor increases respiratory impedance and airway resistance (Vardavas et al., 2012; Palamidas et al., 2017). Cross-sectional studies in Asia surveyed adolescents regarding e-cig use and respiratory symptoms reported increased cough, phlegm and prevalence of asthma in e-cig users including the subset of never smokers (Wang et al., 2016; Cho et al., 2016). Wheeze and bronchitis symptoms were also reported in Californian adolescents who currently or previously used e-cigs (McConnel et al. 2014). A study where sputum samples were collected from population of tobacco smokers, e-cig users and non smokers showed changes in numerous established markers of cigarette smoke exposure (among which ADH3A1 and MMP9) in both smokers and vapers, suggesting that e-cigarette exposure might be harmful for the lung as well (Reidel et al., 2018). In the same study, many innate defense proteins of neutrophil origin were highly represented in e-cig population. According to the authors, this observation, coupled with the

absence of increased number of neutrophil cells, suggests two potential underlying pathogeneses: e-cigarettes may cause altered activation and degranulation of these neutrophils, or e-cigarettes may cause a neutrophilic increase but induce neutrophil death at the same time (Reidel et al., 2018). Results from bronchoscopies on healthy nonsmokers, cigarette smokers, and e-cigarette users suggested that chronic vaping exerts marked biological effects on the lung, such as erythematous airway mucosa, suggesting that inhalation of e-cigarette vapor is not harmless and that e-cig should not have been prescribed as a safe tobacco alternative (Gosh et al., 2018).

During the vaporization process, e-cig produces ultrafine particle – often smaller than those in conventional cigarette (Fuoco et al., 2014) – that are biologically active, trigger inflammatory processes, and are directly implicated in causing cardiovascular events. It is well known that cigarette smoke contains constituents that are involved in the onset of premature cardiovascular diseases, such as oxidizing chemicals, carbon monoxide, volatile organic compounds particulates, heavy metals and nicotine (Benowitz and Burbank, 2016). Nicotine acts as a promoter of cardiovascular events by increasing hearth rate, myocardial contractility and blood pressure (U.S. Department of Health and Human Services, 2010). In addition, nicotine from cigarette smoke enhances myocardial remodeling leading to hypertrophy and fibrosis (van Barlo et al., 2013), promotes development of ventricular fibrillation (Benowitz and Burbank, 2016), and impacts on lipidic balance resulting in dyslipidemia (U.S. Department of Health and Human Services, 2010; Andersson and Arner, 2001). Studies that used devices with effective nicotine delivery have found that e-cigarette use produces the expected heart rate acceleration similar to that seen with cigarette smoking (Benowitz and Burbank, 2016). Changes associated with an increased risk of cardiovascular diseases have been

revealed in e-cig users, which reported raised oxidative stress (Brown et al., 2014; Moheimani et al., 2017), boost in the release of inflammatory mediators (Caponnetto et al., 2013; Higham et al., 2016), and platelet activation, aggregation, and adhesion (Hom et al., 2016). Healthy e-cig users exhibited inhibition of the ability of arteries to dilate in response to the need for more blood flow as well as smokers. Coupled with a shift to full-blown sympathetic nervous system predominance, these changes represent an increased risk of both long-term hearth diseases and acute events (Caponnetto et al., 2013; Higham et al., 2016). A cross-sectional analysis of data in the US 2014 and 2016 National Health Interview Surveys revealed that daily e-cig use was associated with increased odds of having suffered a myocardial infarction (Talal et al., 2018).

Cardiovascular and non-cancer lung diseases kill more smokers than does cancer and it is established that e-cigarettes deliver lower levels of carcinogens than do conventional cigarettes (Goniewicz et al., 2014). Nevertheless, it is important to evidence that bladder carcinogens have been found in urines of e-cig users but not in non-users (Fuller et al., 2018).

HEAT-NOT-BURN TECHNOLOGY: IQOS®

Heat-not-burn (HNB) products are electronic machines that heat modified cigarettes to produce an aerosol for inhalation without causing combustion. PMI created IQOS® (I-Quit-Ordinary-Smoking), where disposable tobacco sticks soaked in propylene glycol are inserted in a holder that heats them at 350 °C (Auer et al., 2017). Claimed as an almost completely safe device, due to the lack of combustion, and thanks to the taste of tobacco without smoke, IQOS® has rapidly reached a great popularity in all the 40 countries in which it has been commercialized since 2014 (Lüdicke et al., 2019). However, since the product is on the global market from only few

years, a small number of studies regarding the effective safety of IQOS® is present in the current literature, many of which have been funded by PMI itself. Users need accurate information about the risks associated to IQOS® from independent researches.

Studies focused on the chemical composition of the IQOS® reported the presence of volatile organic compounds (VOCs), polycyclic aromatic hydrocarbons, and carbon monoxide, (Auer et al., 2017; Cancelada et al., 2019). Based on an estimation of the daily intake of IQOS® emissions (20 stick per day), the predicted daily doses for formaldehyde, acetaldehyde, acrolein, diacetyl, and benzene are comparable those associated with breathing contaminated air at or above recommended limits (Cancelada et al., 2019). A comparison between IQOS® and tobacco cigarette showed that the release of nicotine reaches similar concentration in both the tobacco products, and that IQOS® emits significant concentration of ROS and carbonyl compounds (Salman et al., 2019). The amount of tobacco specific nitrosamines (TSNA) has been found lower compared to tobacco cigarette but significantly higher than from e-cig (Leigh et al., 2018).

In an in-vitro study human bronchial epithelial cells were exposed to e-cig vapor, IQOS® aerosol and cigarette smoke (Sohal et al., 2019) to investigate the cytotoxic effects of the three products. IQOS® and tobacco cigarette exposure showed similar effects on cells in terms of cell mortality and proliferation, chemokine release, and mitochondrial dysfunction, making IQOS® capable to increase oxidative stress, inflammation, infections, airway remodeling and initiate epithelial mesenchymal transition related changes (Sohal et al., 2019). These results are partially in accordance with those by Leigh et al., who found higher cytotoxicity in bronchial epithelial cells exposed to IQOS® compared to control and e-cig group, but lower if compared to tobacco cigarette one (Leigh et al., 2018b).

Acute exposure to IQOS® in rats showed impairment of arterial flow-mediated dilation, suggesting that the use of this product not necessarily avoids the adverse cardiovascular effects of smoking cigarettes (Nabavizadeh et al., 2018).

Prospective clinical studies have not yet been conducted. However, Sharman and colleagues have initiated a 5-year single-center cohort observational study to assess differences in lung function between users of the heated tobacco product, IQOS® with HeatSticks, and smokers of conventional combustible cigarettes (Sharman et al., 2018).

Altogether, these studies have opened a scientific debate on the impact of IQOS® on human health that might influence regulation on this product. For this reason, current evidence is insufficient and further independent investigations are necessary to fully assess the health effects in users and bystanders.

AIM OF THE RESEARCH

TO ASSESS THE TOXICOLOGICAL EFFECTS OF ENDS PERSONALIZATION

Contrary to conventional cigarettes, which differ from each other based essentially on the nicotine ratio and the filter type, e-cigs are designed to personalize as much as possible the habit of vaping.

Flavored liquids, for example, largely address the preferences of vapers, especially among youth and young adults (Harrel et al., 2017; Yingst et al., 2017). A recent study reported a direct correlation between the type and concentration of flavor and the free radical production (Bitzer et al., 2018).

During the last few years, the technology of e-cigs has been improved and the settings of the device are now easily adjustable by users. Besides the e-liquid, in fact, they can arbitrarily combine different values of temperature, voltage and resistance. Of increasing concern are the thermal breakdown products from e-liquids at high temperature, due either to the device design or to unintentional overheating. The achievable temperature inside e-cig, that ranges up to 350°C (Chen et al., 2013; Schripp et al., 2013), is sufficiently high to decompose propylene glycol (PG) or vegetable glycerol (VG). It is reported that PG can undergo oxidation at as low as 127–227 °C to form formaldehyde, acetaldehyde and acrolein (Diaz et al., 2010; Bekki et al., 2014; Wang et al., 2017). Moreover, VG can be thermally dehydrated to acrolein, which can go through further degradation to formaldehyde and acetaldehyde (Nimlos et al., 2006). Wang et al. showed

how over 215 °C the formation of formaldehyde and acetaldehyde increases noticeably, and over 270 °C acrolein can be observed in detectable amounts (Wang et al., 2018).

Strictly related to temperature, the power supplied to e-cig influences the aerosol composition. From basic thermodynamic principles, it can be deduced that more power applied to the atomizer will produce greater vaporization because more energy is available to overcome the heat of vaporization of the e-liquid.

The possibility to arbitrarily adjust the total power of the device by combining different values of voltage and resistance may have a considerable impact on human health (Chausse at al., 2015). Contrary to the common believe that carbonyls are generated only when high voltage is applied (Jensen et al., 2015), it is now stated that toxic aldehydes, such as formaldehyde, are produced even in lower power breath activated devices (Bitzer et al., 2019). Since the combination of voltage applied and resistance value of the filament coil is responsible of the heating power through the Joule effect ($W=V^2/\Omega$) (Chausse et al., 2015), we believe that the extent of the toxicological consequences can be strictly influenced by consumers' habits.

In this study, e-cig devices were set with the same voltage value (3.5 V) in order to determine whether application of low (0.25 Ω) and medium (1.5 Ω) coil resistances affected the carbonyls and ROS generation. First, the formation of formaldehyde, acetaldehyde and acrolein in the vapor was establishes by GC-MS analysis; then the source of oxidants were determined by a modified 2,7-dichlorodihydrofluoresceindiacetate (DCFH-DA) fluorescin derived dye to detect ROS reactivity in e-cig aerosol and pre-vaporized e-liquids in a cell-free system. The biological effects of the resulting non-nicotine vapor were studied in both *in-vitro* and *in-vivo* models.

The toxicity of different vapors on cell viability was investigated by exposing H1299 cells, in an air-liquid interface system, to e-cig aerosols. The effects on the pulmonary oxidative and inflammatory status were then studied in a rat model. By exposing, in two different experiments, Sprague Dawley rats to e-cig and IQOS® aerosol, the consequences of 28 days treatment on lung inflammation, oxidative stress and tissue damage, and on blood homeostasis were examined.

CHAPTER 1

TOXIC ALDEHYDES AND FREE RADICALS GENERATED BY E-CIG

The main constituents of e-liquid are vegetable glycerol (VG), propylene glycol (PG), water, flavorants and nicotine – when present. VG and PG are common food additives, and PG has been used as a diluent in parenteral medications and in some medicinal inhalers. Temperature-dependent thermal degradation of PG and VG results in formation of potentially toxic aldehydes including formaldehyde, acetaldehyde and acrolein (Paschke et al., 2014, Uchiyama et al., 2013). Several studies have also reported that e-cig vapor contains high amounts of free radicals (Lerner et al., 2015; Sussan et al., 2015; Goel et al., 2015). The toxic effects of the aldehydes and the health implications of free radicals are discussed in this chapter.

1.1 FORMALDEHYDE, ACETALDEHYDE AND ACROLEIN

Formaldehyde, acetaldehyde and acrolein are formed by thermal decomposition (pyrolysis) of vegetable glycerol (VG) in the e-liquid when it comes into contact with the heating coil of the atomizer.

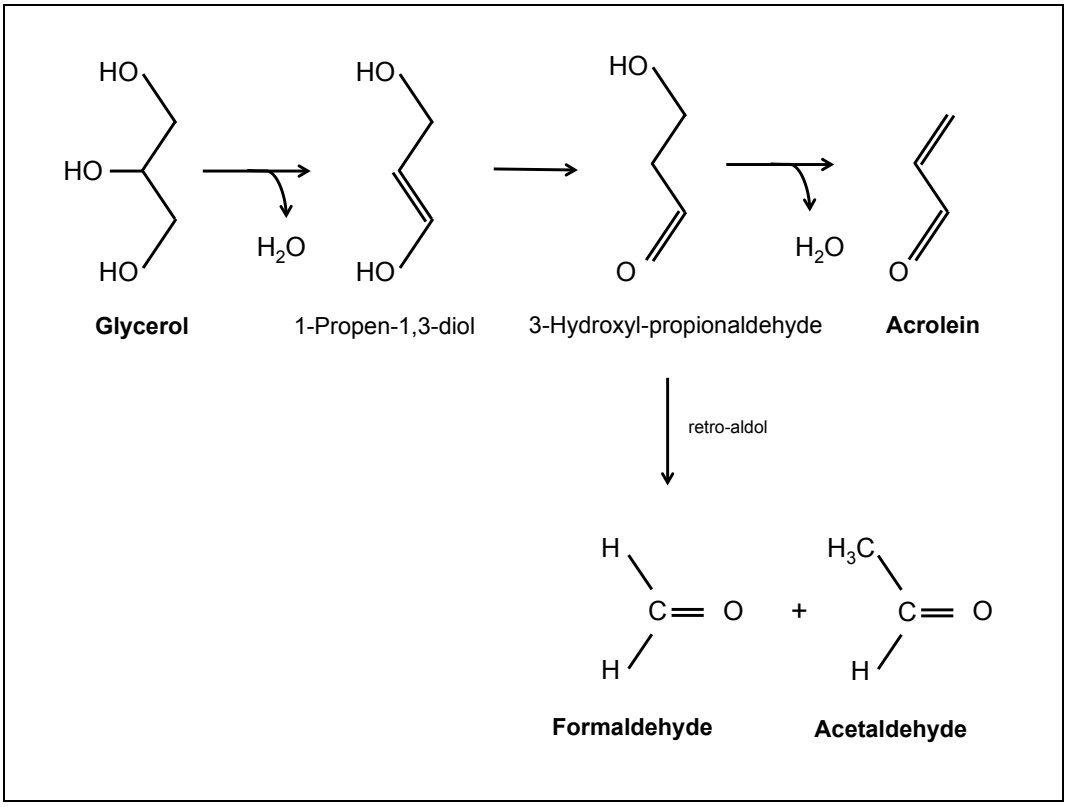

Figure 1. Thermal decomposition (pyrolysis) of glycerol to form formaldehyde, acetaldehyde and acrolein

FORMALDEHYDE – Formaldehyde is a known degradation product of PG that reacts with PG and VG during vaporization to produce hemiacetals (Jensen et al., 2015). It has been demonstrated that more than 2% of the total solvent molecules has converted to formaldehyde-releasing agents, reaching high concentrations (Jensen et al., 2015). Formaldehyde is classified as carcinogen to human (Group 1) by International Agency for Cancer Research. Lower than 0.3 ppm/370 μg m^{-3} concentrations are reported to be protective for the symptoms of sensory irritation for all individuals, including those with self-reported sensitivity to formaldehyde as well as asthmatics (ATSDR, 2007; NAS, 2007a,b). A similar value – 0.3 ppm/380 μg m^{-3} – was set by the American Conference of Governmental Industrial Hygienists as acute (one inhalation) exposure limit. The World Health Organization established a more conservative and even more health

protective value of 100 µg m^{-3} as official indoor air guideline for formaldehyde – defined for 30 min short term average exposure recommended as preventing sensory irritation in the general population – (WHO, 2007). Several studies on e-cig emissions revealed that levels of formaldehyde in vapor exceed these threshold values several times, often depending on the setting of the device (Geiss et al., 2016; Klager et al., 2017).

ACETALDEHYDE – Largely used as a chemical intermediate in the production of herbicides, insecticides, fungicides, pharmaceuticals, flavors, fragrances, dyes, plastics, and synthetic rubber (IARC, 2005), acetaldehyde is also one of the components of cigarette smoke and e-cig vapor. Increasing air concentrations results in deeper penetration of acetaldehyde vapor in the respiratory system, which causes bronchiolitis obliterans (as reported after accidental high-dose occupational exposures) or bronchoconstriction in asthmatics. Acetaldehyde, like formaldehyde and acrolein, is chiefly a portal-of-entry toxicant that targets the upper respiratory mucosa, but it is considerably less potent than these two other aldehydes. Acetaldehyde is classified in Group 2B carcinogens by IARC. In addition, low to moderate air concentrations (25 ppm/45 mg m^{-3} to 200 ppm/363 mg m^{-3}) cause eye and upper respiratory tract irritation. Moderate concentrations (300 ppm or greater) also cause bronchoconstriction in asthmatics (Muttray et al., 2009, Sim and Pattle, 1957). The German Ad-hoc Working Group on Indoor Guidelines of the Indoor Air Hygiene Committee and the States' Supreme Health Authorities (2013) issued an indoor air precautionary guideline value of 100 µg m^{-3} for acetaldehyde to protect public health. Acetaldehyde value in e-

cig vapor was found at least 2.5 larger depending on the battery output (Geiss et al., 2016; Ogunwale et al., 2017).

ACROLEIN – Acrolein is ubiquitously present in cooked foods and in the environment. Chemical reactions responsible for release of acrolein include heat-induced dehydration of glycerol, retro-aldol cleavage of dehydrated carbohydrates, lipid peroxidation of polyunsaturated fatty acids, and Strecker degradation of methionine and threonine (Stevens et al., 2008). Acrolein is listed as an hazardous air pollutant by the United States Environmental Protection Agency (U.S. EPA, 2003). Many studies showed that acute exposure to even low levels of acrolein can induce dyslipidemia (Konklin et al., 2010), vascular injury (Konklin et al., 2006), endothelial dysfunction (Konklin et al., 2009), and platelet activation (Sithu et al., 2010), whereas chronic exposures accelerate cardiovascular disease (Srivastava wt al., 2001; O'Toole et al., 2009; Wang et al., 2008; Ismahil et al., 2011; DeJarnett et al., 2014). Slight eye irritation and "annoyance" or discomfort was observed in human subjects exposed to acrolein at 0.09 ppm/200 μg m^{-3} (Weber-Tschopp et al., 1977). An indoor air guideline value for acrolein of 6.9 μg m^{-3} was proposed by the French Agency for Food, Environmental and Occupational Health and Safety (ANSES, 2013) to protect against effects occurring following short-term exposure (1 h). Several studies reported acrolein concentration in e-cig emissions up to seven folds higher compared to the value indicated by this guideline (Bekki et al., 2014; Geiss et al., 2016; Ogunwale et al., 2017).

1.2 REACTIVE OXYGEN SPECIES AND OXIDATIVE STRESS

Reactive oxygen species (ROS) are radicals with an odd number of electrons that confers them high reactivity with biological molecules, such

as proteins, DNA, and lipids. As direct consequences, free radicals play a dual role in the biological systems, since they can be either harmful or beneficial to living systems. ROS are physiologically involved in signaling pathways in response to infectious agents or in the induction of mitogenic response (Valko et al., 2006). On the other hand, when high levels of free radicals are present in the organism, the development of macromolecule adducts and the generation of oxidative stress occur. The oxidative stress status is the result of the unbalance between the presence of ROS and the activity of removing cellular mechanisms such as scavenger systems, chelating agents, and enzymatic systems.

1.2.1. PHYSIOLOGICAL GENERATION OF ROS

Superoxide radical in cells is produced, among others, by xanthine oxidase (XO), which catalyzes the reaction of hypoxanthine to xanthine and xanthine to uric acid. In both steps, molecular oxygen is reduced, forming the superoxide anion in the first step and hydrogen peroxide in the second (Valko et al., 2004).

Blood cells are additional sources of ROS. Activated macrophages initiate an increase in oxygen uptake that gives rise to a variety of reactive oxygen species, including superoxide anion, nitric oxide and hydrogen peroxide (Conner et al., 1996).

Cytochrome P450 (CYP 450) enzymes are known to be responsible of ROS generation during their catalytic cycle. Several factors determine ROS production by means CYP450, such as the specific CYP450 isoform, the entry of the second electron into the cycle, and the presence and the nature of the substrate.

The immune response against toxic compounds produces ROS, through the release of inflammatory mediators by immunity cells, such as cytokines,

chemokines, interleukins and others from activated Kupffer cells (Klaunig and Kamendulis, 2004).

Human tissues have a substantial ability to tolerate ROS under normal conditions, since they are an essential part of many metabolic pathways. In fact, ROS are the spark of basic energy-producing processes.

Low levels of ROS present in skeletal muscle under basal conditions are a requirement for normal movement, and antioxidant-mediated depletion of ROS from unfatigued skeletal muscle results in the inhibition of their contraction (Gomez-Cabrera et al., 2015). As a consequence, ROS that are produced in exercise have a physiological role, and behave as signals to modulate adaptations of muscle to exercise (Gomez-Cabrera et al., 2015).

Many mechanisms induced by ROS, such as cell cycle arrest and apoptosis, end up with cell death. In fact, direct exposure of cells to ROS, such as H_2O_2, causes multiple intracellular alterations, including the elevation of cytosolic Ca^{2+}, depletion of ATP, oxidation of NADH, and reduction of glutathione. Whether and how ROS contribute to the induction of cell death depends on the signaling and execution pathways that are activated (De Vos et al., 1998). The process that leads to proliferation or cell death depends on the condition of the ROS-producing cell. For example, in cancer, ROS production defends the organism by attacking the DNA of the cancer cell, even if it is limited compared with the proliferation of the normal cell (Valko et al., 2004). On the other hand, ROS are potential carcinogens, as they facilitate mutagenesis, tumor promotion, and progression.

1.2.2. HARMFUL EFFECTS OF ROS

High levels of ROS represent a risk factor for the onset of several diseases and pathological conditions, including cancer and inflammation (Waris and Ahsan, 2006).

MEMBRANE LIPID PEROXIDATION – Double bonds within unsaturated fatty acids chain are attached by ROS, especially by •OH, and the interactions between lipids and free radicals produce peroxides, which are in turn unstable and reactive. In addition, such interactions induce a chain autocatalytic reaction, named propagation, which seriously damages the membrane. This type of damage can reflect in several losses of functions that depend on the type of membrane involved. Breaks on mitochondrial membrane determine ATP reduction with consequent apoptosis, while batters on cytosolic membrane cause the alteration of osmotic equilibrium, with the entry of ions and liquids, and exit of essential metabolites for ATP regeneration. At vascular level, H_2O_2 increases intracellular Ca^{2+} concentration and decreases electrical resistance in human lung microvascular endothelial cells (Suresh et al., 2015). In addition, H_2O_2 increases the expression of adhesion molecules that are important for permeability and signaling transduction in lung epithelium and are closely associated with stress response (Zang et al., 2014; Laitinen et al., 1994).

OXIDATIVE MODIFICATION IN PROTEIN – Free radicals also promote the oxidation of amino acids side chain, crosslinking protein-protein, and the oxidation of protein chain. Oxidative modifications in proteins can lead to the alterations in their functions, as well as their structure, which in turn results in these oxidized proteins undergoing proteolysis (Garcia Moreno et al., 2014). The oxidative damage in these molecules is carried out in three

stages: first, a protein can be slightly modified but its main structure is intact, resulting in a mild reduction of its activity; second, the damage inflicted upon the protein is enough to cause a partial unfolding of the protein and hydrophobic sequences, that are generally covered inside the soluble globular proteins, remain exposed on the surface; third, if the damaged protein has not been identified and degraded into proteasomes, it forms an aggregate with other proteins, lipid, and sugars (Keller et al., 2004).

DNA DAMAGE – One of the preferred target of ROS is DNA, where they are able to create DNA strand breaks, cross-links, and can cause modifications to the purine, pyrimidine and deoxyribose components of DNA (Vilema-Enríquez et al., 2016). Hydroxyl radical reacts with DNA, specifically with the carbon atoms that are forming double bonds in the nitrogenous bases, and subtracts one hydrogen from the methyl group of the thymine, as well as form each of the carbon-hydrogen double bonds of sugar (2-deoxyribose) (Cooke, 2003). H_2O_2-dependent DNA damage triggers a complex network of DNA damage response (DDR) pathways that may initiate DNA repair, arrest cell cycle progression, and cause apoptosis.
DNA impairment often represents the first dangerous circumstance in the multiphasic process of the chemical carcinogenesis, named *initiation*. Adducts formation, indeed, often leads up to a permanent damage on DNA, which characterizes the so-called initiated cell. A cell with an abnormal DNA is not carcinogenic by itself but can assume the ability to replicate and facilitate the development of a tumor, if subjected to the action of a promoting agent. The tumorigenic cell is formed when the clone of the initiated cell begins to proliferate, often acquiring additional mutations (*progression*). DNA alterations due to promoters are reversible and

often indirect, unlike the initiators, which are highly reactive electrophiles species able to directly react with nucleophilic sites, such as those in DNA, RNA and proteins. Cancer develops if the initiators targets are oncogenes, onco-suppressors, apoptosis regulators, DNA-damage repairing regulators, and telomerase. With this background in mind, it is deducible that free radicals and ROS have the characteristics to be perfect initiators, since they directly and permanently damage the DNA, and promoters, because they enhance the oxidative stress in cells (Pierce, 2016).

MUTATIONS – Mutations caused by oxidative DNA damage include a range of specifically oxidized purines and pyrimidines, alkali labile sites, single strand breaks and instability formed directly or by repair process. Studies show that, even if all the bases of DNA can be modified by ROS, mutations are generally related to the modification of GC base pairs (Retel et al., 1993). These mutations are usually base pair substitution, with the G to T transversion as the most frequent mutation in the p53 suppressor gene (Waris and Ahsan, 2006). Cigarette smoke causes accumulation of 8-hydroxydeoxyguanosine (8- OHdG). Lungs from smokers contain higher 8-OHdG levels compared to non-smokers, that could lead to mutations, some of which might be induced by oxygen free radicals, resulting in inflammatory responses, fibrosis and tumor development (Zeinolddiny et al., 2000; Canistro et al., 2017).

Oxidative stress plays a key role in various clinical conditions such as cancer, diabetes, atherosclerosis, chronic inflammation, viral infections (Waris and Ahsan, 2006). Doubtless, chronic obstructive pulmonary disease (COPD) is a pathological condition developed as a consequence of endogenous generation and release of oxidative stressors in the airways

(Likhdar et al., 2011; Rabe et al., 2007). The increased oxidative burden in COPD may contribute to a range of pathogenic processes starting with inactivation of antiproteases, enhancing bronchial inflammation by activating redox-sensitive transcription factors, mucus gland hyperplasia and hypersecretion, corticosteroid resistance, enhanced senescence, activation of neutrophils, macrophages, and fibroblasts, abnormal airway T-cell population, and small airway fibrosis culminating in direct damage to respiratory cells (apoptosis) with defective regeneration (MacNee, 2005; Hansel and Barnes., 2009). The imbalance between ROS and antioxidant defense at pulmonary and systemic level, gene polymorphisms, and activation of transcription factors such as nuclear factor kappa B NF-κB contribute to the molecular pathogenesis of COPD (MacNee and Rhaman 1999).

Generally, chronic inflammation plays a key role in cancer development. Inflammatory mediators that affect the growth of cancer act during the stage of promotion. Moreover, inflammation-inducing factors are also frequently cancer promoters (Karin et al., 2006). In fact, cancer-related inflammation is associated with proliferation and survival of malignant cells, angiogenesis, tumor metastasis, and tumor response to chemotherapeutic drug and hormones (Mantovani et al., 2008). Inflammatory cells release a number of cytokines, chemokines, ROS as inflammatory mediators, soluble mediators of cell death such as Tumor Necrosis Factor-α, interleukins (IL) interferon, and angiogenic factors (Coussens and Werb, 2002). Apart from enhanced proliferation or increased survival, these mediators may also involve the activation of angiogenesis and metastasizing.

CHAPTER 2

DRUG METABOLISM AND ANTIOXIDANT ENZYMES

The wide variety of xenobiotics to which humans are daily exposed is absorbed across the lungs, skin or, more commonly, ingested either unintentionally through food and drinks, or deliberately as drugs for therapeutic or recreational purposes. The common feature of these substances is the lipophilicity and neutrophility at physiological pH. Many xenobiotics are innocuous, but some others can induce biologic responses. Such responses often depend on accumulation of the absorbed substance into the organism with a consequent prolonged activity, or on its conversion into an active metabolite. Drug metabolism is the process that can lead to the termination or modification of xenobiotic biological activity, through three major categories of catalysis: phase I, phase II and phase III reactions (Katzung et al., 2011).

Phase I reactions usually convert the parent drug or xenobiotic to a more polar metabolite by introducing or unmasking a functional group (-OH, -NH_2, -SH). Many phase I products are not polar enough to be rapidly eliminated, so they undergo a subsequent reaction in which an endogenous substrate, such as glucuronic acid, sulfuric acid, acetic acid, or an amino acid, combines with the newly incorporated functional group to form a highly polar conjugate. Such conjugation or synthetic reactions are the hallmarks of phase II metabolism (Katzung et al., 2011).

Biotransformation reactions have several effects on their substrates, being able to produce inactive metabolites or, in some instance, more or

comparable active compounds respect to the initial one. Increased metabolites reactivity results in a large capacity to react both with endogenous molecules and with the wide range of exogenous compounds to which the organism is daily exposed.

Due to the increased ROS generation from the induced catalytic reactions of some metabolizing enzymes, and to the alteration of the antioxidant ones, the exposure to xenobiotics can directly lead to the perturbation of the redox balance of the organism. As previously said, low levels of ROS are essential in many biochemical processes. In fact, response to injury and inflammation evolves with the formation of electrophiles, including oxidants that produce a second level of signaling mimicking the physiological response. At the same time, such signaling is also accompanied by a persistent alteration of homeostasis with elevated levels of oxidized metabolites and macromolecules. These deviations from the redox homeostasis, the aberrant activation of defense and healing mechanisms, and uncontrolled oxidative signaling and damage, evolve into an oxidative stress.

Several variables influence the biotrasformation capability thus generating the so-called "individual toxicity". Genetic factors influence enzyme levels through "genetic polymorphisms" in drug metabolism. Well-defined and clinically relevant genetic polymorphisms in phase I, II and III drug-metabolizing and antioxidant enzymes result in modified efficacy of drug therapy or adverse drug reactions (ADRs). It is right to presume that each person has an own metabolic genetic profile (or fingerprint), identified in genes encoding for drug metabolism enzymes, for xenobiotics transport system, for transcriptional activators, and for their response elements (Evans and Johnson, 2001). Furthermore, absorption, distribution, metabolism, and excretion are easily subject to sex- and age-dependent

modifications because of different body mass compositions, which may impact the solubility of various drugs (Kramer and Testa, 2009). The combination of these elements, together with the personal lifestyle, physiopathological status and environmental factors, influence the individual response to xenobiotic exposure, thus enhancing the variability of the drug-metabolism related effects (Paolini et al., 2004; Kramer and Testa, 2009).

2.1 PHASE I ENZYMES

Many drug-metabolizing enzymes are located in the lipophilic endoplasmic reticulum membranes of the liver and other tissues. When these lamellar membranes are isolated by homogenization and fractionation of the cell, they re-form into vesicles called microsomes. These ones retain most of the morphologic and functional characteristics of the intact membranes, including the features of the rough and smooth endoplasmic reticulum. The smooth microsomes are relatively rich in phase I enzymes responsible for oxidative drug metabolism. In particular, they contain the important class of enzymes known as the mixed function oxidases (MFOs), or monooxygenases. The activity of these enzymes requires both a reducing agent (nicotinamide adenine dinucleotide phosphate [NADPH]) and molecular oxygen. In this oxidation-reduction process, two microsomal enzymes play a key role: the first is a flavoprotein, NADPH-cytochrome P450 oxidoreductase (POR), while the second is a hemoprotein called cytochrome P450 (abbreviated as CYP450 or CYP), which serves as terminal oxidase. CYPs represent the class of enzymes mainly involved in xenobiotics biotransformation. Microsomal drug oxidation requires CYP450, CYP450 reductase, NADPH, and molecular oxygen.

Oxidations represent the most important group of phase I reactions, in quantitative terms. However, other classes of reactions are included in phase I metabolism, such as epoxidations, reductions, hydrolysis, and dehalogenations. Epoxidations are oxidation reactions of alkenes that give cyclic esters in which both carbons of a double bond become bonded to the same oxygen atom. Reductions represent a large rate of reactions catalyzed by enzymes such as alcohol-oxidoreductase, keto-reductase, and aldehyde-reductase; in particular, azo- and nitro-reductions are catalyzed by the POR system and by flavo-protein enzymes. Hydrolysis involve esters, amides and glucosides and are respectively made by esterases, which split esters into an acid and an alcohol, amidases, and epoxide-hydrolases, which convert epoxides to trans-dihydrodiols. Dehalogenations consist in the removal of halogen from a molecule and are classified into three types: reductive, oxidative, and resulting in the formation of a double bond C-C.

2.1.1 CYP450-DEPENDENT MIXED-FUNCTION OXIDASE SYSTEM

For many endogenous and exogenous substances, oxidative metabolism represents the initial step of the biotransformation process. Several enzymatic systems are involved, but the principal is the MFO, which requires both NADPH-cytochrome CYP450 oxidoreductase and CYP. In presence of molecular oxygen and reduced form of NADPH, in a typical reaction, one molecule of oxygen is consumed (reduced) per substrate molecule of substrate, with one oxygen atom appearing in the product, and the other in the form of water.

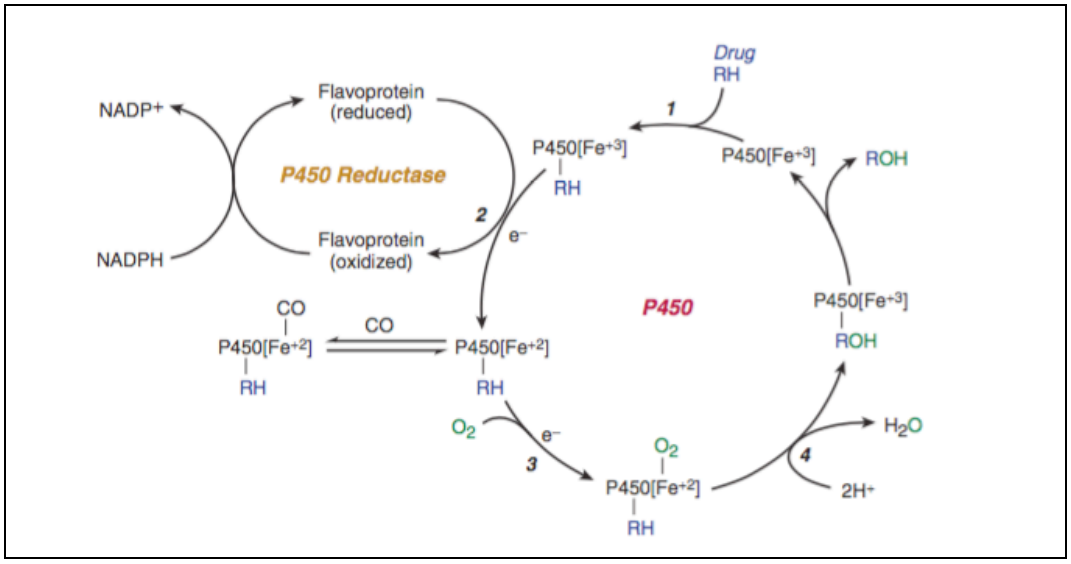

Figure 2. Catalytic cycle of cytochrome P450
Source: Katzung BG, Masters SB, Travor AJ: Basic & Clinical Pharmacology, 12th edition.

The main enzyme of monooxygenase system, CYP450, is a trans-membrane protein having a long N-terminal α-helix, which links the protein to smooth endoplasmic reticulum (SER) membrane, and a catalytic core, which protrudes into cytosol. The core has α and β secondary elements that form a globular structure, highly conserved in all CYPs. By common consent, two faces have been attributed to this structure: distal, which represents the site of interaction with the substrate, and proximal. Between these two faces is located the heme group.

NADPH-cytochrome P450 oxidoreductase has a similar structure to that of CYP450: a N-terminal domain binds the protein to the SER phospholipid matrix and participates in the correct interaction with CYPs, while a C-terminal domain represents the catalytic core that protrudes into cytosol. One mole of this flavoprotein contains 1 mol each of flavin mononucleotide (FMN) and flavin adenine dinucleotide (FAD). This enzyme catalyzes the electrons transfer from reduced coenzyme of NADPH to cytochrome P450 through the coenzymes FMN and FAD (Flück et al., 2007).

2.1.2 PHASE I MODULATION

The variability of drug and xenobiotic metabolism, especially if linked to the phase I enzymes or cytochrome P450, represents an important complicating factor in many areas of pharmacology and toxicology (Pelkonen et al., 2008). Several genetic, endogenous, and environmental factors, which make drug metabolism exceedingly variable and even individualistic, affect CYP activities (Pelkonen et al., 2008).

The human genome has 57 CYP genes, and the function for most of the corresponding enzymes is known at least to some degree (Pelkonen et al., 2008). Fifteen individual CYP enzymes in families 1, 2 and 3 metabolize xenobiotics, including a large number of small molecule drugs currently in use. In particular, CYP3A4 is the most abundant form, responsible alone for the metabolism of more than 50% of prescription drugs and a very large number of other xenobiotics. Besides this, the main represented isoforms in humans are CYP2A1, CYP2A6, CYP2B6, CYP2C8, CYP2C9, CYP2C19, CYP2D6, and CYP2E1. Together, CYP2B6, CYP2C9, CYP2C19, CYP2D6, and CYP3A4 are responsible for more than 90% of known oxidative drug metabolism reactions (Wienkers and Heat 2005; Guengerich, 2008). Some of the chemically dissimilar CYP450 substrate, after repeated exposure, induce CYP450 expression by enhancing the rate of its synthesis or reducing its degradation, while other xenobiotics inactivate cytochrome CYP450 enzyme activity.

INDUCTION – Induction results in accelerated substrate metabolism and usually in a decrease in the pharmacologic action of both the inducer and the co-administered drugs. However, in the case of drugs metabolically transformed to reactive metabolites, enzymatic induction may intensify metabolite-mediated toxicity. Various substrates induce CYP450 isoforms,

having different molecular masses and exhibiting different substrate specificities and immunochemical and spectral characteristics. Increased CYP450 synthesis requires enhanced transcription and translation along with increased synthesis of heme, its prosthetic cofactor. Several intracellular receptors (e.g. Aromatic Hydrocarbon Receptor, AhR; Pregnane X receptor PXR; Constitutive Androstane Receptor, CAR; Peroxisome Proliferator-activated Receptor, PPaR) are able to sense a great variety of xenobiotics and consequently regulate numerous phase I and phase II drug-metabolizing enzymes and drug transporters, in order to adjust the organism to the requirements of the chemical environment (Pelkonen et al., 2008).

The CYPs activity can be also controlled at post-transcriptional and post-translational levels. Significant post-transcriptional regulation has been shown only for few CYPs. Regulation of mRNA stability has been found to mediate xenobiotics induction in few cases. Mechanisms of such regulation act on mRNA transport and splicing (Fucella et al., 1998). Different types of splicing on the same mRNA have been demonstrated. Such splicing produces ribonucleoproteins having different start and stop codons. This situation determines protection against ribonucleases, with a consequent different mRNA stability during cytosolic ribosome transport (Fucella et al., 1998).

CYP2E1 appears to be the only CYP mainly regulated at the post-translational level by xenobiotics such as ethanol, acetone, pyrazole and isoniazid (Carroccio et al., 1994). CYP2E1 half-life is significantly increased by inducing compounds, thanks to a stabilization that may involve inhibition of proteasome degradation pathway (Cederbaum, 2006).

As previously shown in fig. 2, the catalytic cycle of CYP450 produces ROS as byproduct (Paolini et al., 1999). Several factors determine ROS

production by means CYPs, such as the specific CYP450 isoform, the entry of the second electron into the cycle, and the presence and the nature of the substrate. As a consequence of CYP induction, a large amount of ROS is generated and creates an oxidant environment that unbalances the redox equilibrium in the organism.

INHIBITION – CYP450 inactivation is implicated in the majority of the reported clinically relevant drug-drug interactions DDIs (Kamel et al., 2013). It can lead to increased bioavailability of the parent compound, normally subjected to extensive first-pass elimination, or to decreased elimination of compound dependent on metabolism for systemic clearance (Pelkonen et al., 2008). Inactivation may result in increased steady-state concentration and accumulation ratio and non-linear kinetics, as a consequence of the saturation of enzymatic process (Pelkonen et al., 2008). The mechanisms of CYPs inactivation can be distinct into two categories: reversible inhibition and mechanism-based inactivation (MBI).

Reversible inhibition occurs as a result of competition at the active site of enzyme and probably concerns only the first step of the catalytic cycle (Kamel and Harriman, 2013). It involves a rapid association and dissociation between drugs and enzyme and it is divided into competitive, noncompetitive and uncompetitive inhibition. In competitive inhibition, substrate (S) and inhibitor compete to bind the same position on the active site of enzyme (E), with a consequent increase in K_m and unchanged V_{max}. In noncompetitive inhibition, inhibitor and substrate have different active binding sites, and inhibitor has the possibility to bind both the free enzymes and the ES complex. In uncompetitive inhibition, inhibitor binds only the ES complex and prevents the product formation. It is dependent on the amount of the ES complex and, consequently, the amount of substrate

present, so that it is characterized by a decrease in both K_m and V_{max} (Kamel and Harriman, 2013).

Mechanism-based inactivation can occur via the formation of metabolite intermediate complexes or via the strong, covalent binding of reactive intermediates to the protein or heme of CYPs. The specificity of MBI for a CYP enzyme is mainly determined by differential binding affinities of the substrate molecules within the active site of the CYP450, and/or its orientation in the active site rather than by the specific protein residues present in close proximity of the reactive moiety (Kamel and Harriman, 2013; Halper et al., 1999).

2.2 PHASE II ENZYMES

Parent drugs or their phase I metabolites that contain suitable chemical groups often undergo coupling or conjugation reactions with an endogenous substance to yield drug conjugates. In general, conjugates are polar molecules that are readily excreted and often inactive. Their formation involves high-energy intermediates and specific transfer enzymes. Such enzymes, named transferases, may be located into microsomes or cytosol. They catalyze the coupling of an activated endogenous substance with a drug or xenobiotic (or endogenous compound such as bilirubin, the end product of heme metabolism).

Xenobiotic conjugations were once believed to represent terminal inactivation events and as such have been viewed as "true detoxification" reactions. However, this concept must be modified, because it is now known that certain conjugation reactions may lead to the formation of reactive species responsible for the toxicity of the compounds. An example is given by nitrosamines, produced from nitrates and secondary amines, and often found in food such as grilled or fried meat, cheese, beer, or

released by cigarette smoke. Nitrosamines react with cytochrome P450 with formation of hydroxylated intermediates. These products undergo a phase II reaction (conjugation with glutathione) leading to the formation of an electrophilic and genotoxic product.

UDP-glucuronosyltransferases (UGTs) are the key enzymes of the process known as glucuronidation. The formation of glucuronide conjugates is the most important detoxification pathway of the phase II drug metabolism in all vertebrates (Jancova et al., 2010). UGT enzymes are responsible for the metabolism of many xenobiotics and endogenous compounds. The UDP-glucuronosyltransferases (UDPGTs) are a superfamily of membrane-bound enzymes catalyzing the formation of a chemical bond between a nucleophilic O-, N-, S-, or C-atom with uridine-5′-diphospho-α-D-glucuronic acid (UDPGA). All UDPGT enzymes are capable of forming O-linked glucuronides. These ones can be formed through conjugation of UDPGA with aliphatic alcohols, phenols, carboxylic acids, thiols and amines (primary, secondary, tertiary) (Fisher et al., 2001).

Glutathione S-transferase (GST), one of the major phase II "detoxification" enzymes, is also involved in the metabolism of xenobiotics and plays an important role in cellular protection against oxidative stress. The GSTs are a family of enzymes that catalyze the formation of thioether conjugates between the endogenous tripeptide glutathione and xenobiotic compounds. GSTs play a major role in the detoxification of epoxides derived from polycyclic aromatic hydrocarbons (PAHs) and alpha-beta unsaturated ketones. Moreover, a number of endogenous compounds such as prostaglandins and steroids are metabolized via glutathione conjugation (van Bladeren, 2000). The major biological function of glutathione transferases appears to be defending against reactive and toxic electrophiles such as reactive oxygen species (superoxide radical and hydrogen peroxide)

that arise through normal metabolic processes. Many of these are formed by cellular oxidative reactions catalyzed by cytochrome P450 and other oxidases (Sheehan et al., 2001).

2.2.1 PHASE II MODULATION

Several elements are involved in the modulation of genes encoding phase II enzymes, such as the antioxidant response element (ARE), the electrophile response element (ERE), the xenobiotic response element (XRE), aromatic hydrocarbon response element (AhRE), and some nuclear factors as KB or NF-kB, which bound to their regulatory regions (Xu et al., 2005).

INDUCTION – Nrf2 is an intracellular target of MAPK cascade (Rushmore and Kong, 2002), which belongs to the NF-E2 family of nuclear transcriptional factor, while Keap1, its repressor, is a cytoplasmic protein anchored to actin F of cytoskeleton and responsible for cellular stress sensing. Such stress may be caused by reactive oxygen species (ROS) and electrophilic compounds, both phase II inducers (Levonen et al., 2004). They drive the dissociation of the Nfr2-Keap1 complex, with a consequent Nrf2 phosphorylation and translocation to the nucleus, where it dimerizes with Maf protein (Dikova-Kostova et al., 2002). This heterodimer induces recognition and binding to the regulatory sequence ARE, present in the phase II gene promoters (Lee et al., 2005).

INACTIVATION – Phase II enzymes inactivation is based on the same mechanisms of CYPs inactivation. Furthermore, it is frequent the so-called functional inhibition, due to a depletion of cofactors essential for conjugations. This mechanism is especially involved in sulphatation regulation.

2.3 ANTIOXIDANT ENZYMES

The enzymes mainly used as antioxidant defense are catalase, responsible of H_2O_2 transformation, superoxide dismutase (SOD), which catalyzes the dismutation of the superoxide radical $O_2^{\bullet -}$, glutathione peroxidase, which reduces both lipid hydroperoxides to their corresponding alcohols, and free hydroperoxides to water, and NAD(P)H-quinone oxidoreductase.

2.3.1 SUPEROXIDE DISMUTASE (SOD)

Superoxide dismutase is the antioxidant enzyme that catalyzes the dismutation of the highly reactive superoxide anion to O_2 and to the less reactive species H_2O_2, through the reaction:

$$2O_2^{\bullet -} + 2H^+ \rightarrow H_2O_2 + O_2$$

Superoxide is physiologically produced by either an enzymatic system for a biological purpose or by a leak of electrons from the respiratory chain. In humans, there are three forms of SOD discovered in 1970's by Irwin Fridovich: cytosolic Cu/Zn-SOD, mitochondrial Mn-SOD, and extra-cellular SOD (EC-SOD). Cu/Zn-SOD (SOD-1) has been conserved during evolution. Each of the two identical subunits of the enzyme contains the active site, constituted by a copper and a zinc atom bound by a histamine residue (Battistoni et al., 1998; Leah et al., 1998; Stoppolo et al., 1998). Cu/Zn-SOD is believed to play a major role in the first line of antioxidant defense. Mn-SOD is a homotetramer containing one manganese atom per subunit that cycles from Mn (III) to Mn (II) and back to Mn (III) during the two steps dismutation of superoxide (MacMillan-Crow et al., 1998). EC-SOD was found both in the interstitial spaces of tissues and in extracellular

fluids, accounting for the majority of the SOD activity in plasma, lymph, and synovial fluid (Sandstróm et al., 1994).

2.3.2 CATALASE

Catalase (CAT) is a tetrameric enzyme consisting of four identical subunits that contain a single ferriprotoporphyrin group per subunit. CAT reacts very efficiently with H_2O_2 to form water and molecular oxygen through the reaction:

$$2H_2O_2 \rightarrow 2H_2O + O_2$$

In animals, hydrogen peroxide is detoxified by CAT and by glutathione peroxidase (GPx). Even though CAT is not essential for some cell types under normal conditions, it plays an important role in the acquisition of tolerance to oxidative stress in the adaptive response of cells (Thomas et al., 2014).

2.3.3 GLUTATHIONE PEROXIDASE (GPX) AND REDUCTASE (GSSG-RED)

The glutathione peroxidase (GPx), a selenium-containing peroxidase, contains a single seleno-cysteine (Sec) residue in each of the four identical subunits, which is essential for enzyme activity. GPx catalyzes the reduction of hydroperoxides using GSH, in order to protect mammalian cells against oxidative damage.

$$ROOH + 2GSH \rightarrow ROH + GSSG + H_2O$$

Thanks to this property, glutathione metabolism is one of the most essential antioxidant defense mechanisms. Moreover, GPx is able to convert H_2O_2 to two molecules of water, through GSH oxidation:

$$2GSH + H_2O_2 \rightarrow GSSG + 2H_2O$$

The oxidized glutathione can be restored to GSH by another enzyme, the glutathione reductase (GSSG-Red) NADPH-dependent, through the following reaction:

$$GSSG + NADPH + H^+ \rightarrow 2GSH + NADP^+$$

There are two forms of glutathione peroxidase, the first one is selenium-indipendent (GST) and the second one is selenium-dependent (GPx). Humans have four different GPx: GPx1 reduces fatty acids hydroperoxides and H_2O_2 at the expense of glutathione and is present in red blood cells, liver, kidney, lung, main localized in nucleus, cytosol and mitochondria; GPx2 is situated in nucleus and cytosol of gastrointestinal epithelial cells; GPx3 is found in blood circulation and cytosol (kidney, lung, placenta, heart, muscle); GPx4 is present in cytosol, nucleus, and in membrane fractions of several organs and tissues, and it can directly reduce the phospholipid hydroperoxides, fatty acid hydroperoxides, and cholesterol hydroperoxides that are produced in peroxidized membranes and oxidized lipoproteins (Imai et al., 1998).

2.3.4 NAD(P)H-QUINONE OXIDEREDUCTASE (NQO1)

NAD(P)H-quinone oxidoreductase catalyzes the reaction:

$$NADPH + H^+ + quinone \leftrightarrow NADP^+ + semiquinone$$

Quinones are formally derived from aromatic compounds by conversion of an even number of –CH= groups into –C(=O)– groups with any necessary rearrangement of double bonds, resulting in a fully conjugated cyclic dione structure. The quinone's double bond is highly electrophilic and can form covalent bonds with several chemical groups; moreover, quinones are also able to arylate nucleophiles with production of ROS. For this reason, NQO1 is important for the degradation of such reactive compounds, and it has a crucial role in the metabolism of endogenous molecules such as ubiquinone and vitamin E.

2.3.5 ANTIOXIDANT ENZYMES MODULATION

The most known antioxidant enzymes signaling system consists in the activation of the Nrf2 transcription factor and the electrophile response element, EpER (also called antioxidant response element or ARE), to which Nrf2 binds. As mentioned before, Nrf2 is retained in cytosol until the repressor Keap1 is modified by electrophiles. While Nrf2 activation requires modification of Keap1, the repressor does not just simply retain Nrf2 (Forman et al., 2014). Rather, Keap1 causes the rapid turnover of the Nrf2 transcription factor by assisting in Nrf2 ubiquitinylation (Forman et al., 2014). When critical cysteine residues in Keap1 are oxidized or covalently modified, Keap1 is inactivated and the Nrf2 transcription factor half-life is extended (Itoh et al., 1999). However, Keap1 modification, although essential, is not the only reaction involved in the activation of Nrf2 signaling by electrophiles. In fact, even though a crucial aspect of Nrf2 activation is its escape from ubiquitinylation and proteasome degradation, Nrf2 must also be phosphorylated for the translocation to the nucleus

where it activates EpRE-regulated genes (Zang and Hannink, 2003; Huang et al., 2000). Such phosphorylation is made by protein kinases, which are also activated by oxidants and other electrophiles (Jaiswal, 2004).

CHAPTER 3

INFLAMMATION BIOMARKERS

As a consequence of exposure to oxidant and toxic compounds, as well as to the presence of tissue damage, the innate immune system is immediately activated, recruits granulocytes to the injured tissue, produces inflammatory mediators, including pro-inflammatory cytokines and evokes an acute inflammatory process to clear the pathogens and damaged tissues. Innate immune cells, in fact, recognize cell damage with intracellular cell surface-expressed pattern recognition receptors (PRRs) that detect damage-associated molecular patterns (DAMPs) released from injured cells. Activate PRPs oligomerize and assemble large multi-subunit complexes that initiate signaling cascades to trigger the release of factor promoting the recruitment of leukocytes to the region (Newton and Dixit, 2012). When not rapidly resolved, inflammation often becomes chronic (weeks to months to years), and this underlies various chronic disorders such as autoimmune, neurodegenerative, vascular and metabolic diseases and cancer. Lung is particularly dependent on tightly regulated immunological and inflammatory processes, since it is exposed to a large and varied burden of infectious agents as well as a diverse group of noxious gases and particulates during the process of gas exchange. Pulmonary defense from injurious agents involves the recruitment cytokine-regulated host defense mechanisms wherever it interfaces with the external environment (Towes, 2001).

3.1 PRO-INFLAMMATORY CYTOKINES

The generation of inflammation in the lower respiratory tract requires the coordinated expression of both pro- and anti-inflammatory cytokines. Cytokines are involved in normal regulation of all physiological process. As a consequence of the recognition of microbial pathogens or toxic compounds, toll-like receptor (TLR)-mediated signaling results in the production of cytokines, such as tumor necrosis factor α (TNF-α) and interleukin 1 (IL1), that stimulate expression of adhesion molecules on vascular endothelial cells (Kim and Newton, 2012).

3.1.1 INTERLEUKIN 1 (IL1)

The IL1 family consists of 11 members, 7 of which have been demonstrated to have broad pro-inflammatory activity (IL1α, IL1β, IL18, IL33, IL36α, IL36β and IL36γ) while the remaining 4 have antagonistic (IL1Ra, IL36Ra, IL38) or anti-inflammatory (IL37) properties (Barbier et al., 2019). IL1α and IL1β play pivotal roles in the developing of inflammatory responses that can degenerate in severe diseases, such as fibrosis, chronic diseases and cancer. In the extracellular environment, IL1α and mature IL1β bind to their specific receptor (IL1R1) to initiate downstream signaling in several cell types. It has been shown that some chemical substances, such as asbestos and silica, can stimulate the activation and secretion of IL1β (Hornung et al., 2008; Dostert et al., 2008). The pathway involved in this stimulation leads to the accumulation of collagen in lung tissue, thus representing one of the initial events of lung fibrosis (Dostert et al., 2008). Similarly, tobacco smoke has been shown to cause heightened systemic IL1 production in blood mononuclear cells and to stimulate local IL1 responses by bronchial epithelial cells as well (Zeidel et al., 2002). Interestingly, IL1 release has been found to be higher in smokers with

COPD compared to smokers with normal pulmonary function, suggesting that smokers who develop COPD may be particularly susceptible to tobacco smoke-induced inflammatory responses, including IL1 release (Rusznak et al., 2000).

As previously said, non-resolved inflammation can drive genetic events that lead to carcinogenesis. Such events orchestrate the construction of an inflammatory microenvironment, whose intrinsic pattern is strictly linked to cancer promotion (Mantovani, 2004). IL1 has been associated to both pathways in animal and human studies (Mantovani et al., 2018).

In a model of epithelial carcinogenesis, IL1α has been shown to be downstream of Ras activation and to be an essential driver for the activation of NFκB–regulated genes, including cytokines and chemokines required for the establishment of a pro-tumoral microenvironment. In addition, IL1α is involved in the suppression of keratinocyte differentiation markers, leading to neoplastic transformation in a cell-autonomous manner (Cataisson et al., 2012).

In general, IL1 affects multiple aspects of the tumor microenvironment. The mechanisms involved in tumor progression included the stimulation of angiogenesis and induction of endothelial cell adhesion molecules recognized by tumor cells. IL1 activates endothelial cells in a prothrombotic/proinflammatory direction by inducing procoagulant activity and inducing expression of adhesion molecules and inflammatory cytokines (Mantovani et al., 2018). Moreover, IL1 induces in endothelial cells and surrounding stromal cells the production of proangiogenic cytokines such as IL8 (Mantovani et al., 2018).

3.1.2 TUMOR NECROSIS FACTOR α (TNF-α)

TNF-α is a strong pro-inflammatory cytokine, which plays an important role in the immune system during inflammation, cell proliferation, differentiation and apoptosis. Although macrophages and T-cells are thought to be the main producers of TNF-α, other cells can also produce this cytokine, such as B cells, NK-cells, neutrophils, mast cells, endothelial cells, smooth muscle cells, cardiomyocytes, fibroblasts, osteoclasts, osteoblasts, astrocytes, dendritic cells, microglial cells, keratinocytes, adipocytes, adrenocortical cells, and glomerular mesangial cells (Bradley 2008; Lin et al., 2000). It has been determined that cells never create reserves of TNF-α, but stimulation triggers de novo synthesis of this cytokine. Transcriptional, translational, and post-translational regulation mechanisms are involved in TNF-α expression. Chromatin modifications also influence the transcription of TNF-α mRNA (Zelová and Hošek, 2013). Negative feedback is another regulatory mechanism, which has an important role during the biosynthesis of TNF-α. TNF-α itself increases the synthesis of anti-inflammatory factors, such as IL10, corticosteroids, or prostanoids, which are able to negatively regulate its expression (Zelová and Hošek, 2013).

TNF-α plays a key role in several phases of inflammation. It enhances the vasodilatation activity by increasing the production of prostanoids (Mark et al., 2001). Vasodilatation facilitates the penetration of inflammatory mediators and cells into the target tissue, where leukocyte subsequently migrate through the characteristic multiphasic process that includes migration, rolling, adhesion of leukocytes to the endothelium, and chemotaxis to the target site. Specific endogenous molecules such as selectins and integrins drive each of these steps. TNF-α finely regulates the

expression of these molecules on the surface of specific immune cells (Chandrasekharan et al., 2007; Mommsen et al., 2011).

As for IL1, TNF-α is a key molecule in the mediation of inflammatory process to tumor promotion, although its role is paradoxical. According to its name, high-dose local administration of TNF-α has a powerful tumor-necrosis activity, while low-dose chronic production may act as endogenous tumor promoter participating in all steps of tumorigenesis, including cellular transformation, proliferation, growth, invasion, angiogenesis, and metastasis (Szlosarek et al., 2006; Balkwill, 2002; Aggarwal et al., 2006).

3.2 CHEMOKINES

Chemokines are a large family of low-molecular weight polypeptides involved in the migration of inflammatory cells. Their receptors are thought to direct T-lymphocyte homing to the lung respiratory tract. Chemokines have chemotactic and activating effects on leukocyte subsets, and provide a key stimulus for directing leukocytes to areas of injury (Puneet et al., 2005; Bhatia and Moochhala, 2004). Based on cysteine residue positioning, chemokines are classified into four subfamilies: CXC (α); CC (β); C (γ); and CX3C (δ).

CXC chemokines (α subfamily) have a single amino acid residue interposed between the first two canonical cysteine. Some CXC chemokines, of which IL8 (CXCL8) is the prototype, attract polymorphonuclear leukocytes to sites of acute inflammation. CXCL8 also activates monocytes and may direct the recruitment of these cells to vascular lesions (Gerszten et al., 1999; Huo et al., 2001).

Chemokines C, which have only two cysteine residues, are specific for lymphocytes. Only one C chemokine, lymphotactin, has been identified (Nussenblatt et al., 2010).

The δ subfamily is the CX3C family, of which fractalkine (CX3CL1) is the only member (Charo and Ransohoff, 2006). This chemokine exists in two forms: one is fused on cellular surface and is induced by inflammatory cytokines thus promoting the adhesion of monocyte and lymphocyte T, the other is present as soluble form and have a strong chemotactic effect.

The CC chemokine subfamily (β-subfamily) has the first two NH_2-terminal cysteines adjacent to one another with no intervening amino acid, the CC cysteine motif (Puneet et al., 2005). Target cells for CC chemokines are believed to be eosinophils, T cells, and monocytes, although recent studies have shown that these chemokines also contribute to neutrophil infiltration (Bhatia et al., 2005; He et al., 2007). Chemokines perform a variety of functions aside from chemotaxis, including T helper cell differentiation and function, as well as angiogenesis (Turner et al., 2014).

Macrophage inflammatory protein-1α (MIP-1α, also known as CCL3) is a member of the CC chemokine family. CCL3 and related CC chemokines such as CCL4 and CCL5 are classified as inflammatory chemokines because of their ability to induce chemotactic mobilization of monocyte-lineage cells and lymphocytes into inflammatory tissues. CCL3 also regulates the proliferation of hematopoietic stem/progenitor cells (HSPCs) in the bone marrow (BM) (Baba et al., 2014). Intriguingly, CCL3 inhibits the proliferation of primitive progenitor cells but activates the proliferation of more mature progenitor cells, (Verfaillie and Catanzarro, 1994) and can maintain a quiescent status in HSCs by blocking cell cycle entry. Thus, CCL3 potentially contributes to hematopoietic regulation in physiologic and pathologic conditions (Baba et al., 2014).

CHAPTER 4

MATERIALS AND METHODS

4.1 ELECTRONIC CIGARETTE

A commercially available Eleaf Pico e-cig consisting of a 2.5 mL liquid tank made of Pyrex glass and a rechargeable lithium battery (MXJO IMR 18650 3000 mAh 35A 3.7 V High Drain Flat Top Rechargeable Battery) was used for all studies (**Figure 3**). The voltage value was set at 3.5 V and two different coils (Joyetech™, 1.5 Ω and 0.25 Ω) were used to obtain a total wattage of 8±2 W and 40±5 W, respectively. In order to prevent the confounding effect of coil aging, a new element was used for each experiment.

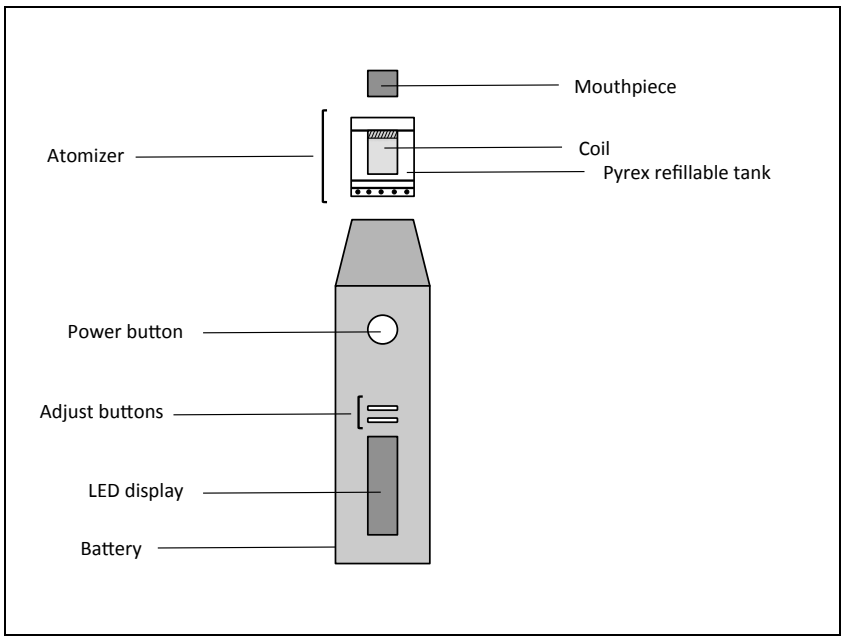

Figure 3: Schematic representation of e-cig device with interchangeable coils.
(Cirillo et al., 2019)

4.2 IQOS®

IQOS® device (2.4 version), produced by Philip Morris International (PMI), was purchased from an authorized shop in Bologna. All IQOS® devices are composed by the same components and work in the same way. Briefly, after inserting the tobacco units in the holder, it is activated by a power button that allows the heating of a platinum-coated blade. The blade simultaneously heats the tobacco stick to temperatures up to 350 °C. In this way, the user can inhale the vapor directly from the tobacco stick. The holder supplies heat to the heated stick for six minutes or 14 puffs, whichever comes first.

4.3 TOBACCO HEETS

Tobacco sticks are called Heets. Tobacco material and three filters compose sticks. The biopolymer film filter (folded film inside the filter chamber) is made of polylactic acid; the filter mouthpiece is made of cellulose acetate, which is similar to a cigarette filter. The tubing, the polymer film filter and the tobacco pad are wrapped in the refill paper and attached to the filter pad by the cartridge paper. Under the Heets there is an aluminum foil designed to prevent ignition of tobacco. PMI produces several types of Heets that vary on the basis of taste intensity, content of nicotine and the flavor. In this experiment the variant Bronze was used.

4.4 E-LIQUIDS

The investiagtions to determine carbonyl compounds in e-cig aerosols employed a PG/VG base solution (50/50, v/v) (Fumador S.r.l., Milan, Italy) without nicotine (eL-N) and with nicotine (18%; eL+N). A red fruits flavor concentrate (Chemfont S.r.l., Rome, Italy) was then added to a final

concentration of 10% (*v/v*). For the studies examining ROS production and the effects on cell viability, the e-cig liquid was composed of a PG/VG base (50/50, *v/v*) (NicVape, USA) without nicotine to which a raspberry flavor concentrate (NicVape, USA) was added at a concentration of 10% (*v/v*).

4.5 DETECTION OF CARBONYL COMPOUNDS: FORMALDEHYDE, ACETALDEHYDE AND ACROLEIN

To establish the presence of formaldehyde, acetaldehyde and acrolein, a 30-L propylene box was filled using the following puff profile: puff on 6 s, puff off 5 s; the puffing sequence was repeated twice (Goel et al., 2015; Canistro et al., 2017; Cardenia et al., 2018). Formaldehyde, acetaldehyde and acrolein were determined by headspace-solid phase microextraction (HS-SPME) coupled to gas chromatography-mass spectrometry (GC/MS), as reported in our previous study (Canistro et al., 2017) with some modifications. A SPME device having a fused-silica fiber (10-mm length) coated with DVB/CAR/PDMS (50/30 mm thickness) was used. After conditioning at 270 °C for 60 min, the SPME fiber was exposed to the box headspace at room temperature. After a 2-min exposure, the fiber was desorbed at 250 °C for 10 min in the injector of the GC/MS system (Q2010 Plus, Shimadzu, Japan). The sample was injected into a RTX-WAX column (30 m, 0.25 mm i.d., 0.25 µm film thickness, Restek, USA) in split mode (1:20 split ratio). Helium was used as carrier gas with a linear velocity of 36.2 cm/sec. The oven temperature was kept at 35 °C for 10 min, then raised to 240 °C at 30 °C/min. Injector and interface temperatures were set at 250 and 230 °C, respectively. Compounds were recognized by comparing their mass spectra and retention time with those of the corresponding chemical standards. The quantification of formaldehyde, acetaldehyde and acrolein signal was carried out by Single

Ion Monitoring (SIM), using 29 m/z, 44 m/z and 56 m/z, respectively. The construction of the calibration curves in this case could not provide reproducible results, due to the difference of vapor pressure of carbonyls when used alone or in presence of other compounds (Liu et al., 2016). Therefore, as suggested in literature (Wang et al., 2017; Geiss et al., 2016), a normalized response factor (Rf) was calculated based on the concentration of carbonyls present in the environment as basal level, according to the following expression:

$$Rf = (A_x - A_y)/A_y$$

where A_x and A_y represent the peak areas of carbonyls detected after and before (basal) the vaping process in the exposure box, respectively.

4.6 CELL-FREE ROS

The ROS production was estimated using the dye 2',7'-dichlorodihydrofluorescein diacetate (DCFH-DA), as previously reported by Lerner et al. (Lerner et al., 2015a). To catalyze the reaction between DCFH and ROS, horseradish peroxidase (HRP) was added. Vapor was pulsed into the bubbler (Ace Glass Inc., Vineland, NJ) at room temperature using the following puffing topography: puff on 4 s, puff off 26 s, flow rate 1.5 L/min; this puffing sequence was repeated 15 times, for a total time of exposure of 7.5 min (total number of puffs: 15). The oxidized dichloro-fluorescein (DCF) fluorescence was measured using a Fluroskan Ascent FL spectrofluorometer (Thermo Fisher Scientific Inc., Waltham, MA) at absorbance/emission maxima of 485 nm/535 nm. H_2O_2 standards were used to calibrate the fluorescence intensity units (FIU) and DCF fluorescence data are expressed as μM of H_2O_2 equivalents. The assay was

conducted using both phosphate buffer (PBS) and cell medium as reaction mixture.

4.7 AIR-LIQUID INTERFACE (ALI) CELL CULTURE AND EXPOSURE

H1299 human lung adenocarcinoma cells were purchased from ATCC (Manassas, VA). The cells were cultured in RPMI 1640 basal media supplemented with 10% fetal bovine serum, 1% penicillin and 1% streptomycin at 37 °C under a 5% CO_2 atmosphere. Before aerosol exposure, cells were plated in 60-mm dishes and grown to 50-70% confluence. Cells were then exposed to air or e-cig vapor in a modified vacuum desiccator (500 mL volume, SP Scienceware, Warminster, PA) using the following puffing topography: puff on 4 s, puff off 26 s, flow rate 15 L/min; this puffing sequence was repeated 15 times, for a total time of exposure of 7.5 min (total number of puffs: 15). In addition to the analytical needs, this topography was also more representative of the real human use of e-cig and allowed us to reinforce the correlation between our results and the actual health risks for e-cig consumers (Norton et al., 2014; Robinson et al., 2015). This treatment protocol was repeated once after 2 h. Cells were exposed to a total number of 30 puffs.

4.8 CELL VIABILITY MEASUREMENT

The 3-(4,5-dimethylthiazol-3-yl)-2,5-diphenyl tetrazolium bromide (MTT) assay (Cat# M5655, Sigma Aldrich, St. Louis, MO) was used to assess cell viability 24 h after e-cig vapor exposure. Briefly, after 24 h exposure, H1299 cells were washed twice with PBS and then incubated with MTT (1 mg/mL) in RMPI 1640 medium at 37 °C for 30 min. The medium was

then removed and dimethyl sulfoxide (DMSO) was added to solubilize the formazan dye; the absorbance was measured at 550 nm using a Multiskan GO microplate spectrophotometer (Thermo Fisher Scientific Inc., Waltham, MA). The viability of cells exposed to e-cig vapor was normalized to the viability of air-exposed cells.

4.9 ANIMAL CARE AND EXPOSURE

The EU Directive (2010/63/EU) guidelines were followed during the entire experiment. The experimental protocol was approved by the Committee on the Ethics of Animal Experiments of the University of Bologna and by the Italian Ministry of Health (Permit number 26832015). The Animal Welfare Committee monitored the proceedings to ensure that all efforts have been made to minimize animal suffering.

4.9.1 E-CIG EXPOSURE

Thirty male Sprague Dawley rats (ENVIGO RMS S.r.l., San Pietro al Natisone, Udine, Italy), 7 weeks old, were housed under standard conditions (12 h light-dark cycle, 22 °C, 60% humidity). Animals had continuous access to water and chow throughout the experiment. After one week of acclimatization, animals were randomly divided into three experimental units: a control group (10 rats), and two treated groups (1.5 Ω and 0.25 Ω) composed by 10 rats each. The treated groups were exposed to the vapor generated by the e-cigarettes (see section 2.2 for details on device settings) for 28 days, as previously reported by Canistro et al. (Canistro et al., 2017) with some modifications. The whole body exposure consisted of 11 cycles of two puffs (6 sec on; 5 sec off; 6 sec on), followed by 20 min of recovery. At the end of each cycle, the animals were moved to a clean

chamber. Five animals were placed in each inhalation chamber, which consisted of a propylene box with a capacity of 30 L. E-cig treated animals were subjected to the procedure for 3 h/day. The levels of O_2, N_2 and CO_2 were monitored by GC/MS to establish safe O_2/N_2 and CO_2/O_2 ratios.

4.9.2 IQOS® EXPOSURE

Twenty male Sprague Dawley rats (ENVIGO RMS S.r.l., San Pietro al Natisone, Udine, Italy), 7 weeks old, were housed under standard conditions (12 h light-dark cycle, 22 °C, 60% humidity). Animals had continuous access to water and chow throughout the experiment. After one week of acclimatization, animals were randomly divided into two experimental groups: IQOS® exposed group and control. Treatment followed the e-cig procedure with some modifications. Treated rats were placed in a home-made exposure chamber having a capacity of 7 L. Two animals per cage were exposed to a total of 8 Heets/day. After the vaporization of each Heets, the chambers were opened and cleaned before starting a new cycle.

4.10 TISSUE COLLECTION

After 24 h from the last exposure, blood was collected from the tail vein. Samples were stored in K_2 EDTA tubes at 4 °C until DNA unwinding assay.

Animals were anesthetized with Zoletil 100 (100 mg/kg b.w.) and sacrificed by decapitation according to the Italian Ministerial guidelines for the species. Lung and liver were removed, immediately frozen into liquid nitrogen, and stored at -80 °C. Lung was homogenized in 150 nM NaCl, 1 mM EDTA, 1% Triton-X, and 20 mM TRIS-HCl pH 7.4, by using a IKA

Ultra-Turrax homogenizer. The homogenate was then centrifuged at 9,000 g for 15 min at 4 °C and the supernatant was collected, which from now on will be labelled as S9 fraction. The cytosolic and microsomal fractions were obtained according to previously reported procedures (Bonamassa et al., 2016).

4.11 PROTEIN CONCENTRATION

Protein concentration was determined according to the method described by Lowry et al. (Lowry et al., 1951), using bovine serum albumin as standard. Samples were properly diluted in order to reach a suitable protein concentration (Canistro et al., 2012).

4.12 ANTIOXIDANT ENZYMES

The following assays were performed on cytosol subcellular fraction from lung and/or liver tissues.

4.12.1 SUPEROXIDE DISMUTASE ACTIVITY (SOD)

The specific activity was assayed spectrophotometrically at 320 nm by monitoring the generation of adenochrome, one of the main products of epinephrine autoxidation at pH 10.2. The dejection of autoxidation was used to calculate SOD activity using the extinction coefficient of 4.02 per mM × cm, and expressed as mol of oxidized epinephrine per min per mg protein, derived by subtracting each test curve from the epinephrine autoxidation standard curve. Activity is expressed in nmol $mg^{-1}min^{-1}$.

4.12.2 NAD(P)H:QUINONE REDUCTASE (NQO1)

NQO1 activity was assayed spectrophotometrically at 600 nm by monitoring the reduction of the blue redox dye of DCPIP (ε = 9.6 mM^{-1} cm^{-1}), and expressed as mol of DCPIP reduced per min per mg protein. Activity is expressed in nmol $mg^{-1}min^{-1}$.

4.12.3 OXIDIZED GLUTATHIONE REDUCTASE ACTIVITY (GSSG-RED)

1.5 mM NADPH was added to 50 mM potassium phosphate buffer, 1 mM EDTA, cytosol sample and 20 mM GSSG. The generation of $NADP^+$ from NADPH due to the reduction of GSSG was recorded at 340 nm for 5 min at 37 °C. GSSG-red activity was calculated using the extinction coefficient of 6.22 per mM x cm, and expressed as mol of NADPH consumed per min per mg protein. Activity is expressed in nmol $mg^{-1}min^{-1}$.

4.12.4 GSH-PEROXIDASE (GSH-PX)

The specific activity was determined following the NADPH consumption at 340 nm for 5 min at 37 °C and expressed as nmol of NADPH consumed per min per mg of protein. All details have been previously reported (Melega et al., 2013). Activity is expressed in nmol $mg^{-1}min^{-1}$.

4.12.5 CATALASE (CAT)

30 mM H_2O_2 was added to the reaction mixture, constituted by 50 mM potassium phosphate buffer and cytosol sample. The decomposition of the substrate was measured at 240 nm and catalase expressed as mol of H_2O_2 consumed per minute per mg protein using a molar extinction coefficient of 43.6 mM^{-1} cm^{-1}. Activity is expressed in µmol mg^{-1} min^{-1}.

4.13 XENOBIOTIC PHASE-I ENZYMES

The following assays were performed on microsomal subcellular fraction from lung tissue; these assays had been previously described in detail by Cirillo et al. (Cirillo et al., 2016).

4.13.1 PENTOXYRESORUFIN O-DEALKYLASE (PROD) – CYP2B1/2, METHOXYRESORUFIN O-DEMETHYLASE (MROD) – CYP1A2 AND ETHOXYRESORUFIN O-DEETHYLASE, (EROD) – CYP1A1

For the reaction mixture (PROD, MROD, EROD), 0.025 mM $MgCl_2$, 200 mM pentoxyresorufin, 5 mM methoxyresorufin and 1.7 mM ethoxyresorufin respectively were mixed with 0.32 mg of proteins and 130 mM NADPH in 2.0 mL 0.05 M Tris-HCl buffer (pH 7.4). Resorufin formation at 37 °C was calculated by comparing the rate of the increase in relative fluorescence to the fluorescence of known amounts of resorufin (excitation 563 nm, emission 586 nm). Activity is expressed in pmol mg^{-1} min^{-1}.

4.13.2 AMINOPYRINE N-DEMETHYLASE (APND) – CYP3A1/2

A total incubation volume of 3 mL, composed of 0.5 mL water solution of 50 mM aminopyrine, 25 mM $MgCl_2$, 1.48 mL of 0.60 mM $NADP^+$, 3.33 mM G6P in 50 mM Tris-HCl buffer (pH 7.4), 0.02 mL G6PDH (0.93 U/mL) and 0.125 mL of sample was incubated for 5 min at 37 °C. The reaction of the released of CH_2O with the Nash reagent generated a yellow color that was read at 412 nm; the molar absorptivity of 8,000 was used for calculation. Activity is expressed in nmol mg^{-1} min^{-1}.

4.13.3 P-NITROPHENOL HYDROXYLASE (P-NPH) – CYP2E1

2 mM p-nitrophenol in 50 mM Tris-HCl buffer (pH 7.4), 5 mM $MgCl_2$, and a NADPH-generating system consisting of 0.4 mM $NADP^+$, 30 mM isocytrate, 0.2 U of isocytrate dehydrogenase and 1.5 mg of proteins were mixed in a total volume of 2 mL. After 10 min of incubation at 37 °C, 0.5 mL of 0.6 N perchloric acid was added to develop the reaction. Precipitated proteins were removed by centrifugation and 1 mL of the resultant supernatant was mixed with 1 mL of 10 N NaOH. Absorbance at 546 nm was immediately recorded and 4-nitrocathecol determined (ε = 10.28 mM^{-1} cm^{-1}). Activity is expressed in nmol mg^{-1} min^{-1}.

4.14 XENOBIOTIC PHASE-II ENZYMES

4.14.1 GLUTATHIONE S-TRANSFERASE (GST)

The incubation mixture consisted of 1 mM glutathione + 1 mM 1-chloro-2,4-dinitrobenzene (CDNB) in methanol + 0.025 mL of sample (cytosol subcellular fraction from lung tissue) in a final volume of 2.5 mL 0.1 M phosphate Na^+/K^+ buffer (pH 6.5). The product of the reaction was read at 340 nm (ε = 9.6 mM^{-1} cm^{-1}). Activity is expressed in nmol $mg^{-1}min^{-1}$ (Sapone et al., 2016).

4.14.2 UDP-GLUCURONOSYL TRANSFERASE (UDP-GT)

The specific activity in microsomal subcellular fraction from lung tissue was determined kinetically using 1-naphtol as substrate (final concentration, 50 mM) by the continuous fluorimetric (excitation 390 nm; emission 440 nm) monitoring of 1-naphtholglucuronide production in the presence of 1 mM uridine-5-diphosphoglucuronic acid. The sensitivity of the reaction was improved by performing the reaction in the presence or absence of Triton

X-100 (0.2%) as a detergent. Activity is expressed in nmol mg^{-1} min^{-1} (Vivarelli et al., 2016b).

4.15 XANTHINE OXIDASE (XO)

XO was spectrophotometrically measured in lung cytosol by quantifying the formation of uric acid at 290 nm. The reaction mixture contained 50 mM sodium phosphate buffer (pH 7.8), hypoxantine (50 μM final concentration) and it was incubated at 37 °C for 5 min. The reaction started with the addition of NAD^+ (Shintani, 2013). Activity is expressed in nmol mg^{-1} min^{-1}.

4.16 ROS CONTENT IN LUNG

2',7'-dichlorofluorescein diacetate (DCFH-DA) was used as a probe for the estimation of ROS content in S9 fraction. Samples were mixed with DCFH-DA (100 μM) at 37 °C for 30 min, and the reaction was then shut down by chilling (Kang et al. 2018). The formation of the oxidized break down product (2',7'-dichlorofluorescein, DCF) was monitored with a fluorescence spectrophotometer (488 nm excitation; 525 nm emission). DCF was quantified using a standard curve, as previously reported by Rodrigues Siqueira et al. (Rodrigues Siqueira et al., 2005) and expressed as molar concentration per mg of protein (nM DCF mg^{-1} protein).

4.17 PROTEIN CARBONYLATION

Protein carbonyl groups were measured as suggested by Levine et al. (Levine et al., 1994); the method is based on the reaction of carbonyls groups with dinitrophenyl-hydrazine (DNPH), to form a stable hydrazine that can be spectrophotometrically monitored at 390 nm. Samples (cytosol

from lung tissue) were prepared according as previously reported (Vivarelli et al., 2018). The results are expressed as nmol of carbonyl groups/mg protein.

4.18 FRAP ASSAY

Ferric Reductive Antioxidant Power (FRAP) was determined in plasma and lung tissues according to the procedure reported by Benzie and Strain (Benzie and Strain, 1996). Briefly, FRAP reagent (900 mL) containing 10 mM 2,4,6-tripyridyl-S-triazine in 40 mM HCl, 300 mM acetate buffer (pH 3.6) and 20 mM $FeCl_3$ was added to 30 µL of plasma or supernatant tissue. The absorbance change (at 593 nm) between the final reading and the blank was calculated for each sample and related to the absorbance of ferric standard solutions. Results are expressed in nmol Fe (III) 0.1 mL^{-1} plasma.

4.19 LIPID HYDROPEROXIDES (LOOHS) IN CELL MEMBRANES

Lipid hydroperoxides in cell membranes (red blood cells and tissue supernatant fraction S9) were estimated by performing FOX assay (Jiang et al. 1992). It is based on the rapid oxidation of Fe^{2+} to Fe^{3+} under acid condition and in the presence of xylenol orange dye. The Fe^{3+} -xylenol orange compounds can be spectrophotometrically monitored at 560 nm. 160 µL of sample were mixed with 840 µL of FOX reagent. The amounts of hydroperoxides were extrapolated by the use of a hydrogen peroxide standard curve. The results are expressed as µM of H_2O_2/mg of protein. Further details on the method can be found in Jiang et al. (Jiang et al., 1992). Results are expressed as µmol H_2O_2 mL^{-1} blood.

4.20 HAEMATOLOGICAL ANALYSIS

The haematological analyses were performed by the Central Laboratory of Clinical Pathology (CLINLAB) of the Department of Veterinary Medical Science (University of Bologna), according to standard methods certified by the Italian National Health Service.

4.21 GENE EXPRESSION STUDIES

4.21.1 NRF2 FUNCTIONAL ACTIVITY

Nrf2 function was evaluated by using Western Blot kit by Thermo Fisher. The analysis was conduced after protein extraction from lung tissue through T-PER Tissue Protein Extraction Reagent (T-PER™ Tissue Protein Extraction Reagent, Thermo Scientific, REF. 78510) and protein quantification (Pierce™ BCA Protein Assay Kit, Thermo Scientific). After gel electrophoresis the transferred nitrocellulose filter was incubated with primary antibody for Nrf2 Polyclonal Antibody (Thermo Fisher Scientific) and then with the secondary antibody (Gt anti-Rb IgG Secondary Antibody, Invitrogen). The filter membrane was then analyzed with ChemiDoc™ reader. The procedure was further repeated throuth incubation with anti-tubulin primary antibody (eBioscience™ Anti-a Tubulin, Invitrogen), the respective secondary antibody (Gt anti-Ms IgG Secondary Antibody, Invitrogen) and reading.

4.21.2 INFLAMMATION BIOMARKERS

Total RNA from lung tissue was isolated using Purelink RNA mini kit (Thermo Fisher Scientific, Waltham, MA, USA), according to manufacturer's recommendation. Briefly, lung samples were homogenized in lysis buffer containing 1% β-mercaptoethanol using a homogenizer

SHM1 (Stuart, Bibby Scientific LTD, Staffordshire, UK) and keeping samples on ice. Homogenized samples were added to an equal volume of 70% ethanol and mixed. The solution was passed through a filter cartridge, having a silica-based membrane that binds RNA. The filter was then washed once with Wash Buffer I and twice with Wash Buffer II (both provided by Thermo Fisher Scientific). RNA was finally eluted with RNase-free water and stored at − 80 °C. RNA samples were quantified using Nanoquant plate (Tecan, Männedorf. Switzerland) and i-control software (Tecan). For each sample, 400 ng of total RNA were reverse transcribed using the High Capacity cDNA Reverse Transcription kit (Thermo Fisher Scientific) with RNase inhibitor according to manufacturer's instructions. Briefly, 10 µL of each sample were added to 10 µL master mix and the mixture was subjected to the appropriate thermo cycling conditions. Finally, relative quantification was performed by real-time PCR (Bio-Rad CFX Connect, Bio-Rad, Hercules, CA, USA) using Universal Master Mix (Thermo Fisher Scientific) and Taqman gene expression assay (Thermo Fisher Scientific) for the following genes: IL1β (Rn00580432_m1), IL6 (Rn01410330_m1), TNFα (Rn99999017_m1), CCL3 (Rn00564660_m1), CCL4 (Rn00671924_m1), CSF2 (Rn01456850_m1), ALDH3A1 (Rn00694669_m1). GAPDH (Rn99999916_s1) and actin (Rn00667869_m1) were used as endogenous controls. Each measurement was performed in triplicate and data were analysed through the 2^-ΔΔCt methods (Livak and Schmittgen, 2001). Rats non-exposed to vapor from e-cig were considered the calibrator of the gene expression experiments.

4.21.3 CYP1A1

Total RNA was extracted form lung tissue by using Trizol reagent ((Life Technologies, CA, USA). Traces of genomic DNA were removed after

treatment with DNase and the obtained RNA was reverse transcribed using RevertAid™ First Strand cDNA Synthesis kit (Fischer Scientific, KS, USA). Levels of mRNA were analyzed by real-time PCR and normalized with the expression of β-actin mRNA, using the following primers:

- β -actin: F5′ -GGCGGCACCACCATGTACCCT-3′ ;

R5′ -AGGGGCCGGACTCGTCATACT-3′ ;

- CYP1A1: F5′ -CAAGAGGAGCTAGACACAGT-3′ ;

R5′ -AGCCTTTCAAACTTGTGTCT-3′ ;

4.22 SCANNING ELECTRON MICROSCOPY (SEM)

Lung and tracheal samples from control and treated animals were dissected and immediately washed in 0.1 M phosphate buffer, to remove blood or any other contaminant. Tissues were fixed with 2.5% glutaraldehyde in 0.1 M phosphate buffer pH 7.2–7.4 for 1 h, post-fixed with 1% osmium tetroxide (OsO_4) in the same buffer for 2 h and, finally, dehydrated with graded ethanol (50-100%, 5 min each). Critical point dried specimens were mounted on aluminum stubs. After 10 nm, gold sputter-coated samples were examined with a Philips SEM at 20 kV (Burattini et al., 2016).

4.23 TRANSMISSION ELECTRON MICROSCOPY (TEM)

Tissues were immediately washed and fixed with 2.5% glutaraldehyde in 0.1 M phosphate buffer for 1 h, post-fixed in 1% OsO_4 for 1 h, alcohol dehydrated and embedded in araldite, as reported by Salucci et al. (Salucci et al., 2017). For ultrastructural analysis thin sections were stained with uranyl acetate and lead citrate and observed with an electron microscope at 80 kV.

4.24 ELECTRON PARAMAGNETIC RESONANCE (EPR)

Immediately before measurement, the frozen lung tissues were dissolved in a physiological solution containing the hydroxylamine "spin trap" bis(1-hydroxy-2,2,6,6-tetramethyl-4-piperidinyl)-decandioate dihydrochloride, which was synthesized in our laboratory, and warmed for 5 min at 37 °C. The samples obtained were transferred and sealed in a calibrated capillary glass tube, which was placed inside the thermostated cavity (at room temperature) of a Bruker ESP 300 EPR spectrometer (Bruker Biospin S.r.l., Rheinstetten, Germany) equipped with a nuclear magnetic resonance gaussmeter for field calibration, a Bruker ER 033M FF-lock (Bruker Biospin S.r.l.) and a Hewlett-Packard 5350B microwave frequency counter (Hewlett Packard, Houston, TX, USA). The actual amount of solution analyzed was chosen so as to cover the entire sensitive area of the instrument cavity. The spectra of the nitroxide radical, generated by the reaction of the probe with the radicals produced in the tissues, were then recorded using the following instrumental settings: modulation amplitude = 1.0 G; conversion time = 163.84 ms; time constant = 163.84 ms; modulation frequency 100 kHz; microwave power = 6.4 mW. e intensity of the rst spectral line of the nitroxide (aN = 16.90 G and g = 2.0056) was used to obtain the relative amount of nitroxide in each examined samples. The calibration of the spectrometer response was done by using a known solution of TEMPO-coline in water and an ER 4119HS Bruker Marker Accessory as internal standard. The hydroxylamine probe solution was prepared following procedure by Vivarelli et al. (2016).

4.25 8-HYDRO-2-DEOXYGUANOSINE (8-OHDG) ASSAY

Guanosine oxidation to 8-OHdG was measured in plasma and lung tissue by employing DNA/RNA Oxidative Damage (High Sensitivity) ELISA Kit (Caymann chemical; Item No. 589320).

DNA from lung tissue was extracted using QIAmp® DNA Investigator Kit (50) (Quiagen; Cat. No. 56504) and used after digestion with DNA Degradase Plus ™ (Cat. No. E2020).

4.26 STATISTICAL ANALYSES

Data referred to as carbonyls compounds are expressed as mean ± standard deviation (SD) of three independent replicates (n=3) and analyzed by means of one-way ANOVA to evaluate the influence of different conditions tested ($p<0.05$). Data referred to as DCFH-DA assay in PBS (vapor condensate and air-liquid interface) are expressed as mean ± standard deviation (SD) of six independent replicates. For DCFH-DA assay in cell medium, results are indicated as relative percentage of the ROS content in control samples arbitrarily set at a value of 100% (mean ± SD of six independent replicates). Cell viability determined by MTT assay is expressed as percentage variation of viable cells relative to control group arbitrarily set at 100% (mean ± SD of six independent replicates). One-way ANOVA, followed by Tukey's multiple comparison test, was carried out at a 95% confidence level ($p \leq 0.05$), to separate means of parameters that were statistically different.

For data referring to the in-vivo study, if not differently specified, results are expressed as mean ± standard deviation (SD) on six independent replicates (n=6) and analyzed by means of one-way ANOVA, followed by Tukey's multiple comparison test. The test was carried out at a 95% confidence level ($p \leq 0.05$), to separate means of parameters that were statistically

different. For gene expression analysis, the set of treatments was compared against a single control mean, by using a one-way ANOVA followed by Dunnet test.

CHAPTER 5

RESULTS

5.1 FORMALDEHYDE, ACETALDEHYDE AND ACROLEIN LEVELS

In general, eL-N generated higher levels of carbonyls than eL+N. Among aldehydes, formaldehyde was the most produced in both liquids, followed by acetaldehyde and acrolein; however, the observed concentrations of carbonyls were strictly related to both the composition of liquids and the resistance value. For eL-N, acrolein, acetaldehyde and formaldehyde levels generated by 0.25 Ω coil were three- to seven-fold higher than those generated by the 1.50 Ω coil (**Figure 4A**). In contrast, the carbonyl content was higher with the 1.50 Ω coil compared to 0.25 Ω coil when eL+N was used. **Figure 4B** shows that when the eL+N was used, the 1.50 Ω coil resulted in the highest generation rate of carbonyls, especially formaldehyde, which was significantly ($p<0.05$) higher than acetaldehyde and acrolein; however, the latter was not significantly affected by the resistance value. Since the eL-N led to the highest production of hazardous carbonyls, an eL-N was chosen for subsequent ROS generation and cell viability experiments.

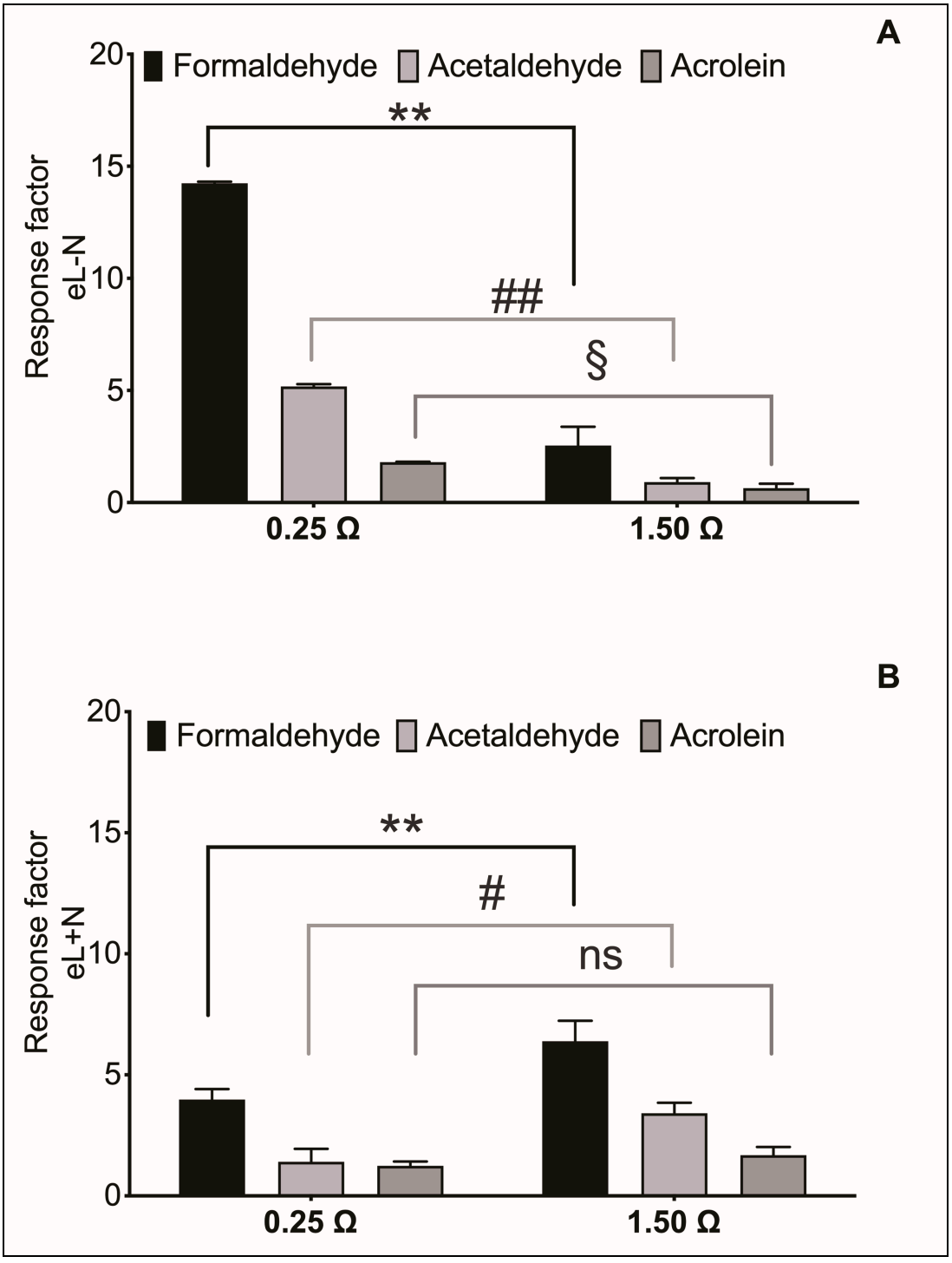

Figure 4. Effects of resistance value (0.25 Ω and 1.5 Ω) on formaldehyde, acetaldehyde and acrolein levels in vapors released by eL-N (without nicotine) (A) and eL+N (with nicotine) (B).

Data represent mean ± SD of three independent replicates.

** $p<0.01$. Significant difference in formaldehyde levels between 0.25 Ω e 1.50 Ω

# $p<0.05$; ## $p<0.01$. Significant difference in acetaldehyde levels between 0.25 Ω e 1.50 Ω

§ $p<0.05$. Significant difference in acrolein levels between 0.25 Ω e 1.50 Ω

5.2 ROS LEVELS GENERATED BY E-CIG VAPOR

ROS levels generated by e-cigs were determined by collecting vapor in PBS and measured in both the bubbler (vapor condensate) and at the ALI using the exposure chamber described above. Results obtained by analyzing the vapor condensate (**Figure 5a**) showed more than six-fold higher levels of ROS in samples obtained with the 0.25 Ω coil compared to air control, and about three-fold higher if compared with 1.5 Ω ($p<0.01$). The same trend was found when ROS levels were measured at the ALI (**Figure 5b**).

To determine if e-cig vapor produced ROS under cell culture conditions, the DCFH-DA assay was conducted using cell media as solvent under the experimental conditions mentioned previously. In both the bubbler and the ALI exposure chamber, the results followed the same trend as those obtained with PBS. The 0.25 Ω coil produced significantly higher levels of ROS when compared to control in both experimental conditions (+82.9%, $p<0.001$ in vapor condensate; +46.3%, $p<0.05$ in ALI) (**Figure 5c** and **5d**). When compared to the control, the 0.25 Ω coil produced increased ROS levels: 143.9% in condensate ($p<0.0002$) and 136.2% in air-liquid interface ($p<0.0001$) (**Figure 5c** and **5d**).

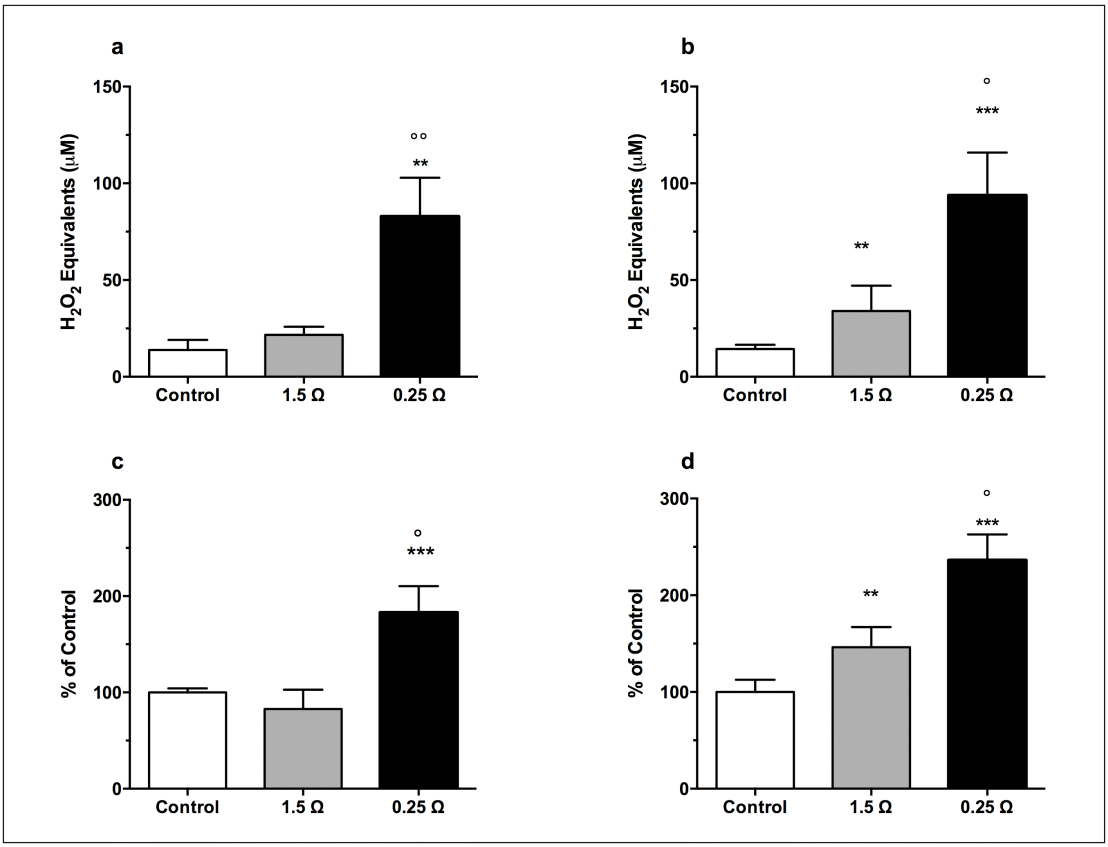

Figure 5. **Effect of resistance values on ROS levels in e-cig vapor.**
Fresh air control and e-cig vapor were pulsed through DCFH-HRP ROS indicator solution in (**a, b**) phosphate buffer and (**c, d**) cell culture media in (**a, c**) vapor condensate and (**b, d**) the ALI during a 7.50 min exposure. Data represent mean ± SD of six independent replicates.
**p<0.01; ***p<0.0002 significant results between 1.5 Ω/0.25 Ω groups and control group using one-way ANOVA (Tukey's multiple comparison test).
°p<0.05; °°p<0.01 significant results between 0.25 Ω and 1.5 Ω group using one-way ANOVA (Tukey's multiple comparison test).

5.3 CELL VIABILITY

H1299 cell viability was measured 24 h after exposure in the experimental chamber. Results from the MTT assay (**Figure 6a**) showed that cell survival was inversely related to the total wattage of the devices. The effect of the 1.5 Ω coil group (10% reduction) had borderline statistical significance (p=0.058). Cell viability decreased to 45.8% (p<0.0001) when cells were exposed to the vapor generated by using the 0.25 Ω coil. Cell viability was observed to be inversely correlated to ROS production in cell medium revealed in the exposure chamber (**Figure 6b**).

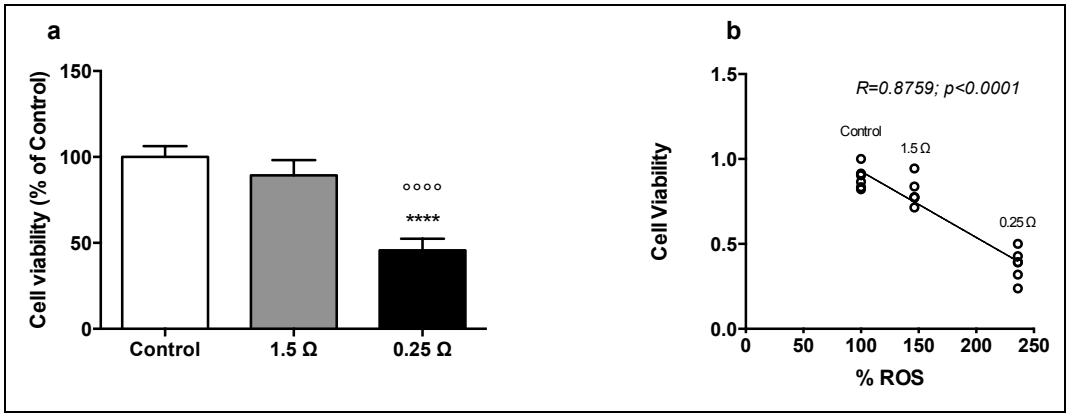

Figure 6. **Relationship between cell viability, coil resistance and ROS generation.**
(**a**) Effect of vapor generated from e-cigs equipped with 1.5 Ω and 0.25 Ω coils on viability of H1299 cells by MTT assay. Data are expressed as percentage relative to viable cells in control arbitrarily set at a value of 100%. Data represent mean ± SD of six independent replicates. **p<0.01; ***p<0.0002 significant results between 1.5 Ω/0.25 Ω groups and control group using one-way ANOVA (Tukey's multiple comparison test).
°p<0.05; °°p<0.01 significant results between 0.25 Ω and 1.5 Ω group using one-way ANOVA (Tukey's multiple comparison test). (**b**) Cell viability in each group inversely correlates vs ROS generation (R=0.8795; p<0.0001).

5.4 ANTIOXIDANT PROFILE AND OXIDATIVE STRESS

A general imbalance of the antioxidant pattern of exposed animals compared to controls is shown in **Figure 7**. Overall, 1.5 Ω group presented the mildest perturbations, whose magnitude became higher after exposure to e-cig vapor generated by the 0.25 Ω coil. This scenario was evident in the pulmonary glutathione reductase (GSSG-red; +156%, p<0.01) and catalase (CAT; -64%, p<0.01) (**Fig. 7a**). The suggested oxidative stress status, due to the strong induction of GSSG-red, was coupled with the opposite behavior of conjugated phase-II glutathione S-transferases (GST) and UDP-glucuronyl-transferase (UDPGT), which are significantly reduced in 1.5 Ω exposed rats but increased in 0.25 Ω group (**Fig. 7b**). To explain the trend of phase II enzymes, the expression of Nrf2, whose target genes are both UDPGT and GST, was evaluated. **Figure 7c** shows the decreased Nrf2 expression in 1.5 Ω group compared to control and 0.25 Ω one. On the other hand, the levels of total glutathione in the lung tissue show an

increasing trend, which is inversely proportional to the resistance value (**Figure 7d**).

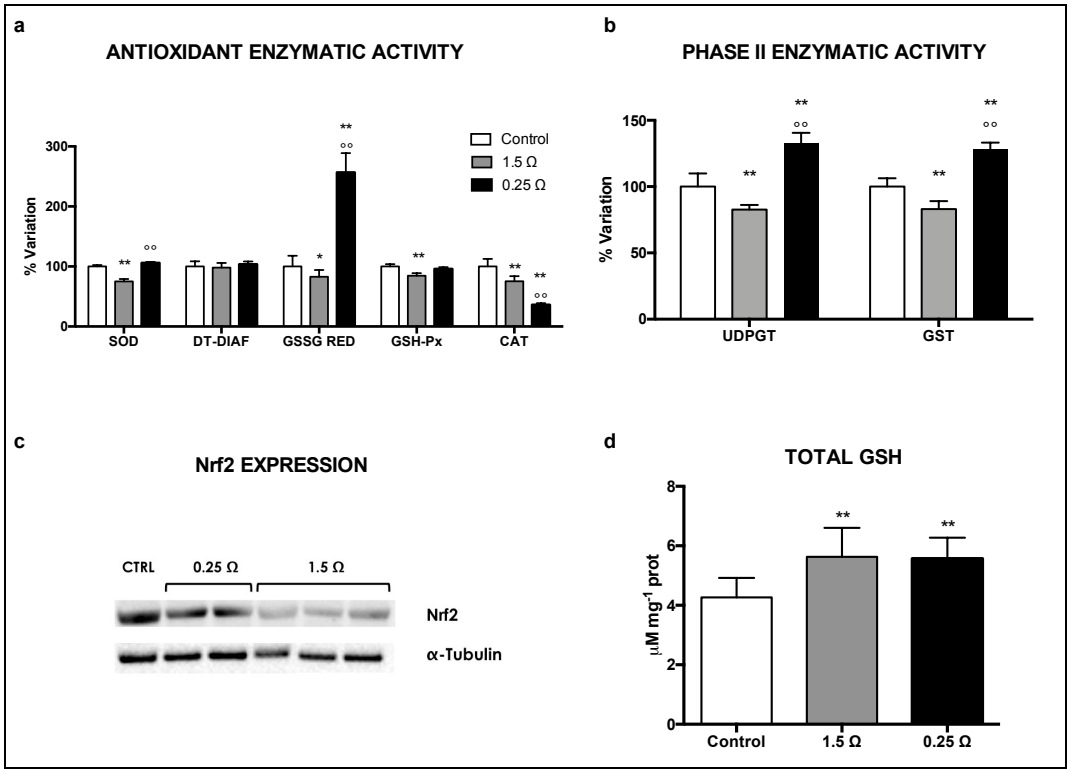

Figure 7. Pulmonary pro-oxidative effects of vapors generated from e-cig equipped with 1.5 Ω or 0.25 Ω coils.
(a) Pulmonary antioxidant enzymes, (b) Phase II enzymes in lung, (c) Nrf2 gene expression, (d) total glutathione content in lung.
(a), (b) Data expressed as percentage variation (mean ± SD of six independent replicates from ten rats) compared to control group arbitrarily set at 100%.
(d) Data expressed as mean ± SD of six independent replicates. Results were analysed by means of one-way ANOVA, followed by Tukey's multiple comparison test.
*p<0.05; **p<0.01 significant results between 1.5 Ω /0.25 Ω groups and control group.
°p<0.05; °°p<0.01 significant results between 0.25 Ω and 1.5 Ω group.

Since the antioxidant enzymatic machinery appeared altered in exposed groups, we investigated the putative ROS sources. Among these, we found in the lung that XO was up-regulated proportionally to the total wattage of the device (**Fig. 8a**). We also hypothesized that changes in cytochrome P450 (CYP) catalytic cycle could be involved in ROS generation and pulmonary toxicity (**Fig. 8b**). We found the higher and biologically significant increase in 0.25 Ω group for both CYP 1A1 (up to 470 %

compared to control, $p<0.01$) and CYP 2E1 (up to 196% vs. control, $p<0.01$).

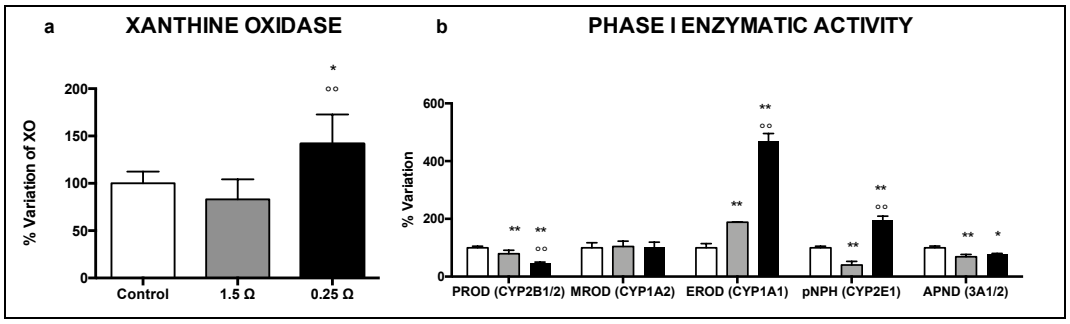

Figure 8. Pulmonary pro-oxidative effects of vapors generated from e-cig equipped with 1.5 Ω or 0.25 Ω coils.
(a) Xanthine oxidase activity in lung, (b) Phase I antioxidant enzymes in lung.
Data expressed as percentage variation (mean ± SD of six independent replicates from ten rats) compared to control group arbitrarily set at 100%.
*p<0.05; **p<0.01 significant results between 1.5 Ω /0.25 Ω groups and control group.
°p<0.05; °°p<0.01 significant results between 0.25 Ω and 1.5 Ω group.

To evaluate if the boost of free radicals was involved in the pulmonary oxidative stress status (OSS), the ROS levels were measured in lung by using DCFH-DA fluorescent probe. **Fig. 9a** shows a ROS increment (about 1.5-fold) in 1.5 Ω exposed group compared to control and 2-fold increase in 0.25 Ω one. Largely used as an oxidative stress biomarker, carbonyl residues in pulmonary proteins were measured (**Fig. 9b**). A slight but statistically significant increasing trend was reported in exposed animals, with an inverse correlation between the carbonylated proteins amount and the coil resistance applied to the device. However, even if statistically significant, the biological meaning of these variations cannot be considered relevant. To examine whether these phenomena affect the antioxidant power at systemic level, we measured the antioxidant capacity using the FRAP approach. Data referred to FRAP in plasma are reported in **Fig. 9c** and show how the antioxidant power was significantly reduced in rats exposed to vapor from 1.5 Ω e-cig compared to control. Animals exposed to 0.25 Ω e-cig vapor presented a non-significant perturbation if

compared to both 1.5 Ω and control group. On the contrary, data referred to hydroperoxide level in erythrocyte membranes (**Fig. 9d**) show a slight but significant increment only in 0.25 Ω group.

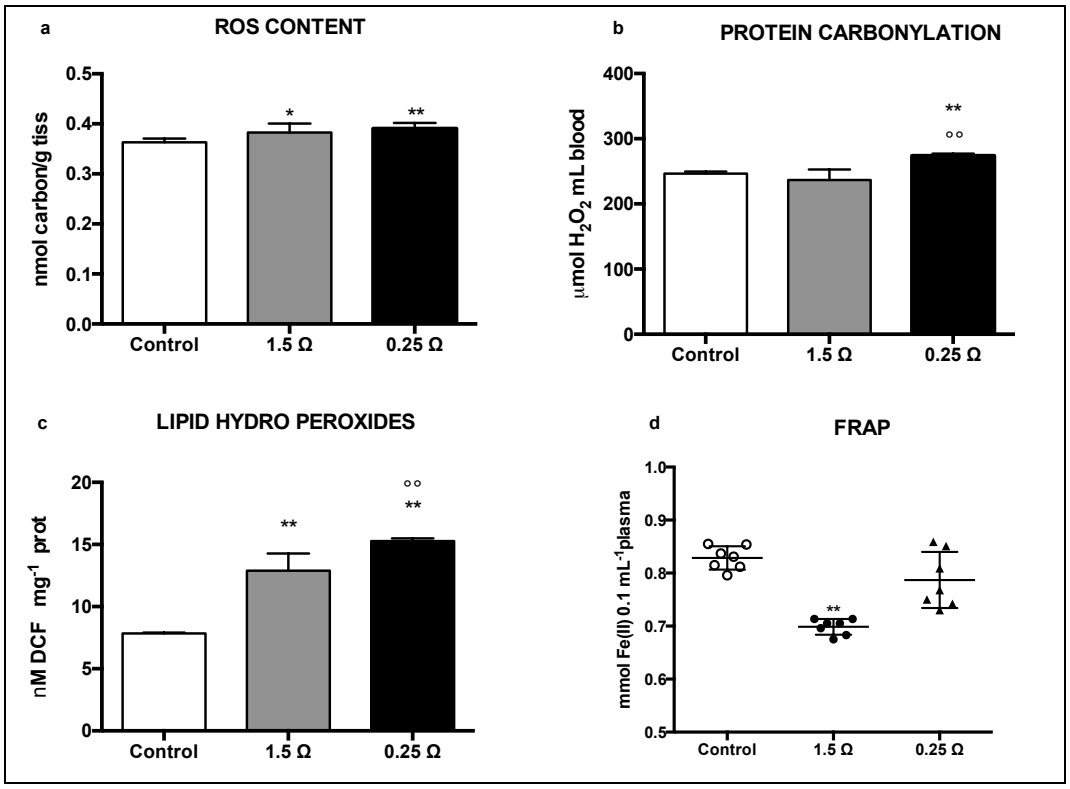

Figure 9. Pro-oxidative effects of vapors generated from e-cig equipped with 1.5 Ω or 0.25 Ω coils.

(a) ROS levels in lung revealed by using DCFH fluorescent dye, (b) Protein carbonylation in lung, (c) FRAP in plasma, (d) Lipid peroxidation of erythrocytes.

Data expressed as mean ± SD of six independent replicates. Results were analysed by means of one-way ANOVA, followed by Tukey's multiple comparison test.

*p<0.05; **p<0.01 significant results between 1.5 Ω /0.25 Ω groups and control group.

°p<0.05; °°p<0.01 significant results between 0.25 Ω and 1.5 Ω group.

Liver is one of the organs that are mainly involved in the biotransformation and detoxification of xenobiotics. Antioxidant enzymatic activity, as well as phase I and phase II ones, were measured in liver to have a vision of the systemic effect of e-cig exposure (**Figure 10**). The general decrease of the antioxidant enzymatic activity in 0.25 Ω group was always significant when compared to 1.5 Ω group and, for GSSG-red and CAT, also when compared to control (**Figure 10a**). This drop was also revealed in

UDPGT, whose activity was significantly reduced in animals exposed to the heaviest condition (**Figure 10b**). As for lung, the activity of hepatic phase I metabolizing enzymes was significantly increased in 0.25 Ω group, thus producing ROS as a consequence of their catalytic cycle (**Figure 10c**).

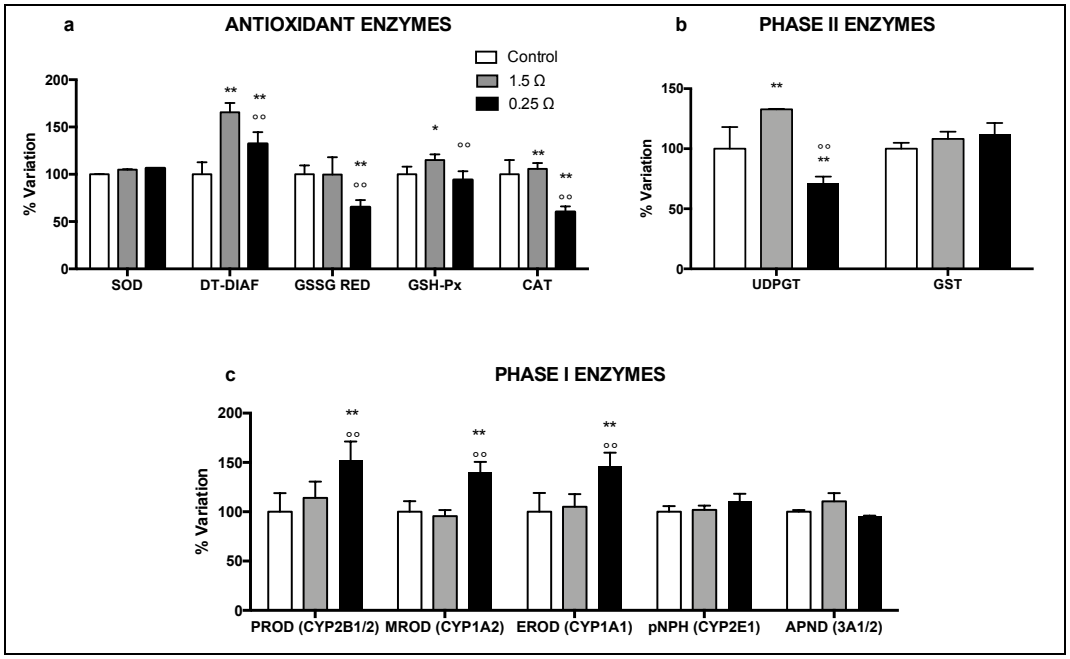

Figure 10. Hepatic pro-oxidative effects of vapors generated from e-cig equipped with 1.5 Ω or 0.25 Ω coils.
(a) Hepatic antioxidant enzymes, (b) Phase II enzymes in liver, (c) Phase I enzymes in liver.
Data expressed as percentage variation (mean ± SD of six independent replicates from ten rats) compared to control group arbitrarily set at 100%.
**p*<0.05; ***p*<0.01 significant results between 1.5 Ω /0.25 Ω groups and control group.
°*p*<0.05; °°*p*<0.01 significant results between 0.25 Ω and 1.5 Ω group.

The disequilibrium of the redox balance suggested a putative role of the e-cig exposure in the development of oxidative damage of the biological macromolecules. Lipids membranes of exposed groups showed higher levels of peroxidation compared to control (**Figure 11a**), and an increasing trend in carbonyl residues in proteins was observed with a direct correlation with the intensity of the exposure (**Figure 11b**). Coupled with the oxidative damage, the total glutathione content at hepatic level decreased as the resistance value decreased (**Figure 11c**), confirming the OSS in liver.

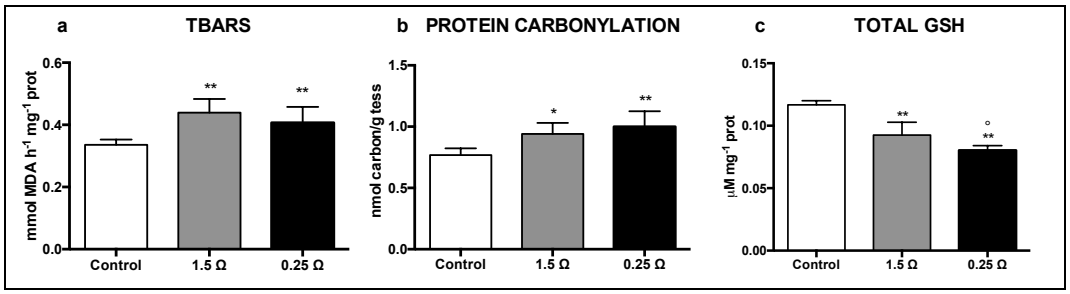

Figure 11. Hepatic pro-oxidative effects of vapors generated from e-cig equipped with 1.5 Ω or 0.25 Ω coils.
(a) Lipid hepatocyte peroxidation, (b) protein carbonylation in liver, (c) total glutathione content in liver. Data expressed as mean ± SD of six independent replicates from ten rats.
*p<0.05; **p<0.01 significant results between 1.5 Ω /0.25 Ω groups and control group.
°p<0.05; significant results between 0.25 Ω and 1.5 Ω group.

5.5 TISSUE DAMAGE

Lung and trachea from each group were analyzed by using SEM (**Figure 12**). **Fig. 12a** and **12d** show lung from control rats. The typical spongy structure was well organized in alveoli and bronchioles: the bronchiole diameter was constant and the air sacs were preserved. Their number and size evidently decreased in lung from 1.5 Ω exposed rats (**Fig. 12b, e**), and the lung structure from 0.25 Ω group was disorganized and showed large areas (*) of airflow collapse (**Fig. 12c, f**). In the same way, trachea from control group presented equilibrated proportion between ciliated cells (cc) and goblet cells (gc) (**Fig. 12g, j**). Trachea from 1.5 Ω group (**Fig. 12h, k**) showed a large area of tissue disruption. In the remaining one, the proportion between cc and gc was maintained. In 0.25 Ω condition, an altered morphology and a deeply changed organization appeared in a large part of the tissue (**Fig. 12i, l**). The diffuse tissue loss at 0.25 Ω condition (**Fig. 12i, l**), was correlated to the presence of apoptotic (ap) and necrotic (n) cells (**Fig. 12l**).

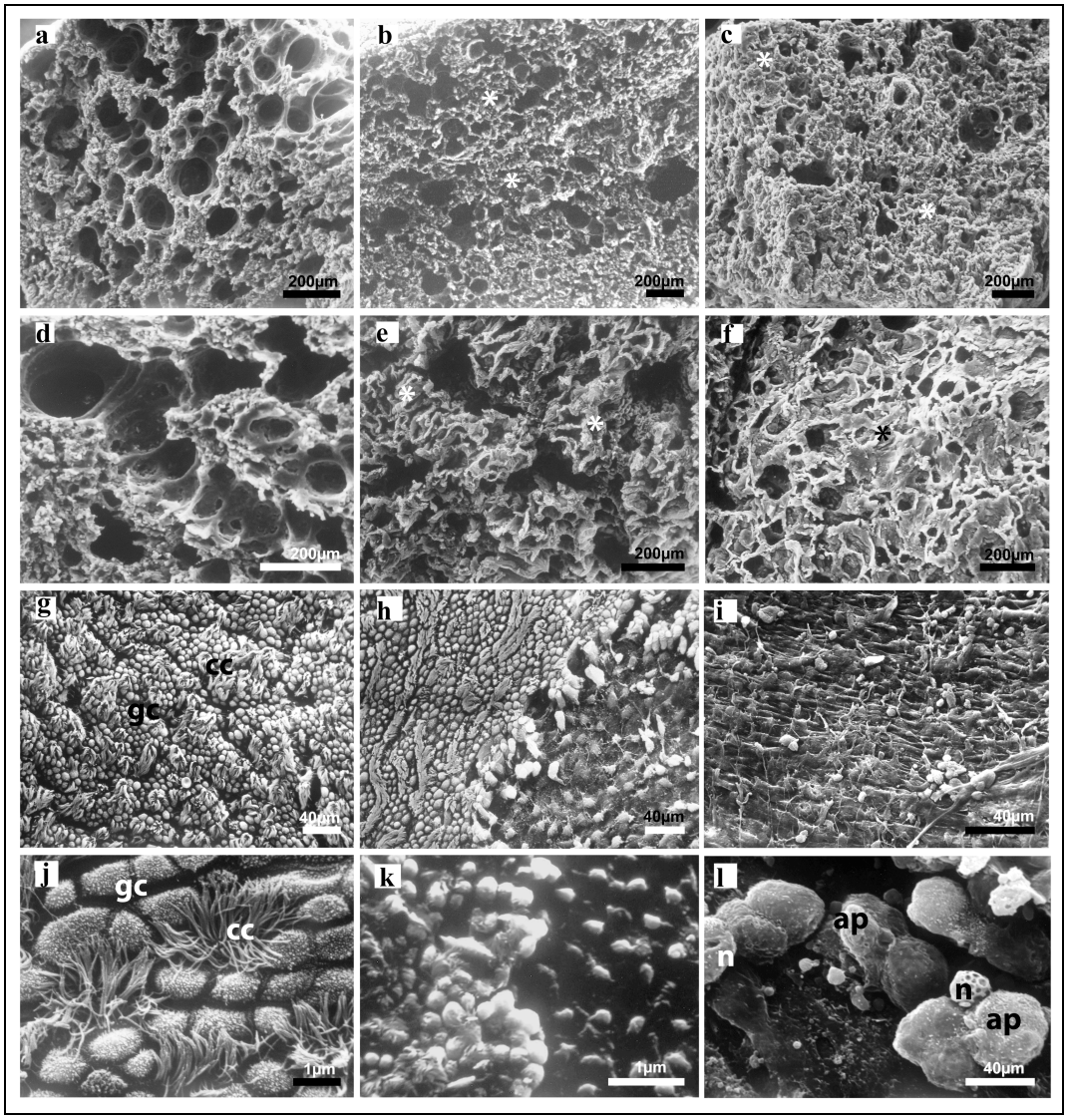

Figure 12. SEM morphologic alterations of lung and trachea tissue in rats exposed to the vapors generated from e-cig equipped with 1.5 Ω or 0.25 Ω coils.
First and second lines report images from lung of control group (a, d), 1.5 Ω group (b, e), and 0.25 Ω group (c, f). Third and fourth lines report images from trachea of control group (g, j) in which both ciliated cells (cc) and goblet cells (gc) are appreciable. 1.5 Ω group (h, k), and 0.25 Ω group (i, l) show large areas without epithelium. * represents areas of alveoli collapse; n = necrotic cells; ap = apoptotic cells. Samples from five rats of each group were analysed.

This behavior was also supported by TEM, as shown in **Figure 13**. Control group (**Fig. 13a**) showed well-preserved airway epithelium cells. At high magnification (**Fig. 13b**), it is possible to observe cilia ultrastructural features. E-cig effects at 1.5 Ω (**Fig. 13c**) and at 0.25 Ω (**Fig. 13d**) showed several morphological changes, including epithelium detachment (**Fig. 13c**) and loss of cilia (**Fig. nd**). These tissue damages were more evident in 0.25

Ω condition, also correlated to the presence of necrotic (**Fig. 13e and 13f**) and apoptotic (**Fig. 13g and nh**) cells. The typical apoptotic cells are characterized by chromatin condensation (**Fig. 13h**) and micronuclei (**Fig. 13g**).

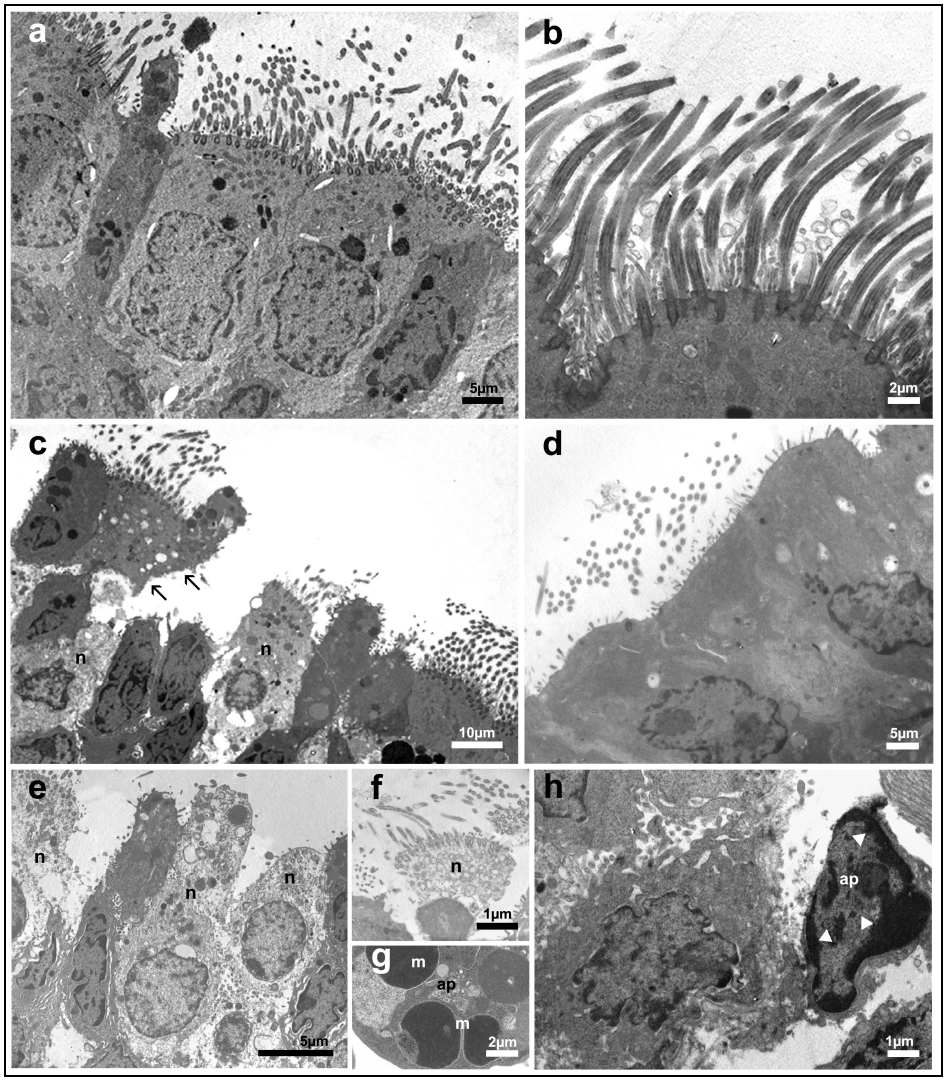

Figure 13. TEM ultrastructural alterations of trachea tissue in rats exposed to the vapors generated from e-cig equipped with 1.5 Ω or 0.25 Ω coils.
First line reports images from trachea epithelium of control group (a, b). Second line described 1.5 Ω group (c), and 0.25 Ω group (d) showing a detachment (g) of epithelium correlated, in both conditions to the presence of necrotic (e, f) and apoptotic (g, h) cells. n = necrotic cells; ap = apoptotic cells; m = micronuclei; ▶ = marginated chromatin. Samples from five rats of each group were analysed.

5.6 MODULATION OF GENE EXPRESSION

Gene expression of pro-inflammatory cytokines such as IL1β, IL6 and TNFα was analysed in rat lung tissue. Although no significant variation was recorded, a trend of increase in gene expression of both IL1β and IL6 was observed after rat exposure to the vapor of e-cig in 0.25 Ω group compared to control (**Fig. 14a,b**). A decrease in the expression of TNFα was recorded (**Fig. 14c**). Besides, the expression of chemokine CCL3 and CCL4, encoding for macrophage inflammatory proteins, showed a significant decrease in 0.25 Ω group compared to control (**Fig. 14d,e**). Similarly, the colony-stimulating factor of macrophage and granulocyte colonies CSF2 showed a decrease in the lung tissue of rats exposed to 0.25 Ω vapor from e-cig (**Fig. 14f**). Finally, due to the critical role of ALDH3A1 in the oxidation of reactive aldehydes and in the cytotoxicity and genotoxicity of cigarette smoke (Jang et al., 2014), we analyzed its expression in rat lung tissue exposed to e-cig vapors.

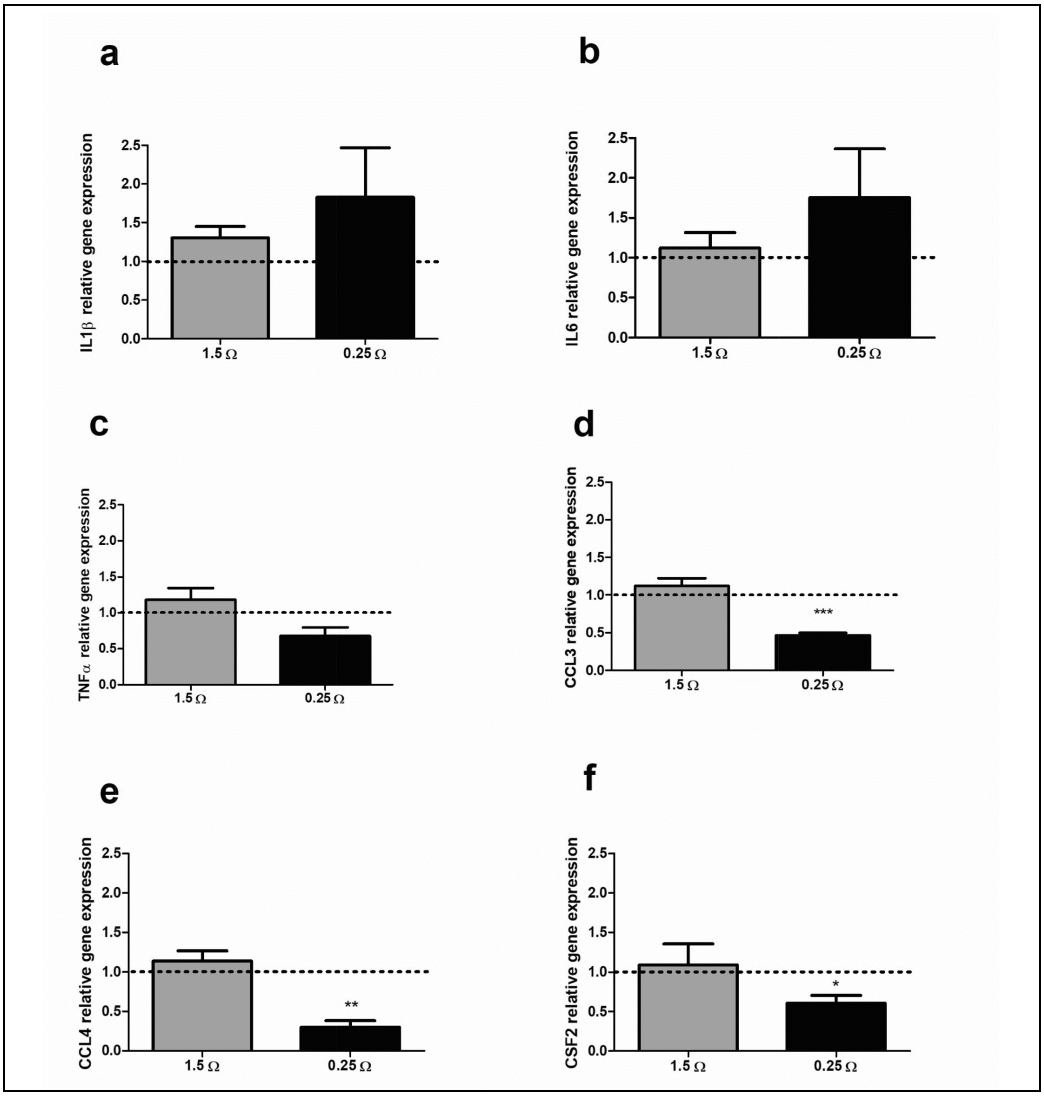

Figure 14. Effects of vapors generate from e-cigs equipped with 1.5 Ω or 0.25 Ω coils on the pulmonary inflammatory pattern.
Relative gene expression of IL1β (a), IL6 (b), TNFα (c), CCL3 (d), CCL4 (e), CSF2 (f). GAPDH and actin were used as endogenous controls. Data are expressed as mean ± SEM of at least four independent replicates. Results were analysed by means of one-way ANOVA followed by Dunnet test. *$p<0.05$; **$p<0.01$ significant results versus control (dashed line). The gene expression analysis was conducted on 7 rats in the control group, 7 rats in the 1.5 Ω group, and 4 rats in the 0.25 Ω group.

5.7 HEMATOLOGICAL PROFILE

The haematocrit and haemoglobin (Hb) levels, as well as the total red blood cell (RBC) and reticulocyte (RC) count, were significantly higher in the 0.25 Ω group compared to those observed in the control (**Fig. 15a-d**). Our model evidenced non-significant changes in the 1.5 Ω group, but the variations resulted more marked when the resistance was decreased to 0.25

Ω. Lymphocytes count (**Fig 15e**) showed a dramatic drop in 0.25 Ω group but a non-significant decrease in 1.5 Ω group if compared to control. Finally, a change in leucocytes profile is reported in **Fig. 15f**, which indicates that the number of circulating neutrophils was about 8-fold higher in 0.25 Ω group ($p<0.01$) compared to control. The alterations of monocytes, eosinophils and basophils followed an increasing but not significant trend in 0.25 Ω group and a non-significant decreasing trend in 1.5 Ω group.

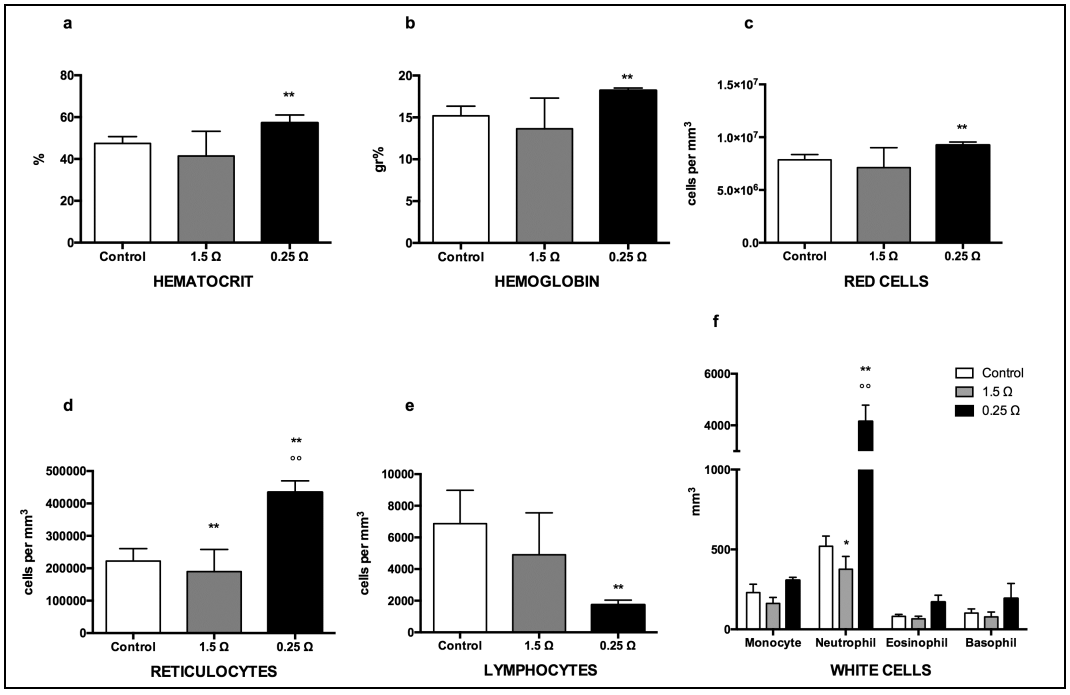

Figure 15. Effects of vapors generate from e-cigs equipped with 1.5 Ω or 0.25 Ω coils on the haematological profile.

(a) Haematocrit; (b) Haemoglobin; (c) red cells; (d) reticulocytes; (e) lymphocytes; (f) white cells. Data expressed as mean ± SD of six independent replicates from ten rats. Results were analysed by means of one-way ANOVA, followed by Tukey's multiple comparison test.

*$p<0.05$; **$p<0.01$ significant results between 1.5 Ω /0.25 Ω groups and control group.

°$p<0.05$; °°$p<0.01$ significant results between 0.25 Ω and 1.5 Ω group.

5.8 EFFECT OF IQOS® EXPOSURE ON ROS GENERATION

To investigate the effects of IQOS® exposure on ROS generation in lung, ROS content in pulmonary tissue was measured with two different techniques. EPR was performed in fragment of lung from each animal and showed a significant increase of ROS levels in treated group, even with a visible dispersion of data (**Figure 16a**). These results were confirmed by performing DCFH-DA assay in lung homogenate (**Figure 16b**).

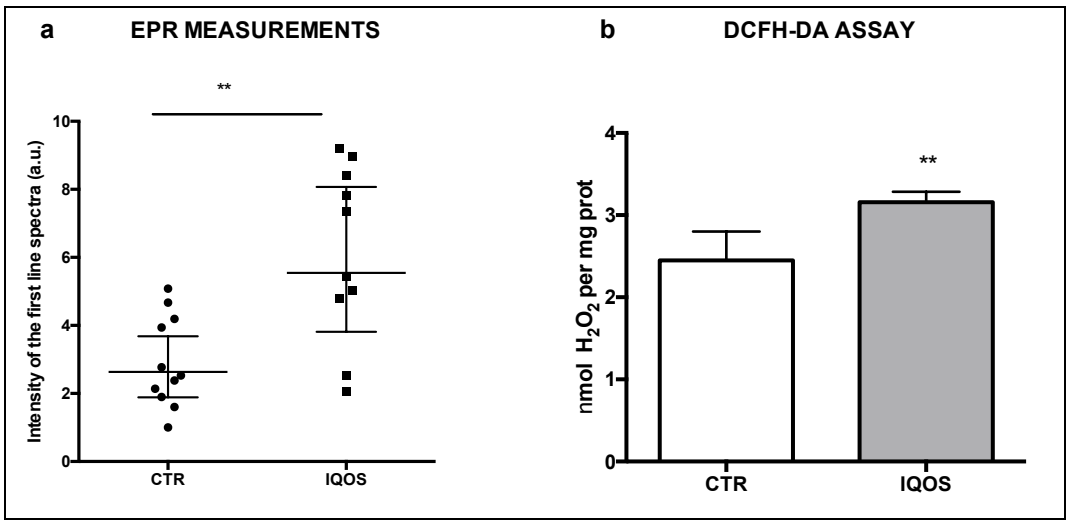

Figure 16. Effects of vapors generate from IQOS® on ROS generation in lung.
ROS levels in lung revealed by EPR measurements (a) and DCFH-DA fluorescent dye (b).
(a) Each point represents an independent measurement from each animal.
(b) Data represents mean ± SD of six independent replicates.
Results were analysed by means of unpaired t-test.
**$p<0.01$ significant results between IQOS® group and control.

5.9 OXIDATIVE EFFECTS OF IQOS® EXPOSURE

As a source of ROS, cytochrome P450 activity was evaluated (Figure n). Animal exposed to IQOS® showed a significant increase in CYP2B1/2 (**Fig 17a**), CYP2A1/2 (**fig 17b**), and especially CYP1A1, whose activity resulted almost nine fold enhanced in exposed group ($p<0.01$) (**fig 17c**). To confirm the increased activity of CYP1A1, the mRNA expression of the

related gene was evaluated and resulted significantly higher in IQOS® group compared to control (**fig 17d**).

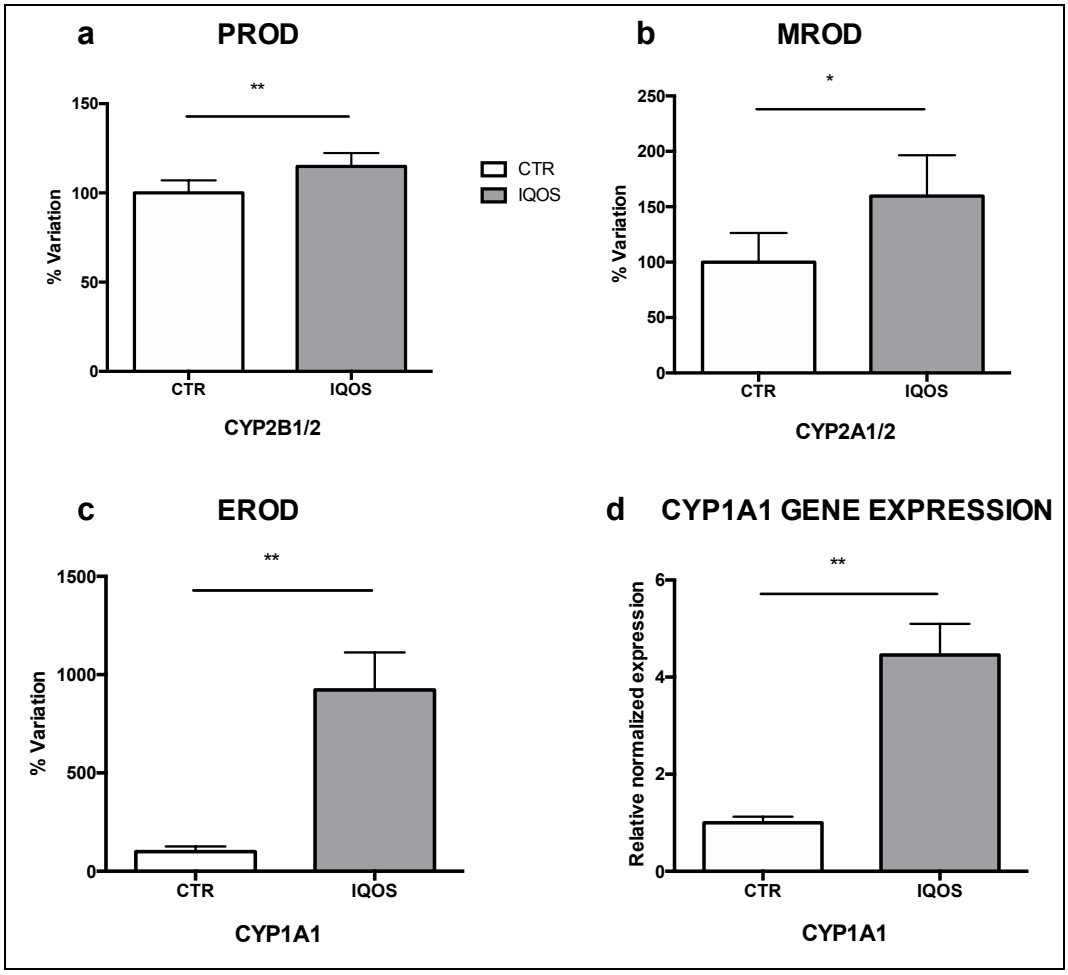

Figure 17. Effects of vapors generate from IQOS® on pulmonary phase I enzymatic activity.
Data were obtained through enzymatic assays performed on microsomal lung fractions using several specific probes: (a) PROD (CYP2B1/2), (b) MROD (CYP1A1/2), (c) EROD (CYP1A1). (d) quantitative evaluation of CYP1A1 gene expression.
(a), (b), (c) Data expressed as percentage variation (mean ± SD of six independent replicates from ten rats) compared to control group arbitrarily set at 100%. Results were analysed by means of unpaired t-test.
*p<0.05; **p<0.01 significant results between IQOS® and control group.

The oxidative effects on biological macromolecule in lung were also evaluated. Both lipid membranes (**fig 18a,b**) and proteins (**fig 18c**) of exposed group showed higher levels of oxidation compared to control. In addition, enhanced lipid peroxidation was found in erythrocytes membranes (**fig 18d**). This suggests the presence of an oxidative

environment also at systemic status that was confirmed by the decreased levels of FRAP in exposed group (**fig 18e**).

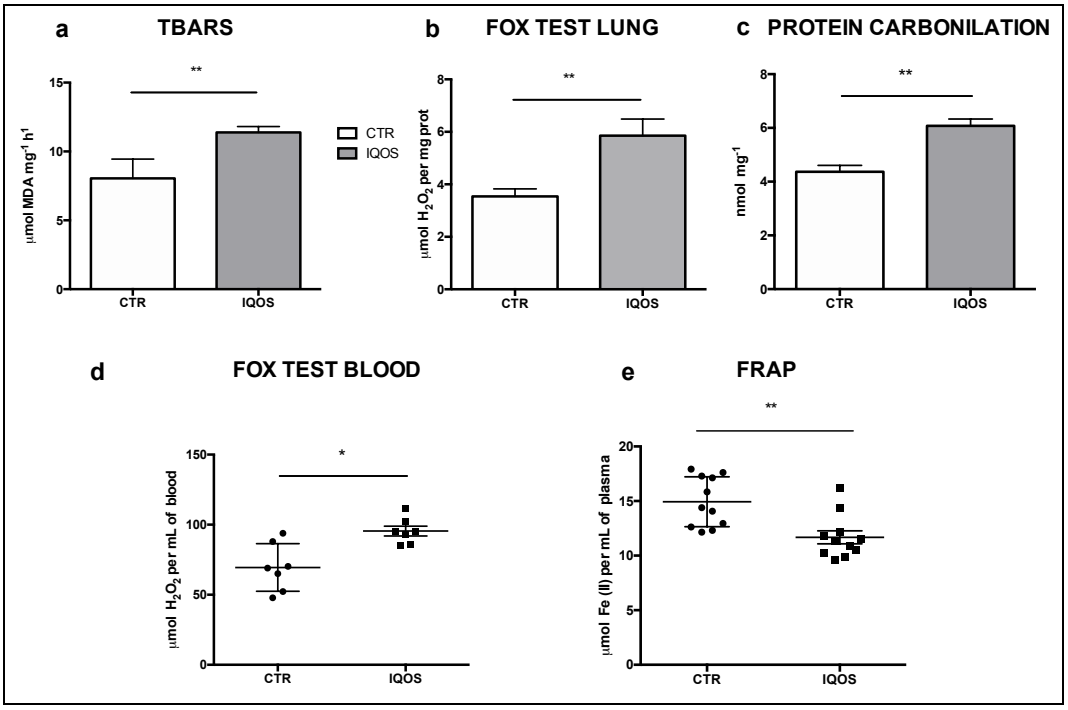

Figure 18. Effects of vapors generate from IQOS® on biological macromolecules.
(a), (b), (c) Data represents mean ± SD of six independent replicates.
(d), (e) Each point represents an independent measurement from each animal.
Results were analysed by means of unpaired t-test.
*p<0.05; **p<0.01 significant results between IQOS® group and control.

5.9 EFFECT OF IQOS® EXPOSURE ON DNA

Widely used as a biomarker to evaluate the load of oxidative stress and carcinogenesis, 8-hydroxy-2-deoxyguanosine (8-OHdG) was measured in plasma (**Figure 19a**) and lung (**Figure 19b**). In rat exposed to IQOS® vapor, the oxidation of guanosine to 8-OHdG was markedly higher compared to control.

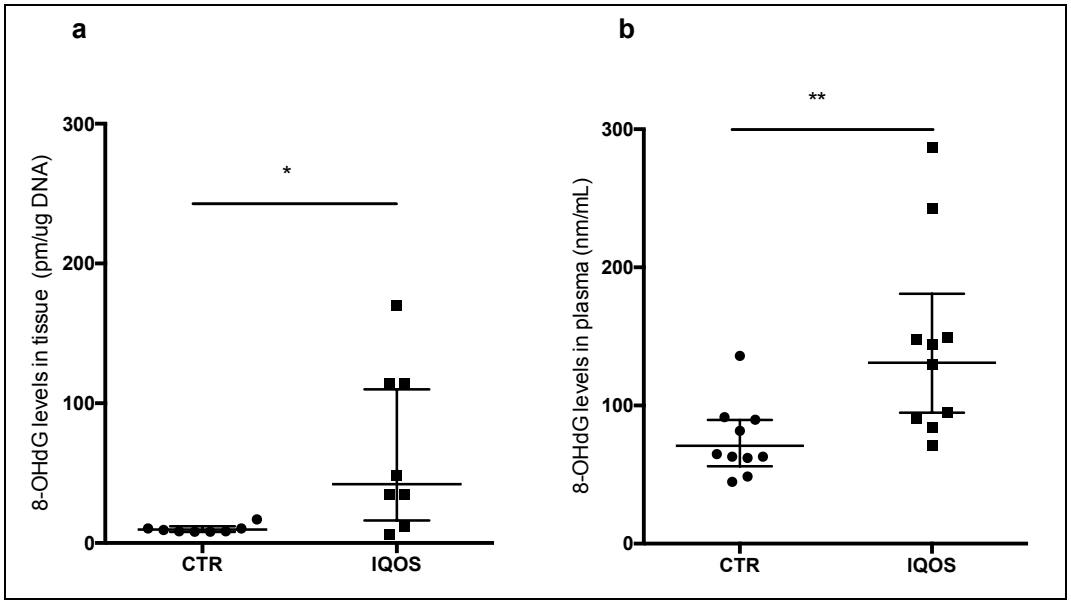

Figure 19. Effects of vapors generate from IQOS® on DNA oxidative damage.
Guanosine oxidation to 8-OGdG in lung (a) and plasma (b).
Data represents mean ± SD of independent replicates from at least 8 animals.
Results were analysed by means of unpaired t-test.
*p<0.05; **p<0.01 significant results between IQOS® group and control.

CHAPTER 6

DISCUSSION AND CONCLUSION

6.1 DISCUSSION

E-cigs are composed of several components that, in many cases, can be modulated or modified according to the consumer's preferences. Among the modifiable components, the coil present in the atomizer is the element that, in combination with the applied voltage, is responsible for the liquid heating. The actual market offers to users a great variety of e-liquids that differ one from each other due to the flavors, PG/VG ratio and the percentage of nicotine. Widely perceived as weapon against addiction, the use of e-cig with nicotine-free liquid is spread, especially among young people. It is well established that thermal decomposition of the PG/VG mixture present in the e-liquid leads to the formation of toxic and carcinogenic carbonyls, such as formaldehyde, acetaldehyde and acrolein (Paschke et al., 2014; Uchiyama et al., 2013).

One of the primary goals of this study was to investigate the role of the e-cig's heating coil resistance with respect to the generation of carbonyls in two liquids that differed for the presence of nicotine. In this experiment, eL-N produced higher levels of carbonyls than eL+N. As reported by Kosmider et al. (2014), the composition of e-liquid significantly affects the content of the released carbonyl compounds. In general, the composition of

the volatile fraction is strictly linked to the thermodynamic equilibrium between the vapor and condensed (liquid) phases; for this reason, when the number and/or the concentration of e-cig liquid ingredients decreases, the competition between molecules in the headspace decreases as well, thus leading to an increase and accumulation of some volatile compounds in the headspace, such as the revealed carbonyls that are characterized by a high vapor pressure. The results of this study are consistent with previous researches demonstrating that the level of carbonyl compounds in e-cig vapors is affected by the presence of nicotine and battery voltage (Kosmider et al., 2014). The latter is a relevant issue considering that e-cigs have become popular during the past decade (Korzun et al., 2019) for having the capacity of modulating the nicotine content of the liquid.

Human exposure to these low molecular weight carbonyls represents a risk factor for occurrence of neoplastic diseases. In particular, formaldehyde and acetaldehyde are classified as Group 1 and Group 2B carcinogens, respectively, by the International Agency for Research on Cancer (IARC, 2012). Acrolein is listed as a hazardous air pollutant by the United States Environmental Protection Agency (U.S. EPA, 2003). The presence of higher carbonyls levels in eL-N liquid overturns the idea that the absence of nicotine makes the liquid safer. There are no doubts that nicotine is the molecule responsible for addiction and cardiovascular risk, and its employment in e-cig is considered a gateway towards the consumption of tobacco cigarette. However, the toxic carbonyls detected in this study represent a risk factor for the onset and development of neoplastic and chronic diseases. This is of particular concern considering that, in many Countries, the nicotine-free e-cig can be sold to adolescent younger than 18 years old.

The generation and subsequent fragmentation of carbonyls is related to the formation of radicals (e.g., hydroxyl radicals), which are responsible for the oxidation and fragmentation of glycols (Geiss et al., 2016). For this reason, ROS levels were measured in both vapor and cell medium using the DCFH-DA assay in a cell-free system. Although the exposure profile was different from the one used for detecting the selected carbonyl compounds, the results exhibited the same trend. The reduction of the coil resistance, and thus the increase of the heating and the total wattage of the device, played an important role in terms of ROS formation. These results appear to confirm the hypothesis of Lerner et al. (Lerner et al., 2015a) who reported that one of the possible sources of ROS could be the heating element.

The biological implications of the ROS and carbonyls were also investigated by examining the effect of e-cig vapor on the viability of H1299 human lung adenocarcinoma cells. Vapor from eL-N significantly reduced cell viability and these effects were directly related to the levels of ROS produced.

High levels of ROS represent a risk factor for the onset of several diseases and pathological conditions, including cancer and inflammation (Waris and Ahsan, 2006). ROS are able to generate DNA strand breaks, cross-links, and can cause modification to the purine, pyrimidine and deoxyribose components of DNA (Halliwell and Gutteridge, 2015). In an in-vivo study, e-cig aerosol caused accumulation of 8-hydroxy-deoxyguanosine (8-OH-dG) which can lead to mutations, with a significant correlation with ROS content, thus probably resulting in inflammatory response and neoplastic development (Canistro et al., 2017).

Others have previously examined the impact of e-cig vapor and e-cig extract on the morphology and viability of lung cells using both air-liquid

interface or direct exposure to e-cig extract (Lerner et al., 2015b; Cervellati et al., 2014; Higham et al., 2018). Ex vivo treatment of bronco-epithelial cells from both patients with COPD and healthy subjects with e-cig extracts increased some inflammatory responses including altered cytokine and chemokine production (Higham et al., 2018).

In support of these data, epidemiological studies have indicated an association between e-cig use and respiratory disorders, especially asthma, bronchitis and COPD (Choi and Bernat, 2018; McConnell et al., 2017; Schweitzer et al., 2017; Wills et al., 2019). Altogether, these findings confirm the pivotal role of oxidative stress induced by e-cig use in the onset and development of respiratory diseases in healthy subjects or in the transition of initial symptomatology in chronic disorders.

In the animal model, an imbalance of the enzymatic antioxidant responses was found. Lung GSSG-red activity was significantly higher in 0.25 Ω group compared to 1.5 Ω and control, in agreement with data referred to heavy smokers, where high levels of GSH are necessary for the detoxification process (Solak et al., 2005). Rats subjected to the vapor from the 1.5 Ω device showed a modest but significant impairment of the detoxifying enzymes, whereas, lowering down Ohms, the deeper changes reflected a general enzymatic up-regulation, due to the higher levels of reactive carbonyl species.

It is known how the induction of CYP superfamily can strongly contribute to ROS overproduction and, at the same time, plays a key role in the increased bioactivation of pre-mutagens and pre-carcinogens (Sapone et al., 2012; Vivarelli et al., 2016). In this study, various cytochrome P450 (CYP)-supported monooxygenase isoforms increased in the 0.25 Ω group compared to 1.5 Ω and control. In 0.25 Ω group, we found the strongest CYP1A1 induction, an isoform that bioactivates arylamines, dioxins,

aromatic amines and polycyclic aromatic hydrocarbons (PAHs), and might culminate in DNA adducts that are known to increase lung cancer risk (Vázquez-Gómez et al., 2018). Likewise, CYP2E1 isoform, markedly boosted in our model, catalyzes the metabolism of a wide variety of xenobiotics, including glycerol, acetaldehyde, aromatic compounds and nitrosamines (Cederbaum, 2014). These data are of particular interest considering that changes in CYP-linked monooxygenases occurred despite the use of nicotine free e-liquid.

In parallel, pulmonary xanthine oxidase (XO) levels were significantly higher in the 0.25 Ω group than in 1.5 Ω and control. Elevated XO was previously found in patients with COPD compared with control subjects (Ichinose et al., 2003), in an animal model of asthma (Sugiura et al., 1999), and in lungs of animals exposed to cigarette smoke (Kim et al., 2013). Since both XO and CYP catalytic cycle are important sources of the superoxide radical, we measured ROS content in the lung tissue. Exposed rats presented significantly higher ROS levels compared to controls, suggesting that e-cig vapors generated an oxidative stress status (OSS). The redox imbalance at systemic level was manifested through the significant reduction of plasma antioxidant capacity (FRAP) in the exposed animals. Consistently, data from 0.25 Ω group showed higher levels of hydroperoxides in erythrocyte membranes. Lipid peroxidation induces alteration of fine structures, fluidity, and permeability and modifies low-density lipoprotein to pro-atherogenic and proinflammatory forms (Greenberg et al., 2008) and generates potentially toxic products with mutagenic and carcinogenic activity (West et al., 2006).

An OSS was also found in liver. The enzymatic redox unbalance was manifested through a drop in the antioxidant enzymatic activity in exposed group, particularly significant in 0.25 Ω group. This decreasing trend was

also observed for UDPGT enzymatic activity, suggesting the inability of hepatic enzymes to detoxify liver from elaborated vapors. Such vapors, however, underwent to the metabolism of phase I enzymes, whose activity resulted enhanced in 0.25 Ω group. It is not surprising that hepatic response was different if compared to the pulmonary one. In an inhalation exposure, in fact, lung is the first organ that comes into contact with gases and reacts with the most aggressive response. The absorption by hematic circulation progressively reduces the concentration of toxicants and oxidants, thus the response at hepatic level is attenuated compared to lung.
Since the lung is the mainly stressed organ inhalation exposure, a particular attention to the pulmonary alterations was given in this study. The OSS level, the impairment of the antioxidant machinery and the macromolecule damages we found, reflected in the morphological alterations at airway level. A loss of the typical organization in bronchioles and alveoli was evident in the 1.5 Ω group, and more conspicuous in the 0.25 Ω one. In particular, e-cig exposed animals reported alveolar destruction and bronchial epithelium disorganization. A demarcation line between a well-organized tissue and a loss of structure area was also revealed in trachea form from the 1.5 Ω group. More evidently, in 0.25 Ω rats, the number of ciliated cells was dramatically reduced and both apoptotic and necrotic cells were present. These alterations are similar to those reported by smokers and COPD patients (Macnee, 2009), and it was recently shown how e-cig aerosol exposure is associated with inflammation along with the loss of epithelial barrier function in lung cells (Gerloff et al., 2017). To further investigate the inflammatory response to e-cig exposure in our experimental settings, a panel of cytokine and chemokine gene expression was measured: only two genes (*i.e.* CCL3 and CCL4) were significantly changed compared to controls and they were all down regulated. The increasing trend of IL1β

and IL6 expression in 0.25 Ω group suggests that the more powerful setting may induce a stronger inflammatory status. Widely recognized as modulator of innate immune defense, IL1β was often found enhanced in COPD patients and may have played a prominent role in its pathophysiology (Botelho et al., 2011), while the release of IL6 from cells exposed to e-cig vapor occurred in a dose-dependent manner in response to the aerosol exposures (Lerner et al., 2015). Smoking impacts both innate and adaptive immunity (Qui et al., 2017), usually decreasing interferon-γ and TNFα (Strezelak et al. 2018). In our model, we recorded a similar trend for TNFα in 0.25 Ω group, supporting the hypothesis that also e-cig vapors may induce an immune response. Furthermore, the expression of CCL3, CCL4 and CSF2 is in line with the reduced expression of TNFα. Even though these data are in contrast with the increased number of white blood cells in 0.25 Ω group, they could be explained in light of the findings by Meuronen and colleagues, that suggested how the inflammatory cells are incapable of producing chemokine mRNA in the lower airways in smokers (Meuronen et al., 2008). Since the protein expression of the significantly dysregulated genes was not analyzed in the present research, further studies need to be carried out to confirm the expression level of studied gene at protein level.

As the influence of OSS and inflammatory processes on the haematological parameters in smokers has been found (Strzelak et al., 2018), the putative changes of haematocrit, Hb levels, RBC and RC count was investigated, and these biomarkers were significantly higher in the 0.25 Ω group than in control. These data are in agreement with the haematological profile of patients with a smoking history (Ugbebor et al., 2011; Anandha Lakshimi et al., 2014; Kalahasthi and Berman, 2016; Malenica et al., 2017). Interestingly, as haematological alterations enhanced with the smoking

intensity (Whitehead et al., 1995; Anandha Lakshimi et al., 2014), our model showed the most marked changes in the 0.25 Ω group. These observations concur in our hypothesis that vaping at low resistances leads to a more intense exposure. Existing data concerning the influence of smoking on lymphocyte profile are affected by numerous confounding factors of subpopulations (Stämpfli and Anderson, 2009; Andreoli et al., 2015). However, the drop in lymphocyte count from 1.5 Ω to 0.25 Ω group is in line with the inversely relation between the lymphocyte count in smokers and the increasing number of tobacco cigarette per day revealed by Sherke et al. (Sherke et al., 2016). Noteworthy, similar results were also obtained in a cross-sectional study conducted on children with the history of indoor exposure to tobacco smoke (El-Hodhod et al., 2010). Changes in leukocyte profile are in accordance with those emerged from clinical trials showing an increment of the neutrophils moving from light- to heavy-smokers, as well as in patients with COPD (Anandha Lakshimi et al., 2014; Jaroenpool et al., 2016). In particular, the high number of circulating neutrophils herein recorded in the 0.25 Ω group, has been previously observed in smokers (Calapai et al., 2009; Andreoli et al., 2015).

The results here presented suggest that the customization of the vaping experience results in a plethora of "personalized toxicological effects", whose repercussions on health are unpredictable. This study shows how two identically settled e-cigs (battery output, temperature and atomizer setting), loaded with the same liquid (PG/VG ratio, nicotine concentration and flavours), could generate different amounts of toxic aldehydes, as a mere effect of the value of the heating element.

To minimize this problem, new strategies have been developing. Among these, the heat not burns technology is assuming wide popularity, especially among current and former smokers (Kopa and Pawliczak, 2019). In addition, there are growing evidences that the market of IQOS® has an impact on adolescent young adults, which are even more attracted by this kind of products (McKelvey et al., 2018). The great popularity of IQOS® is due to solid market strategies – which involves claims, packaging, product design and shops architecture – and to a reasonable number of scientific evidences that support the safety of the device. However, when PMI independent studies are conducted, the results follow a different direction and, on the contrary, recommend caution in the use of IQOS® (Auer et al., 2017; Cancelada et al., 2019; Salman et al., 2019; Sohal et al., 2019).

In this preliminary study, when IQOS® exposed animals were compared to unexposed controls, an oxidative environment in lung was revealed in treated group. To explore whether e-cigs induce toxicological effects, such as those involving cytochrome P450 (CYP) changes, the modulation of carcinogen-metabolizing enzymes in the lungs of rats exposed to IQOS® was analyzed: a significant increase in CYP1A1/2 (activating, for example, polychlorinated biphenyls, aromatic amines, dioxins and PAHs), CYP2B1/2 (activating olefins and halogenated hydrocarbons), and CYP1A1 was found. It was previously discussed how oxidative stress has a pivotal role in the damage of the biological macromolecules, by causing lipid peroxidation, protein carbonylation and oxidative damage to DNA. In this context, lipid membranes, as well as proteins in lung of exposed group resulted significantly more oxidized if compared to control. Guanosine oxidation to 8-OHdG was measured. 8-OHdG is one of the most extensively studied and abundant free radical-induced oxidative DNA

lesions, which also correlates with mutagenesis in bacterial and mammalian cells. IQOS® exposed animal showed significantly higher levels of 8-OHdG compared to control, both in lung and in plasma. This suggests that oxidative stress acted not only al local level, but was spread to the entire organism, thus potentially involving many biological targets. As a confirmation, plasmatic FRAP was also reduced in exposed group. These results are in line not only with other studies on IQOS® (Salman et al., 2019; Sohal et al., 2019; Leigh et al., 2018b) but also with previous researches on e-cig (Canistro et al., 2017; Scheffler et al., 2015) in which oxidative DNA damage was reported in e-cig exposed animals.

6.2 CONCLUSION

The study here presented suggests how difficult is to establish a risk assessment associated to related tobacco products. On one hand, the evolving technology of these devices enhances the number of variables that users can modulate; on the other one, marketing strategies aim to make these products even more appealing, both for young and for smokers who are determined to quit. Personalization allows users to satisfy their needs and to feel gratification from the vaping experience. The idea that low voltage devices are safer is wide spread among population and scientific community (Farsalinos et al., 2017). In addition, heat not burn technology was developed to operate at low voltage to vaporize tobacco sticks without combustion. However, results from this study show how the combination of resistance and voltage, rather than the voltage itself, has an impact on e-cig toxicity. In light of the findings here presented and until robust evidence from epidemiological studies on the putative public health repercussions are provided, the promotion of electronic devices by scientific and public health

agencies as smoking cessation aid should be considered with extreme caution.

REFERENCES

"The Facts on the FDA's New Tobacco Rule". United States Department of Health and Human Services. United States Food and Drug Administration. 2 May 2017.

Ambrose BK et al., Perceptions of the relative harm of cigarettes and e-cigarettes among U.S. youth. Am J Prev Med. 2014 Aug; 47(2 Suppl 1):S53-60.

Amrock SM et al., Perception of e-cigarette harm and its correlation with use among U.S. adolescents. Nicotine Tob Res. 2015 Mar; 17(3):330-6.

ANSES. Proposition de valeurs guides de qualité d'air intérieur. L'acroléine. Avis de l'Anses. Rapport d'expertise collective. Saisine n° 2011-SA-0354. (2013)

Apelberg BJ et al., Enhancing youth tobacco surveillance to inform tobacco product regulation: findings from the 2012 National Youth Tobacco Survey. Am J Prev Med. 2014;47(2 Suppl 1):S1–S3.

ATSDR Revised Health Consultation; Formaldehyde Sampling at FEMA Temporary Housing Units Agency for Toxic Substances and Disease Registry, Baton Rouge, LA (2007, February)

Auer R et al., Heat-Not-Burn Tobacco Cigarettes: Smoke by Any Other Name. JAMA Internal Medicine. 2017;177(7):1050–1052.

Barrington-Trimis JLet al., Flavorings in electronic cigarettes: an unrecognized respiratory health hazard? JAMA. 2014;312(23):2493–4.

Battistoni Aet al., Role of the dimeric structure in Cu,Zn superoxide dismutase. pH-Dependent, reversible denaturation of the mono- meric enzyme from Escherichia coli. J Biol Chem, 1998. 273: 5655-5661.

Behar RZet al., Identification of toxicants in cinnamon-flavored electronic cigarette refill fluids. Toxicol In Vitro. 2014;28(2):198–208.

Bekki Ket al., Carbonyl compounds generated from Electronic Cigarettes. Int J Environ Res Public Health, 2014. 11: 11192-11200.

Benowitz NL and Burbank AD. Cardiovascular toxicity of nicotine: Implications for electronic cigarette use. Trends Cardiovasc Med, 2016. 26(6):515-23.

Bitzer ZTet al., Effect of flavoring chemicals on free radical formation in electronic cigarette aerosols. Free Radic Biol Med, 2018. 120: 72-79.

Bitzer ZT et al., Effects of Solvent and Temperature on Free Radical Formation in Electronic Cigarette Aerosols. Chem Res Toxicol. 2018 16;31(1):4-12.

Bonamassa Bet al., Harmful effects behind the daily supplementation of a fixed vegetarian blend in the rat model. Food Chem Toxicol, 2016. 97: 367-374.

Bradley JR. TNF-mediated inflammatory disease. J Pathol. 2008;2:149–60.

Brown Jet al., Real-world effectiveness of e-cigarettes when used to aid smoking cessation: a cross-sectional population study. Addiction, 2014. 109:1531–40.

Burattini S et al., Melatonin action in tumor skeletal muscle cells: an ultrastructural study. Acta Histochem, 2016. 118(3): 278-285.

Cancelada Let al., Heated Tobacco Products: Volatile Emissions and Their Predicted Impact on Indoor Air Quality. Environ Sci Technol, 2019. 53(13):7866-7876.

Canistro D et al., Black cabbage seed extract affects rat Cyp-mediated biotransformation: organ and sex related differences. Food Chem Toxicol, 2012. 50(8): 2612-21.

Caponnetto P et al. EffiCiency and Safety of an eLectronic cigAreTte (ECLAT) as tobacco cigarettes substitute: a prospective 12-month randomized control design study. PLOS ONE, 2013. 8:e66317.

Carroccio A et al., Ethanol increases content and activity of human cytochrome P4502E1 in a transduced HepG2 cell line. Biochem Biophys Res Commun, 1994. 203:727–733.

Cataisson C et al. IL-1R-MyD88 signaling in keratinocyte transformation and carcinogenesis. J Exp Med, 2012. 209:1689–1702.

Cederbaum A.I., CYP2E1—biochemical and toxicological aspects and role in alcohol-induced liver injury. Mt Sinai J Med, 2006. 73: 657-672.

Cervellati Fet al., Comparative effects between electronic and cigarette smoke in human keratinocytes and epithelial lung cells. Toxicol In Vitro, 2014. 28: 999–1005.

Chandrasekharan UM et al. Tumor necrosis factor alpha (TNF-alpha) receptor-II is required for TNF-alpha-induced leukocyte-endothelial interaction in vivo. Blood. 2007;5:1938–44.

Charo IF and Ransohoff RM. The many roles of chemokines and chemokine receptors in inflammation. N Engl J Med, 2006. 354(6):610-21.

Chen W et al., Exposure assessment to e-cigarettes, part 1: literature review on carbonyl compounds generation from e-cigarettes and affecting factors. In Proceedings of Healthy Buildings, Boulder, 2013, USA.

Cho JH and Paik SY. Association between electronic cigarette use and asthma among high school students in South Korea. PLoS One, 2016. 11: e0151022.

Cirillo S et al., Effects of chlorinated drinking water on the xenobiotic metabolisn in Cyprinus Carpio treated with samples from two Italian municipal networks. Environ Sci Pollut R, 2016. 23(18):18777–18788.

Cirillo S et al., The customizable e-cigarette resistance influences toxicological outcomes: lung degeneration, inflammation and oxidative stress-induced in a rat model. Toxicol Sci, 2019. 127(1): 132-145.

Cirillo S et al., Impact of electronic cigarette heating coil resistance on the production of reactive carbonyls, reactive oxygen species and induction of cytotoxicity in human lung cancer cells in vitro. Reg Tox Pharm, 2019. Oct 17:104500. [Epub ahead of print]

Conklin DJ et al., Acrolein consumption induces systemic dyslipidemia and lipoprotein modification. Toxicol. Appl. Pharmacol, 2010. 243: 1–1210.1016/j.taap.2009.12.010.

Conklin DJ et al., Acrolein generation stimulates hypercontraction in isolated human blood vessels. Toxicol. Appl. Pharmacol, 2006. 217: 277–28810.1016/j.taap.2006.09.009.

Conklin DJet al., Glutathione-S-transferase P protects against endothelial dysfunction induced by exposure to tobacco smoke. Am. J. Physiol. Heart Circ. Physiol, 2009. 296: H1586–H159710.1152/ajpheart.00867.2008.

Cooke MS. Oxidative damage: Mechanism, mutation, and disfunctional relationship. FASEB J, 2003. 17: 1195-1200.

Corsi DJ and Lippert AM. An examination of the shift in school-level clustering of US adolescent electronic cigarette use and its multilevel correlates, 2011–2013. Health Place, 2016. 38: 30–38.

Coussens LM and Werb Z. Inflammation and cancer. Nature, 2002. 420(6917):860–867.

DeJarnett N et al., Acrolein Exposure is Associated with Increased Cardiovascular Disease Risk. J. Am. Heart Assoc, 2014. 3, e00093410.1161/jaha.114.000934.

Diaz E et al., Homogeneous oxidation reactions of propanediols at low temperatures. ChemSusChem, 2010. 3; 1063–70.

Dikova-Kostova et al., Direct evidence that sulphydryl groups of keap 1 are the sensor regulating induction of phase II enzymes that protect against carcinogens and oxidants. Proc Nat Acad Sci USA, 2002. 99: 11908-11913.

Dostert C et al., Innate immune activation through Nalp3 inflammasome sensing of asbestos and silica. Science, 2008. 320:674–677.

Editors. E-cigarettes: Public Health England's evidence-based confusion. Lancet, 2015. 386:829

Evans WE and Johnson JA. Pharmacogenomics: the inherited basis for interindividual difference in drug response. Annu Rev Genomics Hum Genet, 2001. 2: 9-39.

Farsalinos KE et al., Electronic cigarette use in the European Union: analysis of a representative sample of 27 460 Europeans from 28 countries. Addiction, 2016. 111: 2032–2040.

Farsalinos KE et al., E-cigarettes emit very high formaldehyde levels only in conditions that are aversive to users: A replication study under verified realistic use conditions. Food Chem Toxicol, 2017. 109(1):90-94.

Fisher MB et al., The role of he- patic and extrahepatic UDP-glucuronosyltransferases in human drug metabolism. Drug Metabol Rev, 2001. 33: 273–297.

Flück C.E. et al., Clinical, structural and functional implications of mutations and polymorphisms in human NADPH P450 oxydoreductase. Fundam Clin Pharmacol, 2007. 21: 399-410.

Food and Drug Administration (2016). Deeming tobacco products to be subject to the federal food, drug, and cosmetic act, as amended by the family smoking prevention and tobacco control act. Restrictions on the Sale and Distribution of Tobacco Products and Required Warning Statements for Tobacco Products (pp. 28973–29106). U.S. Department of Health and Human Services.

Forman H. J. et al., How do nutritional antioxidant really work: nuclephilic tone and para-hormone versus free radical scavenging in vivo. Free Radic Biol Med, 2014. 66.

Franks AS et al., Do electronic cigarettes have a role in tobacco cessation? Pharmacotherapy, 2018. 38(5); 555–i568.

Fucella et al., Trattato di farmacologia e terapia. Torino UTET, 1998. Pp 24-25.

Fuller T et al., Comparison of Bladder Carcinogens in the Urine of E-cigarette Users Versus Non E-cigarette Using Controls. Sci Rep, 2018. 8(1):507

Fuoco FC et al., Influential parameters on particle concentration and size distribution in the mainstream of e-cigarettes. Environ. Pollut, 2014. 184:523–29

Garcia-Arcos I et al., Chronic electronic cigarette exposure in mice induces features of COPD in a nicotine-dependent manner. Thorax, 2016. 71: 1119–1129.

Garcia-Moreno M et al., The role of oxidative stress in the development of alcoholic liver disease. Rev Gastroenterol Mex, 2014. 7: 135-144.

Geiss, O et al., Correlation of volatile carbonyl yields emitted by e-cigarettes with the temperature of the heating coil and the perceived sensorial quality of the generated vapours. Int. J. Hyg. Environ. Health, 2016. 219 (3): 268–277.

Gerszten REet al. MCP-1 and IL-8 trigger firm adhesion of monocytes to vascular endothelium under flow conditions. Nature, 1999. 398:718-723.

Ghosh A et al., Chronic e-cigarette exposure alters the human bronchial epithelial proteome. Am J Respir Crit Care Med, 2018. 198: 67–76.

Glanz SA and Bareham DW. E-Cigarettes: Use, Effects on Smoking, Risks, and Policy Implications. Annu Rev Public Health, 2018. 39: 215–235.

Gmel G et al., E-cigarette use in young Swiss men: Is vaping an effective way of reducing or quitting smoking? Swiss Med. Wkly, 2016.146:w14271.

Goel R et al., Highly reactive free radicals in electronic cigarette aerosols. Chem Res Tox, 2015. 28: 1675-1677.

Gomez-Cabrera MC et al., Redox modulation of mitochondriogenesis in exercise. Does antioxidant supplementation blunt the benefits of exercise training? Free Radic. Biol. Med, 2015. 86: 37–46

Goniewicz ML et al Levels of selected carcinogens and toxicants in vapor from electronic cigarettes. Tob Control, 2014. 23: 133–139.

Grana Ret al., E-cigarettes: a scientific review. Circulation, 2014. 129(19):1972–86.

Guengerich F.P., Cytochrome P450 and chemical toxicology. Chem Res Toxicol, 2008. 21: 70-83.

Harrell MB et al Flavored e-cigarette use: Characterizing youth, young adult, and adult users. Preventive Medicine Reports, 2017. 5: 33–40.

Higham et al. Electronic cigarette exposure triggers neutrophil inflammatory responses. Respir. Res, 2016 17(1):56

Hirano T et al., Electronic cigarette use and smoking abstinence in Japan: a cross-sectional study of quitting methods. Int. J. Environ. Res. Public Health, 2016. 14:189-202.

Holliday et al., E-cigarette vapour is not inert and exposure can lead to cell damage. Evidence-based dentistry, 2016. 17(1):2–3.

Hom Set al., Platelet activation, adhesion, inflammation, and aggregation potential are altered in the presence of electronic cigarette extracts of variable nicotine concentrations. Platelets, 2016. 27:694–702

Hornung V et al., Silica crystals and aluminum salts activate the NALP3 inflammasome through phagosomal destabilization. Nat Immunol, 2008. 9:847–856.

http://www.atsdr.cdc.gov/substances/formaldehyde/pdfs/revised_formaldehyde_report_1007.pdf

https://www.ons.gov.uk/peoplepopulationandcommunity/healthandsocialcare/healthandlifeexpectancies/bulletins/adultsmokinghabitsingreatbritain/2016.

Huo Y et al. The chemokine KC, but not monocyte chemoattractant protein-1, triggers monocyte arrest on early atherosclerotic endothelium. J Clin Invest, 200. 108:1307-1314.

Husari A et al. Acute exposure to electronic and combustible cigarette aerosols: effects in an animal model and in human alveolar cells. Nicotine Tob Res, 2016. 18: 613–619.

Hwang et al. Electronic cigarette inhalation alters innate immunity and airway cytokines while increasing the virulence of colonizing bacteria. J Mol Med, 2016. 94:667-679.

IARC (International Agency for Research on Cancer). 2006. Preamble to the IARC Monographs on the Evaluation of Carcinogenic Risk to Humans [online]. Available: http://monographs.iarc.fr/ENG/Preamble/index.php.

Imai H et al. Suppression of leukotriene formation in RBL-2H3 cells that overexpressed phospholipid hydroperoxide glutathione peroxidase. J Biol Chem, 1998. 273: 1990 - 1997.

Ismahil MA et al., Chronic oral exposure to the aldehyde pollutant acrolein induces dilated cardiomyopathy. Am. J. Physiol. Heart Circ. Physiol, 2011. 301, H2050–H206010.1152/ajpheart.00120.2011.

Jaiswal AK. NRF2 signaling in coordinated activation of antioxidant genes expression. Free Radic Biol Med, 2004. 36: 1199-1207.

Jamal A et al. Tobacco Use Among Middle and High School Students - United States, 2011–2016. MMWR Morb Mortal Wkly Rep, 2017. 66(23):597-603.

Jancova P et al., Phase II drug metabolizing enzymes. Biomed Pop Med Fac Univ Palacky Olomouc Cech Repub, 2010. 154: 103-116.

Jiang ZY et al., Ferrous ion oxidation in the presence of xylenol orange for detection of lipid hydroperoxide in low density lipoprotein. Anal Biochem, 1992. 202: 384-389.

Kalkhoran S and Glantz SA. E-cigarettes and smoking cessation in real-world and clinical settings: a systematic review and meta-analysis. Lancet Respir Med, 2016. 4: 116–128.

Kang CH et al., Apigenin promotes TRAIL-mediated apoptosis regardless of ROS generation". Food Chem Toxicol, 2018. 111: 623-630, 2018.

Karin M. Nuclear factor-kappaB in cancer development and progression. Nature, 2006. 441:431–436.

Katzung BG et al., Basic and clinical pharmacology, 12th edition. 2011. McGraw Hill.

Keller JN et al., Autophagy, proteosomes, lipofuscin and oxidative stress in the aging brain. Int J Biochem Cell Biol, 2004. 36: 2376-2380.

Klager Set al., Flavoring chemicals and aldehydes in e-cigarette emissions. Envir Sci Tech, 2017. 51(18):10806-13.

Kopa PN and Pawliczak R. IQOS® - a heat-not-burn (HnB) tobacco product - chemical composition and possible impact on oxidative stress and inflammatory response. A systematic review. Toxicol Mech Methods, 2019. 2:1-7.

Kosmider L et al., Cherry-flavoured electronic cigarettes expose users to the inhalation irritant, benzaldehyde. Thorax, 2016. 71(4):376–7.

Kosmider L et al., Nicotine emissions from electronic cigarettes: Individual and interactive effects of propylene glycol to vegetable glycerin composition and device power output. Food Chem Toxicol, 2018. 115:302-305.

KowittSD et al., Perceptions and experiences with flavored non-menthol tobacco products: A systematic review of qualitative studies. International Journal of Environmental Research, 2017. 14. First published on 2017/03/24.

Krämer S and Testa B, The Biochemistry of Drug Metabolism. An introduction. Part 7. Intra-individuals factors affecting drug metabolism. Chemistry and Biodiversity, 2009. 6: 1477-1660.

Kulik M et al., Electronic cigarette use is associated with lower odds of having stopped smoking: a cross-sectional study of 28 European Union countries. Am. J. Prev. Med. 2018. 54(4):603-609.

Laitinen A and Laitinen LA, Airway morphology: epithelium/basement membrane. American Journal of Respiratory and Critical Care Medicine, 1994. 150(5):S14–S17.

Leah RB et al., The copper chaperone CCS directly interacts with copper/zinc superoxide dismutase. J Biol Chem, 1998. 273: 23625–8.

Lee YJ et al. Glucose deprivation-induced cytotoxicity and alterations in mitogen-activated protein kinase activation are mediated by oxidative stress in multidrug-resistant human breast carcinoma cells. J Biol Chem, 1998. 273: 5294 -9.

Leigh NJ et al., Tobacco-specific nitrosamines (TSNA) in heated tobacco product IQOS®. Tob Control, 2018. 27(Suppl 1):s37-s38.

Leigh NJet al., Cytotoxic effects of heated tobacco products (HTP) on human bronchial epithelial cells. Tob Control, 2018. 27(Suppl 1):s26-s29.

Lerner CA et al., Vapors produced by electronic cigarettes and e-juices with flavorings induce toxicity, oxidative stress, and inflammatory response in lung epithelial cells and in mouse lung. PLoS One, 2015. 10: e0116732.

Levonen AL et al., Cellular mechanisms of redox cell signalling: role of cysteine modification in controlling antioxidant defences in response to electrophilic lipid oxidant products. Biochem J, 2004. 378: 373-382.

Lim HH and Shin HS. Determination of volatile organic compounds including alcohols in refill fluids and cartridges of electronic cigarettes by headspace solid-phase micro extraction and gas chromatography-mass spectrometry. Anal Bioanal Chem, 2017. 409(5): 1247–1256.

Lin E et al., Inflammatory cytokines and cell response in surgery. Surgery, 2000. 2: 117–26.

Lisko JG et al., Chemical composition and evaluation of nicotine, tobacco alkaloids, pH, and selected flavors in e-cigarette cartridges and refill solutions. Nicotine Tob Res, 2015. 17: 1270–1278.

Livak KJ and Schmittgen TD. Analysis of relative gene expression data using real-time quantitative PCR and the 2(-Delta Delta C(T)). Method. Methods, 2001. 25(4): 402–408.

Mantovani A et al., IL-1 and IL-1 regulatory pathways in cancer progression and therapy. Immunol Rev, 2018. 281(1): 57–61.

Mantovani A et al., Cancer-related inflammation. Nature, 2008. 454(7203): 436–444.

Manzoli L et al. Cohort study of electronic cigarette use: effectiveness and safety at 24 months. Tob. Control, 2017. 26: 284–92.

McConnell R et al., Electronic cigarette use and respiratory symptoms in adolescents. Am J Respir Crit Care Med, 2017. 195: 1043–1049.

McKee M and Capewell S. Evidence about electronic cigarettes: a foundation built on rock or sand? BMJ, 2015. 351:h4863.

McKelvey K et al., Heated tobacco products likely appeal to adolescents and young adults. Tob Control, 2018. 27(Suppl 1): s41-s47.

Melega S et al., Effect of sprout extract from Tuscan black cabbage on xenobiotic-metabolizing and antioxidant enzymes in rat liver. Mutat Res, 2013. 751: 45-51.

Misra M et al., Comparative In Vitro Toxicity Profile of Electronic and Tobacco Cigarettes, Smokeless Tobacco and Nicotine Replacement Therapy Products: E-Liquids, Extracts and Collected Aerosols. Int J Environ Res Pub H, 2014. 11(11): 11325–47.

Moheimani RS et al. Increased cardiac sympathetic activity and oxidative stress in habitual electronic cigarette users: implications for cardiovascular risk. JAMA Cardiol, 2017. 2: 278–84.

Mommsen P et al., Regulation of L-selectin expression by trauma-relevant cytokines. Pathol Res Pract, 2011. 3: 142–7.

Moses E et al. Molecular impact of electronic cigarette aerosol exposure in human bronchial epithelium. Toxicol Sci, 2017. 155: 248–257.

Muttray A et al., No acute effects of an exposure to 50 ppm acetaldehyde on the upper airways. Int Arch Occup Environ Health, 2009. 82: 481-488.

Nabavizadeh P et al., Vascular endothelial function is impaired by aerosol from a single IQOS® HeatStick to the same extent as by cigarette smoke. Tob Control, 2018. 27(Suppl 1):s13-s19.

Nasim A et al. Patterns of alternative tobacco use among adolescent cigarette smokers. Drug Alcohol Depend, 2012. 124(1-2): 26–33.

National Academy of Sciences. Emergency and Continuous Exposure Guidance Levels for Selected Submarine Contaminants Subcommittee on Emergency and Continuous Exposure Guidance Levels for Selected Submarine Contaminants, Committee on Toxicology, National Research Council, Washington, DC (2007).

Neilson Let al. Development of an in vitro cytotoxicity model for aerosol exposure using 3D reconstructed human airway tissue; application for assessment of e-cigarette aerosol. Toxicol In Vitro, 2015. 29: 1952–1962.

Newton K and Dixit VM. Signaling in innate immunity and inflammation. Cold Spring Harb Prospecr Biol, 2012. 4:a006049.

Nimlos et al., Mechanisms of glycerol dehydration. J Phys Chem A, 2006. 110: 6145–56.

Norton KJ et al., Initial puffing behaviors and subjective responses differ between an electronic nicotine delivery system and traditional cigarettes. Tob Induc Dis, 2014. 12(1):17.

Nutt DJ et al. Estimating the harms of nicotine-containing products using the MCDA approach. Eur Addict Res, 2014. 20: 218–25.

O'Toole et al., Acrolein activates matrix metalloproteinases by increasing reactive oxygen species in macrophages. Toxicol Appl Pharmacol, 2009. 236: 194–20110.

Ogunwale MA et al., Aldehyde Detection in Electronic Cigarette Aerosols. ACS Omega, 2017. 2(3): 1207–1214.

Ogunwale MA et al. Aldehyde detection in electronic cigarette aerosols. ACS Omega, 2017. 2: 1207–14.

Palamidas A et al. Acute effects of short term use of e-cigarettes on airways physiology and respiratory symptoms in smokers with and without airways obstructive diseases and in healthy non smokers. Tob Prev Cessation, 2017. 3: 5.

Pankow JF et al., Benzene formation in electronic cigarettes. PLoS One, 2017. 12(3):e0173055.

Paolini M et al., Co-carcinogenic e ect of beta-carotene. Nature, 1999. 398: 760–761.

Paolini M et al., Parkinson's disease, pesticides and individual vulnerability. TIPS, 2004. 25(3): 124-129

Paschke T et al., Effects of ingredients on cigarette smoke composition and biological activity: a literature overview. Beiträge zur Tab, 2014. 20: 107-247.

Pelkonen O et al., Inhibition and induction of human cytochrome P450 enzymes: current status. Arch Toxicol, 2008. 82: 667-715.

Phillips B et al. A 7-month cigarette smoke inhalation study in C57BL/6 mice demonstrates reduced lung inflammation and emphysema following smoking cessation or aerosol exposure from a prototypic modified risk tobacco product. Food Chem Toxicol, 2015. 80: 328–345.

Pierce AB. Genetics. A conceptual approach. Sixth edition. Blackwells, 2016.

Reidel B et al., E-cigarette use causes a unique innate immune response in the lung, involving increased neutrophilic activation and altered mucin secretion. Am J Respir Crit Care Med, 2018. 197: 492–501.

Robinson RJ et al., Electronic Cigarette Topography in the Natural Environment. PLoS One, 2015. 10(6) :e0129296.

Rodrigues Siqueira I et al., Alexandre Netto Aging affects oxidative state in hippocampus, hypothalamus and adrenal glands of Wistar rats. Life Sci, 2005. 78: 271-278.

Rushmore TH and Kong AN. Pharmacogenomics, regulation and signalling pathways of phase I and phase II drug-metabolizing enzymes. Curr Drug Metab, 2002. 3: 481-490.

Rusznak C et al., Effect of cigarette smoke on the permeability and IL-1beta and sICAM-1 release from cultured human bronchial epithelial cells of never-smokers, smokers, and patients with chronic obstructive pulmonary disease. Am J Respir Cell Mol Biol, 2000. 23: 530-536.

Salman R et al., Free-Base and Total Nicotine, Reactive Oxygen Species, and Carbonyl Emissions From IQOS®, a Heated Tobacco Product. Nicotine Tob Res, 2019. 21(9): 1285-1288.

Salman R et al., Lung Function in Users of a Smoke-Free Electronic Device With HeatSticks (IQOS®) Versus Smokers of Conventional Cigarettes: Protocol for a Longitudinal Cohort Observational Study. JMIR Res Protoc, 2018. 7(11) :e10006.

Salucci S et al., Melatonin prevents mitochondrial dysfunctions and death in differentiated skeletal muscle cells. Microsc Res Tech, 2017. 80(11): 1174-1181.

Sapone A et al., Perturbation of xenobiotic metabolism in Dreissena polymorpha model exposed in situ to surface water (Lake Trasimene) purified with various disinfectants. Chemosphere, 2016. 144: 548-554.

Scheffler S et al., Cytotoxic Evaluation of e-Liquid Aerosol using Different Lung-Derived Cell Models. Int J Environ Res Public Health, 2015. 12(10): 12466–74.

Scheffler S et al., Evaluation of E-cigarette liquid vapor and mainstream cigarette smoke after direct exposure of primary human bronchial epithelial cells. Int J Environ Res Public Health, 2015. 12(4): 3915–25.

Schripp T et al., Does e-cigarette consumption cause passive vaping? Indoor Air, 2013. 23: 25–31.

Schweitzer KS et al. Endothelial disruptive proinflammatory effects of nicotine and e-cigarette vapor exposures. Am J Physiol Lung Cell Mol Physiol, 2015. 309: L175-87.

Sheehan D et al., Structure, function and evolution of glutathione transferases: implications for classification of non-mammalian members of an ancient enzyme superfamily. Biochem J, 2001. 360: 1–16.

Shintani H., "Determination of Xanthine Oxidase". Pharm Anal Acta, 2013. S7: 004.

Sim VM and Pattle RE. Effect of possible smog irritants on human subjects. J Am Med Assoc, 1957. 165: 1908-1913.

Simonavicius E et al., What factors are associated with current smokers using or stopping e-cigarette use? Drug Alcohol Depend, 2017. 173: 139–43.

Sithu SD et al., Exposure to acrolein by inhalation causes platelet activation. Toxicol. Appl. Pharmacol, 2010. 248: 100–11010.

Sohal SS et al., IQOS® exposure impairs human airway cell homeostasis: direct comparison with traditional cigarette and e-cigarette. ERJ Open Res, 2019. 5(1): 00159-2018.

Soneji S et al., Association between initial use of e-cigarettes and subsequent cigarette smoking among adolescents and young adults: a systematic review and meta-analysis. JAMA Pediatr, 2017. 171: 788–97.

Spindle TR et al., Electronic cigarette use and uptake of cigarette smoking: a longitudinal examination of U.S. college students. Addict Behav 2017. 67:66–72

Srivastava S et al., Oral exposure to acrolein exacerbates atherosclerosis in apoE-null mice. Atherosclerosis, 2011. 215: 301–30810.

Stevens JF and Maier CS. Acrolein: sources, metabolism, and biomolecular interactions relevant to human health and disease. Mol Nutr Food Res, 2008. 52(1): 7–25.

Stroppolo ME et al., Cu,Zn superoxide dismutase from Photobacterium leignathi is an hyperefficient enzyme. Biochemistry, 1998. 37: 12287-92.

Suresh K et al. Hydrogen peroxide-induced calcium influx in lung microvascular endothelial cells involves TRPV4. Am J Physiol – Lung Cell Mol Physiol, 2015. 309(12): L1467–L1477.

Sussan TE et al., Exposure to electronic cigarettes impairs pulmonary anti-bacterial and anti-viral defenses in a mouse model. PLoS One, 2015. 10: e0116861.

Talal A et al., Association between electronic cigarette use and myocardial infarction: results from the 2014 and 2016 National Health Interview Surveys Presented at Annu Meet Res Nicotine Tob, 2018. 24th, Baltimore, MD.

Thomas B et al., Comparative evaluation of serum antioxidant levels in periodontally diseased patients: An interventional study. Contemp Clin Dent, 2014. 5(3): 340–344.

Thorne D et al., The mutagenic assessment of an electronic-cigarette and reference cigarette smoke using the Ames assay in strains TA98 and TA100. Mutat Res/Gen Toxicol Environ Mut. 2016. 812:29–38.

U.S. Department of Health and Human Services. How Tobacco Smoke Causes Disease: The Biology and Behavioral Basis for Smoking-Attributable Disease: A Report of the Surgeon General.

U.S. Department of Health and Human Services, Centers for Disease Control and Prevention, National Center for Chronic Disease Prevention and Health Promotion, Office on Smoking and Health; Atlanta, GA: 2010.

U.S. Environmental Protection Agency, 2003. http://epa.gov/airtoxics/188polls.html

Uchiyama S et al., Determination of carbonyl compounds generated from the e-cigarette using coupled silica cartridges impregnated with hydroquinone and 2,4-dinitrophenylhydrazine, followed by high-performance liquid chromatography. Anal Sci, 2013. 29: 1219-1222.

UK Off. Natl. Stat. 2016 Adult smoking habits in Great Britain: 2014 Stat. Bull., Off. Natl. Stat., Newport, UK

Valko M et al., Free radicals, metals and antioxidants in oxidative stress-induced cancer. Chem Biol Interact, 2006. 160(1): 1-40.

van Berlo JH et al., Signaling effectors underlying pathologic growth and remodeling of the heart. The Journal of clinical investigation, 2013. 123(1): 37–45.

Vardavas CI al., Short-term pulmonary effects of using an electronic cigarette: impact on respiratory flow resistance, impedance, and exhaled nitric oxide. Chest, 2012. 141: 1400–1406.

Vilema-Enríquez G et al., Molecular and cellular effects of hydrogen peroxide on human lung cancer cells: potential therapeutic implications. Oxi Med Cell Longev, 2016. 2016:1908164.

Vivarelli F et al., The combined effect of Sango sprout juice and caloric restriction on metabolic disorders and gut microbiota composition in an obesity model. Int J Food Sci Nutr, 2018. 69(2): 192-204.

Vivarelli F et al., Disruption of redox homeostasis and carcinogen metabolizing enzymes changes by administration of vitamin E to rats. Life Sci, 2016. 145: 166-73.

Vivarelli F et al., Raphanus sativus cv. Sango Sprout Juice Decreases Diet-Induced Obesity in Sprague Dawley Rats and Ameliorates Related Disorders. PLoS ONE, 2016. 11: e0150913.

Wang GW et al., Acrolein consumption exacerbates myocardial ischemic injury and blocks nitric oxide-induced PKCε signaling and cardioprotection. J Mol Cell Cardiol, 2008. 44: 1016–1022.

Wang MP et al., Electronic cigarette use and respiratory symptoms in chinese adolescents in hong kong. JAMA Pediatr, 2016. 170: 89–91.

Wang P et al., A device-independent evaluation of carbonyl emissions from heated electronic cigarette solvents. PLoS ONE, 2017. 12(1): e0169811.

Waris G and Ahsan H, Reactive oxygen spices: role in the development of cancer and various chronic conditions. Journal of Carcinogenesis, 2006. 4: 14.

Weber-Tschopp A et al., Experimentally induced irritating effects of acrolein on men (author's transl). Int Arch Occup Environ Health, 1977. 40: 117-130.

WHO Guidelines for Indoor Air Quality: Selected Pollutants, 978 92 890 0213 4. World Health Organization. WHO Regional Office for Europe, Copenhagen, Denmark (2010).

Wienkers LC and Heat TG. Predicting in vivo drug interaction from in vitro drug discovery data. Nat Rev Drug Discov, 2005. 4: 825-833.

Wills TA et al. Risk factors for exclusive e-cigarette use and dual e-cigarette use and tobacco use in adolescents. Pediatrics, 2015. 135(1): e43–e51.

Yingst JM et al., A method for classifying user-reported electronic cigarette liquid flavors. Nicotine Tob Res, 2017. 19(11); 1381-1385.

Yong HH et al. Does the regulatory environment for e-cigarettes influence the effectiveness of e-cigarettes for smoking cessation?: Longitudinal findings from the ITC Four Country Survey. Nicotine Tob. Res, 2017. 19(11): 1268-1276.

Zeidel A et al., Immune response in asymptomatic smokers. Acta Anaesthesiol Scand, 2002. 46: 959-964.

Zelová H and Hošek J. TNF-α signalling and inflammation: interactions between old acquaintances. Inflamm Res, 2013. 62(7): 641-51.

Zhang DD and Hannink M. Distinct cysteine residues in Keap1 are required for Keap1-dependent ubiquitination of Nrf2 and for stabilization of Nrf2 by chemopreventive agents and oxidative stress. Mol Cell Biol, 2003. 23: 8137-8151.

Zhang S et al., Application of the Ca^{2+} indicator fluo-3 and fluo-4 in the process of H2O2 induced apoptosis of A549 cell. Chin J Lung Cancer, 2014. 17(3):197–202.

Zhuang YL et al., Long-term e-cigarette use and smoking cessation: a longitudinal study with US population. Tob Control, 2016. 25: i90–95.

ATTACHMENTS

Regulatory Toxicology and Pharmacology 109 (2019) 104500

Contents lists available at ScienceDirect

Regulatory Toxicology and Pharmacology

journal homepage: www.elsevier.com/locate/yrtph

Impact of electronic cigarette heating coil resistance on the production of reactive carbonyls, reactive oxygen species and induction of cytotoxicity in human lung cancer cells *in vitro*

Silvia Cirillo[a], Jose F. Urena[b], Joshua D. Lambert[b,c], Fabio Vivarelli[a], Donatella Canistro[a], Moreno Paolini[a], Vladimiro Cardenia[d], Maria Teresa Rodriguez-Estrada[e,f], John P. Richie Jr.[g], Ryan J. Elias[b,*]

[a] Department of Pharmacy and Biotechnology, Alma Mater Studiorum-University of Bologna, Italy
[b] Department of Food Science, The Pennsylvania State University, College of Agricultural Sciences, University Park, PA, USA
[c] Center for Molecular Carcinogenesis and Toxicology, The Pennsylvania State University, University Park, PA, USA
[d] Department of Agricultural, Forest and Food Sciences, University of Turin, Italy
[e] Department of Agricultural and Food Sciences, Alma Mater Studiorum-University of Bologna, Italy
[f] Interdepartmental Centre for Industrial Agrofood Research, Alma Mater Studiorum-University of Bologna, Italy
[g] Department of Public Health Sciences, Pennsylvania State University Tobacco Center of Regulatory Science (TCORS), The Pennsylvania State University, College of Medicine, Hershey, PA, USA

ARTICLE INFO

Keywords:
E-cig
Resistance
Oxidative stress
Carbonyl compounds
Lung cancer cells

ABSTRACT

Electronic cigarette (e-cigarette; e-cig) use has grown exponentially in recent years despite their unknown health effects. E-cig aerosols are now known to contain hazardous chemical compounds, including carbonyls and reactive oxygen species (ROS), and these compounds are directly inhaled by consumers during e-cig use. Both carbonyls and ROS are formed when the liquid comes into contact with a heating element that is housed within an e-cig's atomizer. In the present study, the effect of coil resistance (1.5 Ω and 0.25 Ω coils, to obtain a total wattage of 8 ± 2 W and 40 ± 5 W, respectively) on the generation of carbonyls (formaldehyde, acetaldehyde, acrolein) and ROS was investigated. The effect of the aerosols generated by different coils on the viability of H1299 human lung carcinoma cells was also evaluated. Our results show a significant ($p < 0.05$) correlation between the low resistance coils and the generation of higher concentrations of the selected carbonyls and ROS in e-cig aerosols. Moreover, exposure to e-cig vapor reduced the viability of H1299 cells by up to 45.8%, and this effect was inversely related to coil resistance. Although further studies are needed to better elucidate the potential toxicity of e-cig emissions, our results suggest that these devices may expose users to hazardous compounds which, in turn, may promote chronic respiratory diseases.

1. Introduction

Electronic cigarettes (e-cigarettes, e-cigs) have been on the consumer market for almost a decade and are marketed as an alternative to conventional combustion cigarettes. E-cigs have been promoted as a potential approach to aid in smoking cessation (Franks et al., 2018). Of particular concern, e-cig popularity has grown rapidly among young people worldwide. In 2014, e-cig use among US adolescents surpassed the use of conventional cigarette for the first time (Arrazola et al., 2014). While e-cigs do not produce carcinogenic combustion products such as polycyclic aromatic hydrocarbons, and e-cig liquids do not contain tobacco associated carcinogens (e.g., nitrosoamines), there is growing evidence that e-cigs do generate harmful substances during their use. Several authors have reported the presence of reactive carbonyls, including formaldehyde, acetaldehyde, acetone and others, in e-cigarette vapor (Goniewicz et al., 2014; Ogunwale et al., 2017; Bitzer et al., 2019). In addition, both stable, long-lived radicals (Lerner et al., 2015a, 2015b; Sussan et al., 2015) and short-lived, highly reactive radicals (Goel et al., 2015) have been found in e-cig vapor. Oxidative stress induced by cigarette smoke has been shown to play a key role in the pathogenesis of cancer (Pryor, 1997), cardiovascular disease (Messner and Bernhard, 2014), and chronic obstructive pulmonary disease (COPD) (Centers for Disease Control and Prevention, 2010; Domej et al., 2014; Kirkham and Rahman, 2006). Likewise, e-cig vapor can induce oxidative stress that

* Corresponding author.
E-mail address: elias@psu.edu (R.J. Elias).

https://doi.org/10.1016/j.yrtph.2019.104500
Received 26 April 2019; Received in revised form 10 October 2019; Accepted 12 October 2019
Available online 17 October 2019

can lead to inflammation (Lerner et al., 2015a; Muthumalage et al., 2018; Scott et al., 2018), cytotoxicity *in vitro* (Scott et al., 2018; Vasanthi Bathrinaraynan et al., 2018; Scheffler et al., 2015; Zhang et al., 2012) and toxicity *in vivo* that may increase cancer risk (Canistro et al., 2017).

In contrast to conventional cigarettes, which differ primarily in terms of nicotine content, tobacco variety and filter type, e-cigs are highly customizable with respect to their operating parameters and the chemical composition of their liquids. These liquids are available in a wide-variety of flavors and nicotine levels, and e-cig devices can be programmed to achieve variable power output and variable heating coil resistance levels. Unlike conventional cigarettes, the possibility to choose among such different flavors (e.g., fruit, dessert, tobacco) is particularly appealing to adolescents and young adults (Harrell et al., 2017; Yingst et al., 2017).

In most cases, modern e-cig devices consist of a mouthpiece, a refillable cartridge, a lithium battery and a heating atomizer. Users activate the heating coil in the atomizer by depressing the device's power button during inhalation; thus, the flavored liquid is rapidly vaporized by passing through the heating element. With new generation devices, users can modulate the e-cig liquid vaporization process by selecting atomizers with different coil resistances, by applying different voltages across the coils, and/or by controlling the operating temperature of the atomizer. According to recent reports, the design and operation settings of e-cigs may have a significant impact on human health (Chausse et al., 2015). Contrary to the initial hypothesis that voltages higher than 3.3 V and up to 5 V are responsible for formaldehyde generation in e-cig aerosols (Jensen et al., 2015), it is now well established that formaldehyde is produced even under lower powered, breath-activated devices (Bitzer et al., 2019). Most of the hazardous carbonyls detected in e-cig vapors are produced during the thermal decomposition of vegetable glycerol (VG) and propylene glycol (PG), the major chemical constituents of most e-cig liquids. In a recent study, significant amounts of formaldehyde and acetaldehyde were detected at temperatures greater or equal to 215 °C when PG and VG were vaporized by an e-cig, while acrolein was observed when VG was subjected to a temperature in excess of 270 °C (Wang et al., 2017). The heating power of the device is a function of the combination of the coil's resistance value and the voltage applied by the e-cig's battery (i.e., the Joule effect) (Chausse et al., 2015). As such, consumers who use a low-voltage device are able to obtain the same power of a high-voltage e-cig by selecting an appropriate coil.

The aim of the present study was to determine the effect of coil resistance (1.5 Ω and 0.25 Ω coils, to obtain a total wattage of 8 ± 2 W and 40 ± 5 W, respectively) on carbonyl and ROS generation by e-cigs and to evaluate the biological effects of the resulting e-cig vapors on the viability of H1299 human lung adenocarcinoma cells following exposure using an *in vitro* air-liquid interface (ALI) exposure system.

2. Material and methods

2.1. E-cigarette devices and settings

A commercially available Eleaf Pico e-cig consisting of a 2.5 mL liquid tank made of Pyrex glass and a rechargeable lithium battery (MXJO IMR 18650 3000 mAh 35A 3.7 V High Drain Flat Top Rechargeable Battery) was used for all studies (Fig. 1). The voltage value was set at 3.5 V and two different coils (Joyetech™, 1.5 Ω and 0.25 Ω) were used to obtain a total wattage of 8 ± 2 W and 40 ± 5 W, respectively. In order to prevent the confounding effect of coil aging, a new element was used for each experiment.

2.2. E-liquids

Studies to determine carbonyl compounds in e-cig aerosols used a PG/VG base solution (50/50, *v/v*) (Fumador S.r.l., Milan, Italy) without nicotine (eL-N) and with nicotine (18%; eL + N). A red fruits flavor concentrate (Chemfont S.r.l., Rome, Italy) was then added to a final concentration of 10% (*v/v*). For studies examining ROS production and effects on cell viability, the e-cig liquid was composed of a PG/VG base (50/50, *v/v*) (NicVape, USA) without nicotine to which a raspberry flavor concentrate (NicVape, USA) was added at a concentration of 10% (*v/v*).

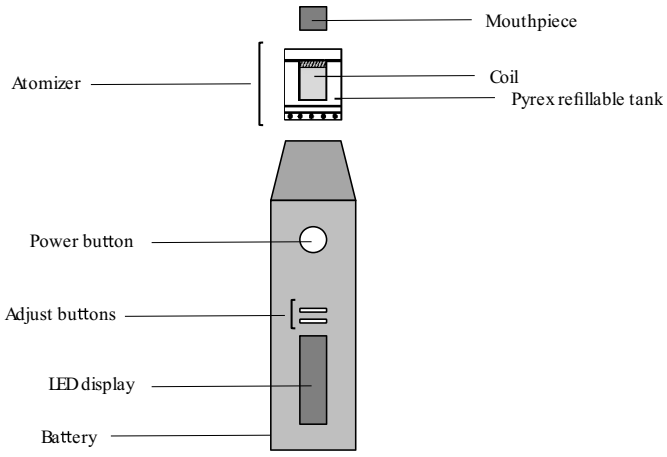

Fig. 1. Schematic representation of the e-cig device used for the study.

2.3. Detection of carbonyl compounds: formaldehyde, acetaldehyde and acrolein

To establish the presence of formaldehyde, acetaldehyde and acrolein, a 30-L propylene box was filled using the following puff profile: puff on 6 s, puff off 5 s; the puffing sequence was repeated twice (Goel et al., 2015; Canistro et al., 2017; Cardenia et al., 2018). Formaldehyde, acetaldehyde and acrolein were determined by headspace-solid phase microextraction (HS-SPME) coupled to gas chromatography-mass spectrometry (GC/MS), as reported in our previous study (Canistro et al., 2017) with some modifications. A SPME device having a fused-silica fiber (10-mm length) coated with DVB/CAR/PDMS (50/30 mm thickness), was used. After conditioning at 270 °C for 60 min, the SPME fiber was exposed to the box headspace at room temperature. After a 2-min exposure, the fiber was desorbed at 250 °C for 10 min in the injector of the GC/MS system (Q2010 Plus, Shimadzu, Japan). The sample was injected into a RTX-WAX column (30 m, 0.25 mm i.d., 0.25 μm film thickness, Restek, USA) in split mode (1:20 split ratio). Helium was used as carrier gas with a linear velocity of 36.2 cm/s. The oven temperature was kept at 35 °C for 10 min, then raised to 240 °C at 30 °C/min. Injector and interface temperatures were set at 250 and 230 °C, respectively. Compounds were recognized by comparing their mass spectra and retention time with those of the corresponding chemical standards. The quantification of formaldehyde, acetaldehyde and acrolein signal was carried out by Single Ion Monitoring (SIM), using 29 *m/z*, 44 *m/z* and 56 *m/z*, respectively. The construction of the calibration curves in this case could not provide reproducible results, due to the difference of vapor pressure of carbonyls when used alone or in presence of other compounds (Liu et al., 2016). Therefore, as suggested in literature (Wang et al., 2017; Geiss et al., 2016), a normalized response factor (Rf) was calculated based on the concentration of carbonyls present in the environment as basal level, according to the following expression:

$$Rf = (A_x - A_y)/A_y$$

where A_x and A_y represent the peak areas of carbonyls detected after and before (basal) the vaping process in the exposure box, respectively.

2.4. Cell-free ROS

The ROS production was estimated using the dye 2′,7′-

dichlorodihydrofluorescein diacetate (DCFH-DA), as previously reported by Lerner et al. (2015a). To catalyze the reaction between DCFH and ROS, horseradish peroxidase (HRP) was added. Vapor was pulsed into the bubbler (Ace Glass Inc., Vineland, NJ) at room temperature using the following puffing topography: puff on 4 s, puff off 26 s, flow rate 1.5 L/min; this puffing sequence was repeated 15 times, for a total time of exposure of 7.5 min (total number of puffs: 15). The oxidized dichloro-fluorescein (DCF) fluorescence was measured using a Fluroskan Ascent FL spectrofluorometer (Thermo Fisher Scientific Inc., Waltham, MA) at absorbance/emission maxima of 485 nm/535 nm; H_2O_2 standards were used to calibrate the fluorescence intensity units (FIU). DCF fluorescence data are expressed as μM of H_2O_2 equivalents. The assay was conducted using both phosphate buffer (PBS) and cell medium as reaction mixture.

2.5. Air-liquid interface cell culture and exposure

H1299 human lung adenocarcinoma cells were purchased from ATCC (Manassas, VA). The cells were cultured in RPMI 1640 basal media supplemented with 10% fetal bovine serum, 1% penicillin and 1% streptomycin at 37 °C under a 5% CO_2 atmosphere. Before aerosol exposure, cells were plated in 60-mm dishes and grown to 50–70% confluence. Cells were then exposed to air or e-cig vapor in a modified vacuum desiccator (500 mL volume, SP Scienceware, Warminster, PA) using the following puffing topography: puff on 4 s, puff off 26 s, flow rate 15 L/min; this puffing sequence was repeated 15 times, for a total time of exposure of 7.5 min (total number of puffs: 15). In addition to the analytical needs, this topography was also more representative of the real human use of e-cig and allowed us to reinforce the correlation between our results and the actual health risks for e-cig consumers (Norton et al., 2014; Robinson et al., 2015). This treatment protocol was repeated once after 2 h. Cells were exposed to a total number of 30 puffs.

2.6. Cell viability measurement

The 3-(4,5-dimethylthiazol-3-yl)-2,5-diphenyl tetrazolium bromide (MTT) assay (Cat# M5655, Sigma Aldrich, St. Louis, MO) was used to assess cell viability 24 h after e-cig vapor exposure. Briefly, 24 h after exposure, H1299 cells were washed twice with PBS and then incubated with MTT (1 mg/mL) in RMPI 1640 medium at 37 °C for 30 min. The medium was then removed and dimethyl sulfoxide (DMSO) was added to solubilize the formazan dye; the absorbance was measured at 550 nm using a Multiskan GO microplate spectrophotometer (Thermo Fisher Scientific Inc., Waltham, MA). The viability of cells exposed to e-cig vapor was normalized to the viability of air-exposed cells.

2.7. Statistical analysis

Data referred to as carbonyls compounds are expressed as mean ± standard deviation (SD) of three independent replicates (n = 3) and analyzed by means of one-way ANOVA to evaluate the influence of different conditions tested ($p < 0.05$). Data referred to as DCFH-DA assay in PBS (vapor condensate and air-liquid interface) are expressed as mean ± standard deviation (SD) of six independent replicates. For DCFH-DA assay in cell medium, results are indicated as relative percentage of the ROS content in control samples arbitrarily set at a value of 100% (mean ± SD of six independent replicates). Cell viability determined by MTT assay is expressed as percentage variation of viable cells relative to control group arbitrarily set at 100% (mean ± SD of six independent replicates). One-way ANOVA, followed by Tukey's multiple comparison test, was carried out at a 95% confidence level ($p \leq 0.05$), to separate means of parameters that were statistically different.

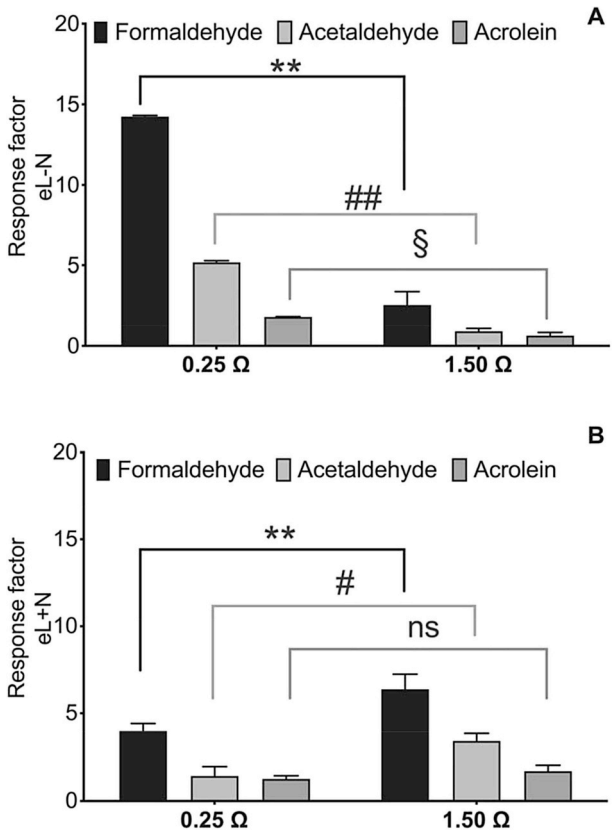

Fig. 2. Effects of resistance value (0.25 Ω and 1.5 Ω) on formaldehyde, acetaldehyde and acrolein levels in vapors released by eL-N (without nicotine) (A) and eL + N (with nicotine) (B). Data represent mean ± SD of three independent replicates. Different letters (a-b) for each aldehyde denote statistically different means (Tukey's test; $p < 0.05$) related to the resistance values; different letters (x-z) for each resistance value denote statistically different means (Tukey's test; $p < 0.05$) related to carbonyls.

3. Results

3.1. Formaldehyde, acetaldehyde and acrolein levels

In general, eL-N generated higher levels of carbonyls than eL + N. Formaldehyde was the main aldehyde produced in both liquids, followed by acetaldehyde and acrolein; however, the observed concentrations of carbonyls were strictly related to both the composition of liquids and the resistance value. For eL-N, acrolein, acetaldehyde and formaldehyde levels generated by 0.25 Ω coil were three-to seven-fold higher than those generated by the 1.50 Ω coil (Fig. 2A). In contrast, the carbonyl content was higher with the 1.50 Ω coil compared to 0.25 Ω coil when eL + N was used (Fig. 2B). Fig. 2B shows that when the eL + N was used, the 1.50 Ω coil resulted in the highest generation rate of carbonyls, especially formaldehyde, which was significantly ($p < 0.05$) higher than acetaldehyde and acrolein; however, the latter was not significantly affected by the resistance value. Since the eL-N led to the highest production of hazardous carbonyls, an eL-N was chosen for subsequent ROS generation and cell viability experiments.

3.2. ROS levels generated by e-cig vapor in PBS

ROS levels generated by e-cigs were determined by collecting vapor in PBS and measured in both the bubbler (vapor condensate) and at the ALI using the exposure chamber described above. Results obtained by analyzing the vapor condensate (Fig. 3A) showed more than six-fold higher levels of ROS in samples obtained with the 0.25 Ω coil compared to air control, and about three-fold higher if compared with 1.5 Ω

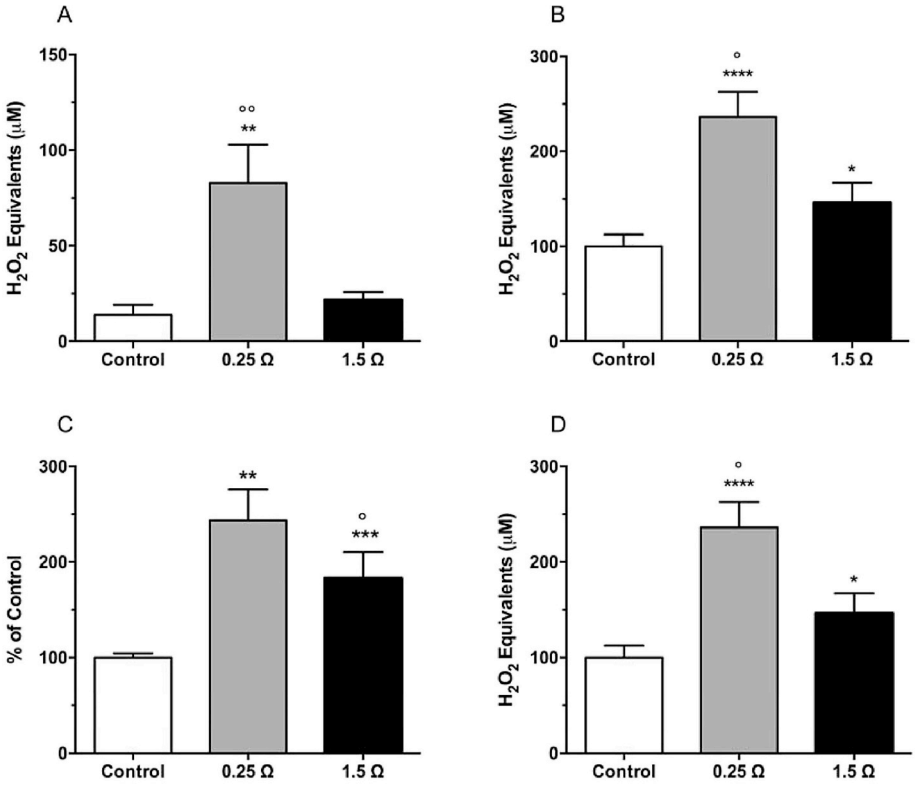

Fig. 3. Effect of resistance values on ROS levels in e-cig vapor. Fresh air control and e-cig vapor were pulsed through DCFH-HRP ROS indicator solution in (**A, B**) phosphate buffer and (**C, D**) cell culture media in (**A, C**) vapor condensate and (**B, D**) the ALI during a 7.50 min exposure. Data represent mean ± SD of six independent replicates. $^{**}p < 0.01$; $^{***}p < 0.0002$ significant results between 1.5 Ω/0.25 Ω groups and control group using one-way ANOVA (Tukey's multiple comparison test). $^{\circ}p < 0.05$; $^{\circ\circ}p < 0.01$ significant results between 0.25 Ω and 1.5 Ω group using one-way ANOVA (Tukey's multiple comparison test).

($p < 0.01$). The same trend was found when ROS levels were measured at the ALI (Fig. 3B).

3.3. ROS levels generated by e-cig vapor in cell medium

To determine if e-cig vapor produces ROS under cell culture conditions, the DCFH-DA assay was conducted using cell media as solvent under the experimental conditions mentioned previously. In both the bubbler and the ALI exposure chamber, the results followed the same trend as those obtained with PBS. The 0.25 Ω coil produced significantly higher levels of ROS when compared to control in both experimental conditions (+82.9%, $p < 0.001$ in vapor condensate; +46.3%, $p < 0.05$ in the air-liquid interface) (Fig. 3C and D). When compared to the control, the 0.25 Ω coil produced increased ROS levels: 143.9% in condensate ($p < 0.0002$) and 136.2% in air-liquid interface ($p < 0.0001$) (Fig. 3C and D).

3.4. Cell viability

H1299 cell viability was measured 24 h after exposure in the experimental chamber. Results from the MTT assay (Fig. 4A) showed that cell survival was inversely related to the total wattage of the devices. The effect of the 1.5 Ω coil group (10% reduction) had borderline statistical significance ($p = 0.058$). Cell viability decreased to 45.8% ($p < 0.0001$) when cells were exposed to the vapor generated by using the 0.25 Ω coil. Cell viability was observed to be inversely correlated to ROS production in cell medium revealed in the exposure chamber (Fig. 4B).

4. Discussion

E-cigs are composed of several components which, in many cases, can be modulated or modified according to a consumer's preferences. Among the modifiable components, the coil that is present in the atomizer is the element that, in combination with the applied voltage, is responsible for heating the liquid, which is generally composed of variable percentages of PG, VG, flavors and nicotine. It is well-established that thermal decomposition of the PG-VG mixture leads to the formation of toxic and carcinogenic carbonyls, such as formaldehyde, acetaldehyde and acrolein (Paschke et al., 2014; Uchiyama et al., 2013). Several studies have also reported that e-cig vapor contains relatively high levels of free radical species (Lerner et al., 2015a, 2015b; Sussan et al., 2015; Pryor, 1997), which are known to be important causal factors in many tobacco related diseases and disorders, such as cardiovascular diseases, COPD and cancer (Messner and Bernhard, 2014; Dekhuijzen, 2004; MacNee and Rahman, 2001).

In the present study, we investigated the role of an e-cig's heating coil resistance with respect to the generation of carbonyls and ROS. Here, we report for the first time that the levels of selected hazardous carbonyls and ROS increase as coil resistance is reduced. The presence or absence of nicotine was also observed to affect the production of carbonyls with eL-N producing higher levels of carbonyls than eL+N. As reported by Kosmider et al. (2014), the composition of e-cig significantly affects the composition of the released carbonyl compounds. In general, the composition of the volatile fraction is strictly linked to the thermodynamic equilibrium between the vapor and condensed (liquid) phases, but there are other aspects that could have contributed to the detected differences. In fact, it has been observed that the carbonyl production is highest when low resistance coils are used, because more e-liquid is consumed at higher wattage settings (Kosmider et al., 2014; Geiss et al., 2016); in addition, the temperature of the e-cig device may also be higher and this can lead to increased carbonyl concentrations as well (Kosmider et al., 2014; Geiss et al., 2016). On the other hand, when nicotine e-liquid is used, carbonyl production is likely lower because nicotine increases pH of the liquid and this may impair the formation of carbonyls, as their production is acid-catalyzed. Our results are consistent with previous studies demonstrating that the level of carbonyl compounds in e-cig vapors is affected by presence of nicotine and battery voltage (Kosmider et al., 2014). The latter is a relevant issue considering that e-cigs have become popular during the past decade

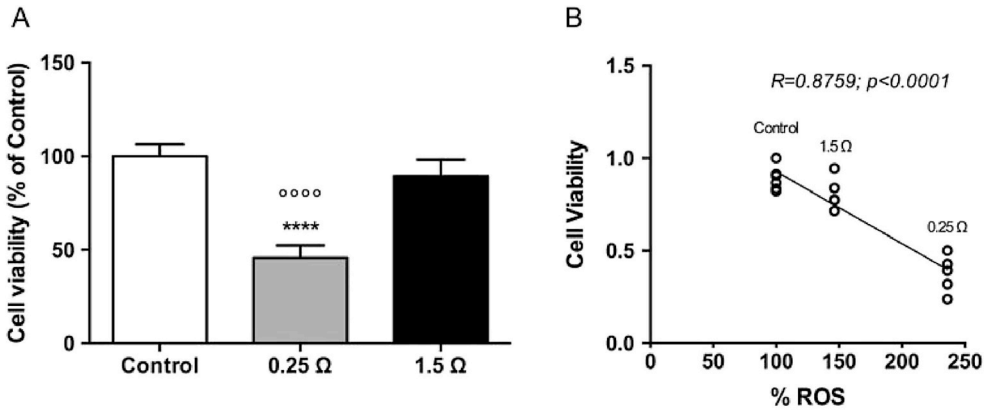

Fig. 4. Relationship between cell viability, coil resistance and ROS generation. (**A**) Effect of vapor generated from e-cigs equipped with 1.5 Ω and 0.25 Ω coils on viability of H1299 cells by MTT assay. Data are expressed as percentage relative to viable cells in control arbitrarily set at a value of 100%; Data represent mean ± SD of six independent replicates. $^{**}p < 0.01$; $^{***}p < 0.0002$ significant results between 1.5 Ω/0.25 Ω groups and control group using one-way ANOVA (Tukey's multiple comparison test). $^{\circ}p < 0.05$; $^{\circ\circ}p < 0.01$ significant results between 0.25 Ω and 1.5 Ω group using one-way ANOVA (Tukey's multiple comparison test). (**B**) Cell viability in each group inversely correlates vs. ROS generation (R = 0.8795; $p < 0.0001$).

(Korzun et al., 2019) for having the capacity of modulating the nicotine content of the liquid.

Human exposure to these low molecular weight carbonyls represents a risk factor for occurrence of neoplastic diseases. In particular, formaldehyde and acetaldehyde are classified as Group 1 and Group 2B carcinogens, respectively, by the International Agency for Research on Cancer (IARC, 2012). Acrolein is listed as a hazardous air pollutant by the United States Environmental Protection Agency (U.S. EPA, 2003). The presence of higher carbonyls levels in eL-N liquid overturns the idea that the absence of nicotine makes the liquid safer. There is no doubt that nicotine is the molecule responsible for addiction and its employment in e-cig is considered a gateway towards the consumption of tobacco cigarette. However, the toxic carbonyls detected in this study represent a risk factor for the onset and development of neoplastic and chronic diseases (Primack et al., 2015; Soneji et al., 2017). This is of particular concern considering that, in many Countries, the nicotine-free e-cig can be sold to adolescent younger than 18 years old.

The generation of carbonyls is related to the formation of radicals (e.g., hydroxyl radicals), which are responsible for the oxidation and fragmentation of glycols (Geiss et al., 2016). For this reason, the ROS levels were measured in both vapor and cell medium using the DCFH-DA assay in a cell-free system. Although the exposure profile was different from the one used for detecting the selected carbonyl compounds, the results exhibited the same trend. The reduction of the coil resistance, and thus the increase of the heating and the total wattage of the device, played an important role in terms of ROS formation. Our results appear to confirm the hypothesis of Lerner et al. (2015a) who reported that one of the possible sources of ROS could be the heating element. We examined the biological implications of the ROS and carbonyls by examining the effect of e-cig vapor on the viability of H1299 human lung adenocarcinoma cells. We found that vapor from eL-N significantly reduced cell viability and that these effects were directly related to the levels of ROS produced.

High levels of ROS represent a risk factor for the onset of several diseases and pathological conditions, including cancer and inflammation (Waris and Ahsan, 2006). ROS are able to create DNA strand breaks, cross-links, and can cause modification to the purine, pyrimidine and deoxyribose components of DNA (Halliwell, 2014). In an *in-vivo* study, e-cig aerosol caused accumulation of 8-hydroxy-deoxyguanosine (8-OH-dG) which can lead to mutations, with a significant correlation with ROS content, thus probably resulting in inflammatory response and neoplastic development (Canistro et al., 2017).

Others have previously examined the impact of e-cig vapor and e-cig extract on the morphology and viability of lung cells using both air-liquid interface or direct exposure to e-cig extract (Lerner et al., 2015b; Cervellati et al., 2014; Higham et al., 2018). *Ex vivo* treatment of bronco-epithelial cells from both patients with COPD and healthy subjects with e-cig extracts increased some inflammatory responses including altered cytokine and chemokine production (Higham et al., 2018).

In support of these data, epidemiological studies have indicated an association between e-cig use and respiratory disorders, especially asthma, bronchitis and COPD (Choi and Bernat, 2018; McConnell et al., 2017; Schweitzer et al., 2017; Wills et al., 2015). Altogether, these findings confirm the pivotal role of oxidative stress induced by e-cig use in the onset and development of respiratory diseases in healthy subjects or in the transition of initial symptomatology in chronic disorders.

5. Conclusions

In conclusion, the technology of newer generation e-cigs allows users to easily switch among heating elements in order to generate more or less aerosols and/or to intensify or reduce the flavor intensity of e-liquids. The ability to manipulate these parameters, together with the option that consumers have to select different e-liquid flavors and nicotine content, allows users to use e-cigs without any indication on its potential risks. Since the device and liquids used in this study are commercially-available, we believe that the exposure conditions, and consequently the generated carbonyls and ROS levels, are relevant to public health. Based on the results of this present study, the use of lower resistance coils coupled with an intermediate voltage setting (i.e., 3.5 V) can potentially represent a considerable health concern. Our results indicate how the generation of thermal degradation by-products depends not only on the applied voltage but also on resistance. Our study demonstrates the need for e-cig consumers to be cautious when assuming that low-voltages may be synonymous with “safer” devices (Thomson and Lewis, 2015), and in a broader sense, reiterates that after more than a decade of research, a “safe level” of exposure from e-cig aerosols cannot yet be established.

Author contributions

The manuscript was written through contributions of all authors. All authors have given approval to the final version of the manuscript.

Funding

This research was supported by the Basic Research Funding [RFO 2016, Alma Mater Studiorum-Università di Bologna, Italy]; the Marco Polo fellowship program [Alma Mater Studiorum-Università di Bologna, Italy]; and the USDA National Institute of Food and Agriculture and Hatch Appropriations under Project #PEN04691 and Accession #1018545. This work was also supported in part by the National Institute on Drug Abuse of the National Institutes of Health and the Center for Tobacco Products of the U.S. Food and Drug

Administration [under Award Number P50-DA-036107]. The content is solely the responsibility of the authors and does not necessarily represent the official views of the National Institutes of Health or the Food and Drug Administration.

Declaration of competing interest

The authors declare that they have no known competing financial interests or personal relationships that could have appeared to influence the work reported in this paper.

Abbreviations

ROS	reactive oxygen species
COPD	chronic obstructive pulmonary disease
PG	propylene glycol
VG	vegetable glycerol
DCFH-DA	2′,7′-dichloro-dihydro-fluorescein diacetate
HRP	horseradish peroxidase
DCF	dichloro-fluorescein
H_2O_2	hydrogen peroxide
MTT	3-(4,5-Dimethylthiazol-3-yl)-2,5-diphenyl Tetrazolium Bromide FIU, fluorescence intensity units IARC, International Agency for Research on Cancer
U.S. EPA	United States Environmental Protection Agency
HS-SPME	headspace-solid phase microextraction
GC/MS	gas chromatography/mass spectrometry
Rf	response factor
eL-N	liquid without nicotine
eL + N	liquid with nicotine
ALI	air-liquid interface

References

Arrazola, R.A., Singh, T., Corey, C.G., Husten, C.G., Neff, L.J., Apelberg, B.J., Bunnel, R.E., Choiniere, C.J., King, B.A., Cox, S., McAfee, T., Caraballo, R.S., 2014. Tobacco use among middle and high school students – United States, 2011-2014. MMWR Morb. Mortal. Wkly. Rep.

Bitzer, Z.T., Goel, R., Reilly, S.M., Bhangu, G., Trushin, N., Foulds, J., Muscat, J., Richie, J.P., 2019. Emissions of free radicals, carbonyls, and nicotine from the NIDA Standardized Research Electronic Cigarette and comparison to similar commercial devices. Chem. Res. Toxicol (Epub ahead of print).

Canistro, D., Vivarelli, F., Cirillo, S., Marquillas, C.B., Buschini, A., Lazzaretti, M., Marchi, L., Cardenia, V., Rodriguez-Estrada, M.T., Lodovici, M., et al., 2017. E-Cigarettes induce toxicological effects that can raise the cancer risk. Sci. Rep. 7 (1), 2028.

Cardenia, V., Vivarelli, F., Cirillo, S., Paolini, M., Canistro, D., Rodriguez-Estrada, M.T., 2018. The effect of electronic-cigarettes aerosol on rat brain lipid profile. Biochimie 153, 99–108.

Centers for Disease Control and Prevention, 2010. In How Tobacco Smoke Causes Disease: the Biology and Behavioral Basis for Smoking-Attributable Disease: A Report of the Surgeon General. Centers for Disease Control and Prevention, Atlanta, GA.

Cervellati, F., Muresan, X.M., Sticozzi, C., Gambari, R., Montagner, G., Forman, H.J., Torricelli, C., Maioli, E., Valacchi, G., 2014. Comparative effects between electronic and cigarette smoke in human keratinocytes and epithelial lung cells. Toxicol. In Vitro 28 (5), 999–1005.

Chausse, P., Naughton, G., Dutheil, F., 2015. Electronic cigarettes resistance value of the heating filament could be the key to lung toxicity. Chest e29–e30.

Choi, K., Bernat, D., 2018. E-cigarette use among Florida youth with and without asthma. Am. J. Prev. Med. 51, 446–453.

Dekhuijzen, P., 2004. Antioxidant properties of N-acetylcysteine: their relevance in relation to chronic obstructive pulmonary disease. Eur. Respir. J. 23 (4), 629–636.

Domej, W., Oettl, K., Renner, W., 2014. Oxidative stress and free radicals in COPD–implications and relevance for treatment. Int. J. Chronic Obstr. Pulm. Dis. 9, 1207–1224.

Franks, A.S., Sando, K., McBane, S., 2018. Do electronic cigarettes have a role in tobacco cessation? Pharmacotherapy 38 (5), 555–i568.

Geiss, O., Bianchi, I., Barrero-Moreno, J., 2016. Correlation of volatile carbonyl yields emitted by e-cigarettes with the temperature of the heating coil and the perceived sensorial quality of the generated vapours. Int. J. Hyg Environ. Health 219 (3), 268–277.

Goel, R., Durand, E., Trushin, N., Prokopczyk, B., Foulds, J., Elias, R.J., Richie, J.P., 2015. Highly reactive free radicals in electronic cigarette aerosols. Chem. Res. Toxicol. 28, 1675–1677.

Halliwel, B., 2014. Cell culture, oxidative stress, and antioxidants: avoiding pitfalls. Biomed. J. 37 (3), 99–105.

Goniewicz, M.L., Knysak, J., Gawron, M., Kosmider, L., Sobczak, A., Kurek, J., Prokopowicz, A., Jablonska-Czapla, M., Rosik-Dulewska, C., Havel, C., Jacob 3rd, P., Benowitz, N., 2014. Levels of selected carcinogens and toxicants in vapor from electronic cigarettes. Tob. Control 23, 133–139.

Harrell, M.B., Weaver, S.R., Loukas, A., Creamer, M., Marti, C.N., Jackson, C.D., Heath, J.W., Nayak, P., Perry, C.L., Pechacek, T.F., Eriksen, M.P., 2017. Flavored e-cigarette use: characterizing youth, young adult, and adult users. Prev. Med. Rep. 5, 33–40.

Higham, A., Bostock, D., Booth, G., Dungwa, J.V., Singh, D., 2018. The effect of electronic cigarette and tobacco smoke exposure on COPD bronchial epithelial cell inflammatory responses. Int. J. Chronic Obstr. Pulm. Dis. 23 (13), 989–1000.

International Agency for Research on Cancer (IARC, 2012. Agents Classified by IARC, vols. 1–112 Monographs, Geneva, Switzerland. http://monographs.iarc.fr/ENG/Classification/List_of_Classification_Vol1-112.pdf.

Jensen, R.P., Luo, W., Pankow, J.F., Strongin, R.M., Peyton, D.H., 2015. Hidden formaldehyde in e-cigarette aerosols. N. Engl. J. Med. 372 (4), 392–394.

Kirkham, P., Rahman, I., 2006. Oxidative stress in asthma and COPD: antioxidants as a therapeutic strategy. Pharmacol. Ther. 111, 476–494.

Korzun, T., Munhenzva, I., Escobedo, J.O., Strongin, R.M., 2019. Synthetic food dyes in electronic cigarettes. Dyes Pigments 160, 509–513.

Kosmider, L., Sobczak, A., Fik, M., Knysak, J., Zaciera, M., Kurek, J., Goniewicz, M.L., 2014. Carbonyl compounds in electronic cigarette vapors: effects of nicotine solvent and battery output voltage. Nicotine Tob. Res. 16 (10), 1319–1326.

Lerner, C.A., Sundar, I.K., Watson, R.M., Elder, A., Jones, R., Done, D., Kurtzman, R., Ossip, D.J., Robinson, R., McIntosh, S., Rahman, I., 2015a. Environmental health hazards of e-cigarettes and their components: oxidants and copper in e-cigarette aerosols. Environ. Pollut. 198, 100–107.

Lerner, C.A., Sundar, I.K., Yao, H., Gerloff, J., Ossip, D.J., McIntosh, S., Robinson, R., Rahman, I., 2015b. Vapors produced by electronic cigarettes and e-juices with flavorings induce toxicity, oxidative stress, and inflammatory response in lung epithelial cells and in mouse lung. PLoS One 10, e0116732.

Liu, J., Wang, B., Tai, C., Wu, L., Zhao, H., Guan, J., Chen, L., 2016. An effective method to detect volatile intermediates generated in the bioconversion of coal to methane by gas chromatography-mass spectrometry after *in-situ* extraction using headspace solid-phase micro-extraction under strict anaerobic conditions. PLoS One 11 (10), e0163949.

MacNee, W., Rahman, I., 2001. Is oxidative stress central to the pathogenesis of chronic obstructive pulmonary disease? Trends Mol. Med. 7 (2), 55–62.

McConnell, R., Barrington-Trimis, J.L., Wang, K., Urman, R., Hong, H., Unger, J., Samet, J., Leventhal, A., Berhane, K., 2017. Electronic cigarette use and respiratory symptoms in adolescents. Am. J. Respir. Crit. Care Med. 195, 1043–1049.

Messner, B., Bernhard, D., 2014. Smoking and cardiovascular disease: mechanisms of endothelial dysfunction and early atherogenesis. Arterioscler. Thromb. Vasc. Biol. 34, 509–515.

Muthumalage, T., Prinz, M., Ansah, K.O., Gerloff, J., Sundar, I.K., Rahman, I., 2018. Inflammatory and oxidative responses induced by exposure to commonly used e-cigarette flavoring chemicals and flavored e-liquids without nicotine. Front. Physiol. 11, 8–1130.

Norton, K.J., June, K.M., O'Connor, R.J., 2014. Initial puffing behaviors and subjective responses differ between an electronic nicotine delivery system and traditional cigarettes. Tob. Induc. Dis. 12 (1), 17. https://doi.org/10.1186/1617-9625-12-17.

Ogunwale, M.A., Mingxiao, L., Mandapati, V., Ramakrishnam, R., Chen, Y., Nantz, H., Conklin, D.J., Fu, X.A., 2017. Aldehyde detection in electronic cigarette aerosols. Chem. Res. Toxicol. 2, 1207–1217.

Paschke, T., Scherer, G., Heller, W.D., 2014. Effects of ingredients on cigarette smoke composition and biological activity: a literature overview. Beitr. Tabakforsch. 20, 107–247.

Primack, B.A., Soneji, S., Stoolmiller, M., Fine, M.J., Sargent, J.D., 2015. Progression to traditional cigarette smoking after electronic cigarette use among US adolescents and young adults. JAMA Pedr. Nov 169 (11), 1018–1023.

Pryor, W.A., 1997. Cigarette smoke radicals and the role of free radicals in chemical carcinogenicity. Environ. Health Perspect. 105 (Suppl. 4), 875–882.

Robinson, R.J., Hensel, E.C., Morabito, P.N., Roundtree, K.A., 2015. Electronic cigarette topography in the natural environment. PLoS One 10 (6), e0129296. https://doi.org/10.1371/journal.pone.0129296.

Scheffler, S., Dieken, H., Krischenowski, O., Aufderheide, M., 2015. Cytotoxic evaluation of e-liquid aerosol using different lung-derived cell models. Int. J. Environ. Res. Public Health 12, 12466–12474.

Schweitzer, R.J., Wills, T.A., Tam, E., Pagano, I., Choi, K., 2017. E-cigarette use and asthma in a multiethnic sample of adolescents. Prev. Med. 105, 226–231.

Scott, A., Lugg, S.T., Aldridge, K., Lewis, K.E., Bowden, A., Mahida, R.Y., Grudzinska, F.S., Dosanjh, D., Parekh, D., Foronjy, R., Sapey, E., Naidu, B., Thickett, D.R., 2018. Pro-inflammatory effects of e-cigarette vapour condensate on human alveolar macrophages. Thorax Aug 13. pii: thoraxjnl-2018-211663.

Soneji, S., Barrington-Trimis, J.L., Wills, T.A., Leventhal, A.M., Unger, J.B., Gibson, L.A., Yang, J., Primack, B.A., Andrews, J.A., Miech, R.A., Spindle, T.R., Dick, D.M., Eissenberg, T., Hornik, R.C., Dang, R., Sargent, J.D., 2017. JAMA Pediatr 172 (1), 98 2018 Jan 1.

Sussan, T.E., Gajghate, S., Thimmulappa, R.K., Ma, J., Kim, J.H., Sudini, K., Consolini, N., Cormier, S.A., Lomnicki, S., Hasan, F., Pekosz, A., Biswal, S., 2015. Exposure to electronic cigarettes impairs pulmonary anti-bacterial and anti-viral defenses in a mouse model. PLoS One 10, e0116861.

Thomson, R.H., Lewis, P.M., 2015. More on hidden formaldehyde in e-cigarette aerosols. N. Engl. J. Med. 372 (16), 1575–1576.

Uchiyama, S., Ohta, K., Inaba, Y., Kunugita, N., 2013. Determination of carbonyl compounds generated from the e-cigarette using coupled silica cartridges impregnated with hydroquinone and 2,4-dinitrophenylhydrazine, followed by high-performance

liquid chromatography. Anal. Sci. 29, 1219–1222.
U.S. Environmental Protection Agency, 2003. http://epa.gov/airtoxics/188polls.html.
Vasanthi Bathrinarayanan, P., Brown, J.E.P., Marshall, L.J., Leslie, L.J., 2018. An investigation into E-cigarette cytotoxicity in-vitro using a novel 3D differentiated co-culture model of human airways. Toxicol. In Vitro 52, 255–264.
Waris, G., Ahsan, H., 2006. Reactive oxygen species: role in the development of cancer and various chronic conditions. J. Carcinog 11, 5–14.
Wang, P., Chen, W., Liao, J., Matsuo, T., Ito, K., Fowles, J., et al., 2017. A device-independent evaluation of carbonyl emissions from heated electronic cigarette solvents. PLoS One 12 (1), e0169811.
Wills, T.A., Knight, R., Williams, R., Pagano, I., Sargent, J.D., 2015. Risk factors for exclusive e-cigarette use and dual e-cigarette and tobacco use in adolescents. Pediatrics 135, e43–e51.
Yingst, J.M., Veldheer, S., Hammett, E., Hrabovsky, S., Foulds, J., 2017. A method for classifying user-reported electronic cigarette liquid flavors. Nicotine Tob. Res. 19 (11), 1381–1385.
Zhang, Z., Kleinstreuer, C., Feng, Y., 2012. Vapor deposition during cigarette smoke inhalation in a subject-specific human airway model. J. Aerosol Sci. 53, 40–60.

OXFORD

SOT | Society of Toxicology
academic.oup.com/toxsci

TOXICOLOGICAL SCIENCES, 172(1), 2019, 132–145

doi: 10.1093/toxsci/kfz176
Advance Access Publication Date: August 6, 2019
Research Article

The Customizable E-cigarette Resistance Influences Toxicological Outcomes: Lung Degeneration, Inflammation, and Oxidative Stress-Induced in a Rat Model

Silvia Cirillo,[*] Fabio Vivarelli,[*,1] Eleonora Turrini,[†] Carmela Fimognari,[†] Sabrina Burattini,[‡] Elisabetta Falcieri,[‡] Marco Bruno Luigi Rocchi,[‡] Vladimiro Cardenia,[§] Maria Teresa Rodriguez-Estrada,[¶,‖] Moreno Paolini,[*,1] and Donatella Canistro[*]

[*]Department of Pharmacy and Biotechnology, Alma Mater Studiorum—University of Bologna, 40126 Bologna; [†]Department for Life Quality Studies, Alma Mater Studiorum—University of Bologna, 47921 Rimini; [‡]Department of Biomolecular Sciences, University of Urbino Carlo Bo, 61029 Urbino; [§]Department of Agricultural, Forest and Food Sciences, University of Turin; [¶]Department of Agricultural and Food Sciences, Alma Mater Studiorum—University of Bologna, 40127 Bologna; and [‖]Interdepartmental Centre for Industrial Agrofood Research, Alma Mater Studiorum—University of Bologna, 47521 Cesena, Italy

[1]To whom correspondence should be addressed at Department of Pharmacy and Biotechnology, Alma Mater Studiorum—University of Bologna, Via Irnerio 48, 40126 Bologna, Italy. Emails: fabio.vivarelli3@unibo.it and moreno.paolini@unibo.it.

ABSTRACT

Despite the knowledge gap regarding the risk-benefit ratio of the electronic cigarette (e-cig), its use has grown exponentially, even in teenagers. E-cig vapor contains carcinogenic compounds (eg, formaldehyde, acetaldehyde, and acrolein) and free radicals, especially reactive oxygen species (ROS) that cause toxicological effects, including DNA damage. The role of e-cig voltage customization on molecule generation has been reported, but the effects of the resistance on e-cig emissions and toxicity are unknown. Here, we show that the manipulation of e-cig resistance influences the carbonyls production from nonnicotine vapor and the oxidative and inflammatory status in a rat model. Fixing the voltage at the conventional 3.5 V, we observed that the amount of the selected aldehydes increased as the resistance decreased from 1.5 to 0.25 Ω. Under these conditions, we exposed Sprague Dawley rats to e-cig aerosol for 28 days, and we studied the pulmonary inflammation, oxidative stress, tissue damage, and blood homeostasis. We found a perturbation of the antioxidant and phase II enzymes, probably related to the increased ROS levels due to the enhanced xanthine oxidase and P450-linked monooxygenases. Furthermore, frames from scanning electron microscope showed a disorganization of alveolar and bronchial epithelium in 0.25 Ω group. Overall, various toxicological outcomes, widely recognized as smoke-related injuries, can potentially occur in e-cig consumers who use low-voltage and resistance device. Our study suggests that certain "tips for vaping safety" cannot be established, and encourages further independent investigations to help public health agencies in regulating the e-cig use.

Key words: electronic cigarette; resistance; oxidative stress; inflammation; animal model.

Electronic cigarettes (e-cigarettes, e-cigs) have been distributed on the global market for almost a decade as both potential approach to aid smoking cessation (Franks *et al.*, 2018) and safe alternative to combustion cigarettes. However, evidence on quit smoking remains inconclusive and, actually, the Center for Disease Control and Prevention (CDC), Food and Drug Administration (FDA), and Georgia State University stated that the number of teens who had never smoked but use e-cigs increased 3 times during the period 2011–2013 (Lestari *et al.*, 2018). Furthermore, a great deal of studies testifies its dangerousness. Although in the early years it was extensively spread the message about e-cig safety, current literature reports a growing number of evidence on harmful outcomes deriving from the device use (Cardenia *et al.*, 2018; Lerner *et al.*, 2015; McConnell *et al.*, 2017; Sussan *et al.*, 2015; Vivarelli *et al.*, 2019). E-cig vapor, same as tobacco smoke, induces carcinogen metabolizing enzymes and oxidative stress, which play a key role in the pathogenesis of chronic, inflammatory, and degenerative diseases, including chronic obstructive pulmonary disease (COPD) and cancer (Lerner *et al.*, 2015; Muthumalage *et al.*, 2018; Scott *et al.*, 2018). In fact, several toxicological aspects closely related to cancer have been investigated in *in vitro* systems (Scheffler *et al.*, 2015; Scott *et al.*, 2018; Vasanthi Bathrinarayanan *et al.*, 2018; Zhang *et al.*, 2012) and confirmed in *in vivo* ones (Canistro *et al.*, 2017; Lee *et al.*, 2018).

E-cig consists of a mouthpiece, a refillable cartridge, a lithium battery, and a heating atomizer. In the majority of the devices, a power button allows the user to activate the heating element during inhalation, thus producing the flavored vapor. The wide variety of e-liquids on the market, together with the continuous evolution in the e-cig technologies, makes these devices extremely customizable. Although the e-liquid is generally composed by vegetable glycerol (VG), propylene glycol (PG), water, and an impressive variety of flavors and nicotine at different concentrations, the personalization of the vaporization process is responsible for different emission levels of toxic and/or carcinogenic carbonyl compounds, such as formaldehyde, acetaldehyde, acrolein (Bitzer *et al.*, 2018; Goniewicz *et al.*, 2014), and reactive free radicals (Goel *et al.*, 2015; Lerner *et al.*, 2015; Sussan *et al.*, 2015). The exposure to aldehydes derived from e-cig vapors is considered a risk factor for human health. In particular, formaldehyde and acetaldehyde are classified as Group 1 and Group 2B carcinogens, respectively, by the International Agency for Research on Cancer (IARC, 1999, 2012). Acrolein is listed as hazardous air pollutant by the U.S. Environmental Protection Agency (2003). Moreover, the generation of carbonyls is related to the formation of radicals (eg, hydroxyl radicals), which are responsible for the oxidation and fragmentation of glycols (Geiss *et al.*, 2016) and the possibility to arbitrarily adjust the total power of the device by combining different voltage and resistance levels may have a considerable impact on human health (Chausse *et al.*, 2015). Indeed, according to a recent online forum survey addressed to vaping users, the majority of respondents vaped at high wattage (89% $>$ 20 W, of which 33% $>$ 60 W) using coils with low resistance (92% $<$ 1 Ω, of which 65% $<$ 0.5 Ω) (Chaumont *et al.*, 2018). Moreover, another study compared vapers from 2 different geographical areas (Germany and Belgium) and reported that the mean coil resistance used by the Germany users group was 1.3 Ω, whereas the mean for Belgium users was 0.4 Ω (Smets *et al.*, 2019).

Contrary to the customary statements that carbonyl compounds are generated only when high voltage is applied (Jensen *et al.*, 2015), it has been observed that carcinogenic aldehydes, such as formaldehyde, are produced even in lower power breath activated e-cig (Bitzer *et al.*, 2019). Because the combination of applied voltage and resistance value of the filament coil is responsible for the device heating power through the Joule effect (Chausse *et al.*, 2015), we believe that the extent of the toxicological effects can be strictly influenced by the consumers' habits.

In this investigation, we have therefore set e-cig devices at a fixed voltage value (the most commonly used 3.5 V) in order to determine whether application of low (0.25 Ω) and medium (1.5 Ω) coil resistances affects the carbonyls generation and the biological effects of the resulting nonnicotine vapor on the pulmonary oxidative and inflammatory status in a rat model. Lung damage and blood homeostasis were also studied.

MATERIALS AND METHODS

E-cigarette, liquid refill, and device settings. A commercially available e-cig (Eleaf Pico) powered by a rechargeable lithium battery (IMR 18650 3000 mAh 35A 3.7 V High Drain Flat Top Rechargeable Battery) was used for this study. The device was set at 3.5 V and equipped with 2 different coils (1.5 and 0.25 Ω) to obtain a total wattage of 8 ± 2 and 40 ± 5 W, respectively. These resistance values were chosen because they are considered as "safe" and "hazardous," respectively, according to the information given to the users. The 2.5-ml Pyrex glass tank was refilled with a nicotine-free e-liquid composed by propylene glycol/vegetable glycerin (PG/VG) base solution (50/50, vol/vol) and red fruits flavor added to a final concentration of 10% (vol/vol).

Determination of carbonyl compounds. Volatile carbonyl compounds were determined by headspace-solid phase micro extraction (HS-SPME) coupled to gas chromatography-mass spectrometry (GC/MS Q2010 Plus, Shimadzu, Japan). Volatile compounds were extracted from the box headspace at room temperature for 2 min, by using a triphasic SPME device (DVB/CAR/PDMS, 50/30 mm thickness, 10-mm length), which had been previously conditioned at 270°C for 60 min. Once the volatile compounds had adsorbed onto the SPME fiber, the latter was desorbed in the GC/MS injector at 250°C for 10 min. A RTX-WAX column (30 m × 0.25 mm i.d. × 0.25 μm film thickness, Restek) was used for the chromatographic separation and the injection was carried out in the split mode, with a 1:20 split ratio. The carrier gas was helium, and its linear velocity was set at 36.2 cm/s. The oven temperature program comprised an initial isotherm at 35°C for 10 min, which was afterwards risen to 240°C at 30°C/min. The injector and interface temperatures were fixed at 250°C and 230°C, respectively. To recognize the compounds of interest, the mass spectra and retention time were compared with those of the corresponding standards. Both the acquisition and integration were performed in the single ion-monitoring mode. Formaldehyde, acetaldehyde, and acrolein were recognized and quantified by their corresponding characteristic ions (*m/z* 29, 44, and 56, respectively). As suggested in literature (Geiss *et al.*, 2016; Wang *et al.*, 2017), a normalized response factor (Rf) was calculated using the amount of aldehydes present in the environment as basal level, according to the following expression:

$$Rf = (A_x - A_y)/A_y,$$

where A_x and A_y represent the peak areas of aldehydes detected after and before (basal) the vaping process in the exposure box, respectively.

Animal care and exposure. The EU Directive (2010/63/EU) guidelines were followed during the entire experiment. The experimental protocol was approved by the Committee on the Ethics of Animal Experiments of the University of Bologna and by the Italian Ministry of Health (Permit number 26832015). The Animal Welfare Committee monitored the proceedings to ensure that all efforts have been made to minimize animal suffering. Thirty male Sprague Dawley rats (ENVIGO RMS S.r.l., San Pietro al Natisone, Udine, Italy), 7 weeks old, were housed under standard conditions (12 h light-dark cycle, 22°C, 60% humidity). Animals had continuous access to water and chow throughout the experiment. After 1 week of acclimatization, animals were randomly divided into 3 experimental units: a control group (10 rats), and 2 treated groups (1.5 and 0.25 Ω) composed by 10 rats each. The treated groups were exposed to the vapor generated by the e-cigarettes (see Determination of carbonyl compounds section for details on device settings) for 28 days, as previously reported by Canistro *et al.* (2017) with some modifications. The whole body exposure consisted of 11 cycles of 2 puffs (6 s on; 5 s off; 6 s on), followed by 20 min of recovery. At the end of each cycle, the animals were moved to a clean chamber. Five animals were placed in each inhalation chamber, which consisted of a propylene box with a capacity of 30 l. E-cig treated animals were subjected to the procedure for 3 h/day. The levels of O_2, N_2, and CO_2 were monitored by GC/MS to establish safe O_2/N_2 and CO_2/O_2 ratios.

Tissue collection. After 24 h from the last exposure, blood was collected from the tail vein. Samples were stored in K_2 EDTA tubes at 4°C until DNA unwinding assay.

Animals were anesthetized with Zoletil 100 (100 mg/kg b.w.) and sacrificed by decapitation according to the Italian Ministerial guidelines for the species. Lung was removed, immediately frozen into liquid nitrogen, and stored at −80°C. Lung was homogenized in 150 nM NaCl, 1 mM EDTA, 1% Triton-X, and 20 mM Tris-HCl pH 7.4, by using a IKA Ultra-Turrax homogenizer. The homogenate was then centrifuged at 9000 × g for 15 min at 4°C and the supernatant was collected, which from now on will be labeled as S9 fraction. The cytosolic and microsomal fractions were obtained according to previously reported procedures (Bonamassa *et al.*, 2016).

Protein concentration. Protein concentration was determined according to the method described by Lowry *et al.* (1951), using bovine serum albumin as standard. Samples were properly diluted in order to reach a suitable protein concentration (Canistro *et al.*, 2012).

Antioxidant enzymes

The following assays were performed on cytosol subcellular fraction from lung tissue. Where not differently declared, the methods were previously described by Vivarelli *et al.* (2016).

Superoxide dismutase activity (SOD). The enzymatic activity was assayed spectrophotometrically at 320 nm by monitoring the generation of adrenochrome, one of the main products of epinephrine autoxidation at pH 10.2. The dejection of autoxidation was used to calculate SOD activity using the extinction coefficient of 4.02 per mM × cm, and expressed as mol of oxidized epinephrine per min per mg protein, derived by subtracting each test curve from the epinephrine autoxidation standard curve. Activity is expressed in nmol/mg/min.

NAD(P)H: quinone reductase (NQO1) from lung tissue. NQO1 activity was assayed spectrophotometrically at 600 nm by monitoring the reduction of the blue redox dye of DCPIP ($\varepsilon = 9.6\ mM^{-1}\ cm^{-1}$), and expressed as mol of DCPIP reduced per min per mg protein. Activity is expressed in nmol/mg/min.

Oxidized glutathione reductase activity (GSSG-red) from lung tissue. 1.5 mM NADPH was added to 50 mM potassium phosphate buffer, 1 mM EDTA, cytosol sample, and 20 mM GSSG. The generation of $NADP^+$ from NADPH due to the reduction of GSSG was recorded at 340 nm for 5 min at 37°C. GSSG-red activity was calculated using the extinction coefficient of 6.22 per mM × cm, and expressed as mol of NADPH consumed per min per mg protein. Activity is expressed in nmol/mg/min.

GSH-Peroxidase (GSH-Px) from lung tissue. The enzymatic activity was determined following the NADPH consumption at 340 nm for 5 min at 37°C and expressed as nmol of NADPH consumed per min per mg of protein. All details have been previously reported (Melega *et al.*, 2013). Activity is expressed in nmol/mg/min.

Catalase (CAT). Thirty millimolar H_2O_2 was added to the reaction mixture, constituted by 50 mM potassium phosphate buffer and cytosol sample. The decomposition of the substrate was measured at 240 nm and catalase activity was expressed as mol of H_2O_2 consumed per minute per mg protein using a molar extinction coefficient of $43.6\ mM^{-1}\ cm^{-1}$. Activity is expressed in μmol/mg/min.

Xenobiotic phase I enzymes. The following assays were performed on microsomal subcellular fraction from lung tissue; these assays had been previously described in detail by Cirillo *et al.* (2016).

Pentoxyresorufin O-dealkylase (PROD) activity-CYP2B1/2, methoxyresorufin O-demethylase (MROD) activity-CYP1A2, and ethoxyresorufin O-deethylase, (EROD) activity-CYP1A1. For the reaction mixture (PROD, MROD, EROD), 0.025 mM $MgCl_2$, 200 mM pentoxyresorufin, 5 mM methoxyresorufin, and 1.7 mM ethoxyresorufin, respectively, were mixed with 0.32 mg of proteins and 130 mM NADPH in 2.0 ml 0.05 M Tris-HCl buffer (pH 7.4). Resorufin formation at 37°C was calculated by comparing the rate of the increase in relative fluorescence to the fluorescence of known amounts of resorufin (excitation 563 nm, emission 586 nm). Activity is expressed in pmol/mg/min.

Aminopyrine N-demethylase (APND) activity-CYP3A1/2. A total incubation volume of 3 ml, composed of 0.5 ml water solution of 50 mM aminopyrine, 25 mM $MgCl_2$, 1.48 ml of 0.60 mM $NADP^+$, 3.33 mM G6P in 50 mM Tris-HCl buffer (pH 7.4), 0.02 ml G6PDH (0.93 U/ml), and 0.125 ml of sample was incubated for 5 min at 37°C. The reaction of the released of CH_2O with the Nash reagent generated a yellow color that was read at 412 nm; the molar absorptivity of 8000 was used for calculation. Activity is expressed in nmol/mg/min.

p-Nitrophenol hydroxylase (*p*-NPH) activity-CYP2E1. Two millimolar *p*-nitrophenol in 50 mM Tris-HCl buffer (pH 7.4), 5 mM $MgCl_2$, and an NADPH-generating system consisting of 0.4 mM $NADP^+$, 30 mM isocytrate, 0.2 U of isocytrate dehydrogenase, and 1.5 mg of proteins were mixed in a total volume of 2 ml. After 10 min of incubation at 37°C, 0.5 ml of 0.6 N perchloric acid was added to develop the reaction. Precipitated proteins were removed by centrifugation and 1 ml of the resultant supernatant was mixed with 1 ml of 10 N NaOH. Absorbance at 546 nm was immediately recorded and 4-nitrocathecol determined ($\varepsilon = 10.28\ mM^{-1}\ cm^{-1}$). Activity is expressed in nmol/mg/min.

Xenobiotic phase II enzymes. Glutathione S-transferase (GST) (Sapone *et al.*, 2016). The incubation mixture consisted of 1 mM glutathione + 1 mM 1-chloro-2,4-dinitrobenzene (CDNB) in methanol + 0.025 ml of sample (cytosol subcellular fraction

from lung tissue) in a final volume of 2.5 ml 0.1 M phosphate Na^+/K^+ buffer (pH 6.5). The product of the reaction was read at 340 nm ($\varepsilon = 9.6\,mM^{-1}\,cm^{-1}$). Activity is expressed in nmol/mg/min.

UDP-glucuronosyl transferase (UDP-GT) (Vivarelli *et al.*, 2016). The activity in microsomal subcellular fraction from lung tissue was determined kinetically using 1-naphtol as substrate (final concentration, 50 mM) by the continuous fluorimetric (excitation 390 nm; emission 440 nm) monitoring of 1-naphthol-glucuronide production in the presence of 1 mM uridine-5-diphosphoglucuronic acid. The sensitivity of the reaction was improved by performing the reaction in the presence or absence of Triton X-100 (0.2%) as a detergent. Activity is expressed in nmol/mg/min.

Xanthine oxidase. Xanthine oxidase (XO) was spectrophotometrically measured in lung cytosol by quantifying the formation of uric acid at 290 nm. The reaction mixture contained 50 mM sodium phosphate buffer (pH 7.8), hypoxanthine (50 μM final concentration), and it was incubated at 37°C for 5 min. The reaction started with the addition of NAD^+ (Shintani, 2013). Activity is expressed in nmol/mg/min.

ROS content in lung. 2′,7′-Dichlorofluorescein diacetate (DCFH-DA) was used as a probe for the estimation of reactive oxygen species (ROS) content in S9 fraction. Samples were mixed with DCFH-DA (100 μM) at 37°C for 30 min, and the reaction was then shut down by chilling (Kang *et al.*, 2018). The formation of the oxidized break down product (2′,7′-dichlorofluorescein, DCF) was monitored with a fluorescence spectrophotometer (488 nm excitation; 525 nm emission). DCF was quantified using a standard curve, as previously reported by Rodrigues Siqueira *et al.* (2005) and expressed as molar concentration per mg of protein (nM DCF/mg protein).

Protein carbonylation. Protein carbonyl groups were measured as suggested by Levine *et al.* (1994); the method is based on the reaction of carbonyls groups with dinitrophenyl-hydrazine (DNPH), to form a stable hydrazine that can be spectrophotometrically monitored at 390 nm. Samples (cytosol from lung tissue) were prepared according as previously reported (Vivarelli *et al.*, 2018). The results are expressed as nmol of carbonyl groups/mg protein.

FRAP assay. Ferric reductive antioxidant power (FRAP) was determined in plasma and lung tissues according to the procedure reported by Benzie and Strain (1996). Briefly, FRAP reagent (900 ml) containing 10 mM 2,4,6-tripyridyl-S-triazine in 40 mM HCl, 300 mM acetate buffer (pH 3.6), and 20 mM $FeCl_3$ was added to 30 μl of plasma or supernatant tissue. The absorbance change (at 593 nm) between the final reading and the blank was calculated for each sample and related to the absorbance of ferric standard solutions. Results are expressed in nmol Fe (III) $0.1\,ml^{-1}$ plasma.

Lipid hydroperoxides in red blood cell membranes. Lipid hydroperoxides in red blood cells (RBCs) were estimated by performing FOX assay (Jiang *et al.*, 1992). It is based on the rapid oxidation of Fe^{2+} to Fe^{3+} under acid condition and in the presence of xylenol orange dye. The Fe^{3+}-xylenol orange compounds can be spectrophotometrically monitored at 560 nm. One hundred and sixty microliters of sample was mixed with 840 μl of FOX reagent. The amounts of hydroperoxides were extrapolated by the use of a hydrogen peroxide standard curve. The results are expressed as μM of H_2O_2/mg of protein. Further details on the method can be found by Jiang *et al.* (1992). Results are expressed as μmol H_2O_2/ml blood.

Hematological analysis. The hematological analyses were performed by the Central Laboratory of Clinical Pathology (CLINLAB) of the Department of Veterinary Medical Science (University of Bologna), according to standard methods certified by the Italian National Health Service.

Gene expression studies. Total RNA from lung tissue was isolated using Purelink RNA mini kit (ThermoFisher Scientific, Waltham, Massachusetts), according to manufacturer's recommendation. Briefly, lung samples were homogenized in lysis buffer containing 1% β-mercaptoethanol using a homogenizer SHM1 (Stuart, Bibby Scientific LTD, Staffordshire, UK) and keeping samples on ice. Homogenized samples were added to an equal volume of 70% ethanol and mixed. The solution was passed through a filter cartridge, having a silica-based membrane that binds RNA. The filter was then washed once with Wash Buffer I and twice with Wash Buffer II (both provided by ThermoFisher Scientific). RNA was finally eluted with RNase-free water and stored at −80°C. RNA samples were quantified using Nanoquant plate (Tecan, Männedorf, Switzerland) and i-control software (Tecan). For each sample, 400 ng of total RNA were reverse transcribed using the High Capacity cDNA Reverse Transcription kit (ThermoFisher Scientific) with RNase inhibitor according to manufacturer's instructions. Briefly, 10 μl of each sample were added to 10 μl master mix and the mixture was subjected to the appropriate thermocycling conditions. Finally, relative quantification was performed by real-time PCR (Bio-Rad CFX Connect, Bio-Rad, Hercules, California) using Universal Master Mix (ThermoFisher Scientific) and TaqMan gene expression assay (ThermoFisher Scientific) for the following genes: IL1β (Rn00580432_m1), IL6 (Rn01410330_m1), TNF-α (Rn99999017_m1), CCL3 (Rn00564660_m1), CCL4 (Rn00671924_m1), CSF2 (Rn01456850_m1), ALDH3A1 (Rn00694669_m1). GAPDH (Rn99999916_s1), and actin (Rn00667869_m1) were used as endogenous controls. Each measurement was performed in triplicate and data were analyzed through the $2^{-\Delta\Delta Ct}$ methods (Livak and Schmittgen, 2001). Rats nonexposed to vapor from e-cig were considered the calibrator of the gene expression experiments.

Scanning electron microscopy. Lung and tracheal samples from control and treated animals were dissected and immediately washed in 0.1 M phosphate buffer, to remove blood or any other contaminant. Tissues were fixed with 2.5% glutaraldehyde in 0.1 M phosphate buffer pH 7.2–7.4 for 1 h, postfixed with 1% osmium tetroxide (OsO_4) in the same buffer for 2 h and, finally, dehydrated with graded ethanol (50%–100%, 5 min each). Critical point dried specimens were mounted on aluminum stubs. After 10 nm, gold sputter-coated samples were examined with a Philips scanning electron microscopy (SEM) at 20 kV (Burattini *et al.*, 2016).

Transmission electron microscopy. Tissues were immediately washed and fixed with 2.5% glutaraldehyde in 0.1 M phosphate buffer for 1 h, postfixed in 1% OsO_4 for 1 h, alcohol dehydrated and embedded in araldite, as reported by Salucci *et al.* (2017). For ultrastructural analysis thin sections were stained with uranyl acetate and lead citrate and observed with an electron microscope at 80 kV.

Statistical analyses. If not differently specified, results are expressed as mean ± standard deviation (SD) on 6 independent

Table 1. Effects of Resistance Value (0.25 and 1.5 Ω) on Formaldehyde, Acetaldehyde, and Acrolein Relative Levels in Vapors Released by E-cig

	Formaldehyde	Acetaldehyde	Acrolein
0.25 Ω	13.20 ± 0.35**	5.04 ± 0.15**	1.60 ± 0.09**
1.50 Ω	2.84 ± 0.42*	0.80 ± 0.16*	0.66 ± 0.17*

All data are reported as mean ± standard deviation of 2 independent replicates of the relative aldehydes levels compared with their environment (basal) level. A normalized response factor (Rf) was calculated using the amount of aldehydes present in the environment as basal level, according to the following expression:

$$Rf=(A_x- A_y)/A_y,$$

where A_x and A_y represent the peak areas of aldehydes detected after and before (basal) the vaping process in the exposure box, respectively. For calculation details, please refer to Materials and Methods section.

*$p < .05$.

**$p < .01$ significant results between 0.25 and 1.5 Ω group, using one-way ANOVA (Tukey's test).

replicates ($n = 6$) and analyzed by means of one-way ANOVA, followed by Tukey's multiple comparison test. The test was carried out at a 95% confidence level ($p \leq .05$), to separate means of parameters that were statistically different. For gene expression analysis, the set of treatments was compared against a single control mean, by using a one-way ANOVA followed by Dunnett's test.

RESULTS

Levels of Formaldehyde, Acetaldehyde, and Acrolein

Among the 3 monitored aldehydes, formaldehyde was the most abundant in e-cig vapors, followed by acetaldehyde and acrolein; however, the observed levels of carbonyls were strictly related to the resistance value. Acrolein, acetaldehyde, and formaldehyde levels generated by 0.25 Ω coil were 3- to 7-fold higher than those generated by the 1.501 Ω coil (Table 1).

Antioxidant Profile and Oxidative Stress

A general imbalance of the antioxidant pattern of exposed animals compared with control is shown in Figure 1. Overall, 1.5 Ω group presented the mildest perturbations, whose magnitude became higher after exposure to e-cig vapor generated by the 0.25 Ω coil. This scenario was evident in the pulmonary glutathione reductase (GSSG-red; +156%, $p < .01$) and catalase (CAT; −64%, $p < .01$) (Figure 1a). The suggested oxidative stress status (OSS), due to the strong induction of GSSG-red, was coupled with the opposite behavior of conjugated phase II GST and UDP-glucuronyl-transferase (UDPGT), which is significantly reduced in 1.5 Ω exposed rats but increased in 0.25 Ω group (Figure 1b).

Because the antioxidant enzymatic machinery appeared altered in exposed groups, we investigated the putative ROS sources. Among these, we found in the lung that XO was upregulated proportionally to the total wattage of the device (Figure 1c). We also hypothesized that changes in cytochrome P450 (CYP) catalytic cycle could be involved in ROS generation and pulmonary toxicity (Figure 1d). We found the higher and biologically significant increase in 0.25 Ω group for both CYP 1A1 (up to 470% compared with control, $p < .01$) and CYP 2E1 (up to 196% vs control, $p < .01$).

To evaluate if the boost of free radicals was involved in the pulmonary OSS, the ROS levels were measured in lung by using DCFH-DA fluorescent probe. Figure 1e shows an ROS increment (about 1.5-fold) in 1.5 Ω exposed group compared with control and 2-fold increase in 0.25 Ω one. Largely used as an oxidative stress biomarker, carbonyl residues in pulmonary proteins were measured (Figure 1f). A slight but statistically significant increasing trend was reported in exposed animals, with an inverse correlation between the carbonylated proteins amount and the coil resistance applied to the device. However, even if statistically significant, the biological meaning of these variations cannot be considered relevant. To examine whether these phenomena affect the antioxidant power at systemic level, we measured the antioxidant capacity using the FRAP approach. Data referred to FRAP in plasma are reported in Figure 1g and show how the antioxidant power was significantly reduced in rats exposed to vapor from 1.5 Ω e-cig compared with control. Animals exposed to 0.25 Ω e-cig vapor presented a nonsignificant perturbation if compared with both 1.5 Ω and control group. On the contrary, data referred to hydroperoxide level in erythrocyte membranes (Figure 1h) show a slight but significant increment only in 0.25 Ω group.

Tissue Damage

Lung and trachea from each group were analyzed by using SEM (Figure 2). Figures 2a and 2d show lung from control rats. The typical spongy structure was well organized in alveoli and bronchioles: the bronchiole diameter is constant and the air sacs are preserved. Their number and size evidently decreased in lung from 1.5 Ω exposed rats (Figs. 2b and 2e), and the lung structure from 0.25 Ω group was disorganized and showed large areas (*) of airflow collapse (Figs. 2c and 2f). In the same way, trachea from control group presented equilibrated proportion between ciliated cells (cc) and goblet cells (gc) (Figs. 2g and 2j). Trachea from 1.5 Ω group (Figs. 2h and 2k) showed a large area of tissue disruption. In the remaining one, the proportion between cc and gc was maintained. In 0.25 Ω condition, an altered morphology and a deeply changed organization appeared in a large part of the tissue (Figs. 2i and 2l). The diffuse tissue loss at 0.25 Ω condition (Figs. 2i and 2l) was correlated to the presence of apoptotic (ap) and necrotic (n) cells (Figure 2l).

This behavior was also supported by transmission electron microscopy (TEM), as shown in Figure 3. Control group (Figure 3a) showed well-preserved airway epithelium cells. At high magnification (Figure 3b), it is possible to observe cilia ultrastructural features. E-cig effects at 1.5 Ω (Figure 3c) and at 0.25 Ω (Figure 3d) showed several morphological changes, including epithelium detachment (Figure 3c) and loss of cilia (Figure 3d). These tissue damages were more evident in 0.25 Ω condition, also correlated to the presence of necrotic (Figs.3e and 3f) and apoptotic (Figs. 3g and 3h) cells. The typical apoptotic cells are characterized by chromatin condensation (Figure 3h) and micronuclei (Figure 3g).

Modulation of Gene Expression

Gene expression of proinflammatory cytokines such as IL1β, IL6, and TNF-α was analyzed in rat lung tissue. Although no significant variation was recorded, a trend of increase in gene expression of both IL1β and IL6 was observed after rat exposure to the vapor of e-cig in 0.25 Ω group compared with control (Figs. 4a and 4b). A decrease in the expression of TNF-α was recorded (Figure 4c). Besides, the expression of chemokine CCL3 and CCL4, encoding for macrophage inflammatory proteins, showed a significant decrease in 0.25 Ω group compared with control (Figs. 4d and 4e). Similarly, the colony-stimulating factor of macrophage and granulocyte colonies CSF2 showed a decrease in the lung tissue of rats exposed to 0.25 Ω vapor from e-cig (Figure 4f). The inflammation alterations after exposure to

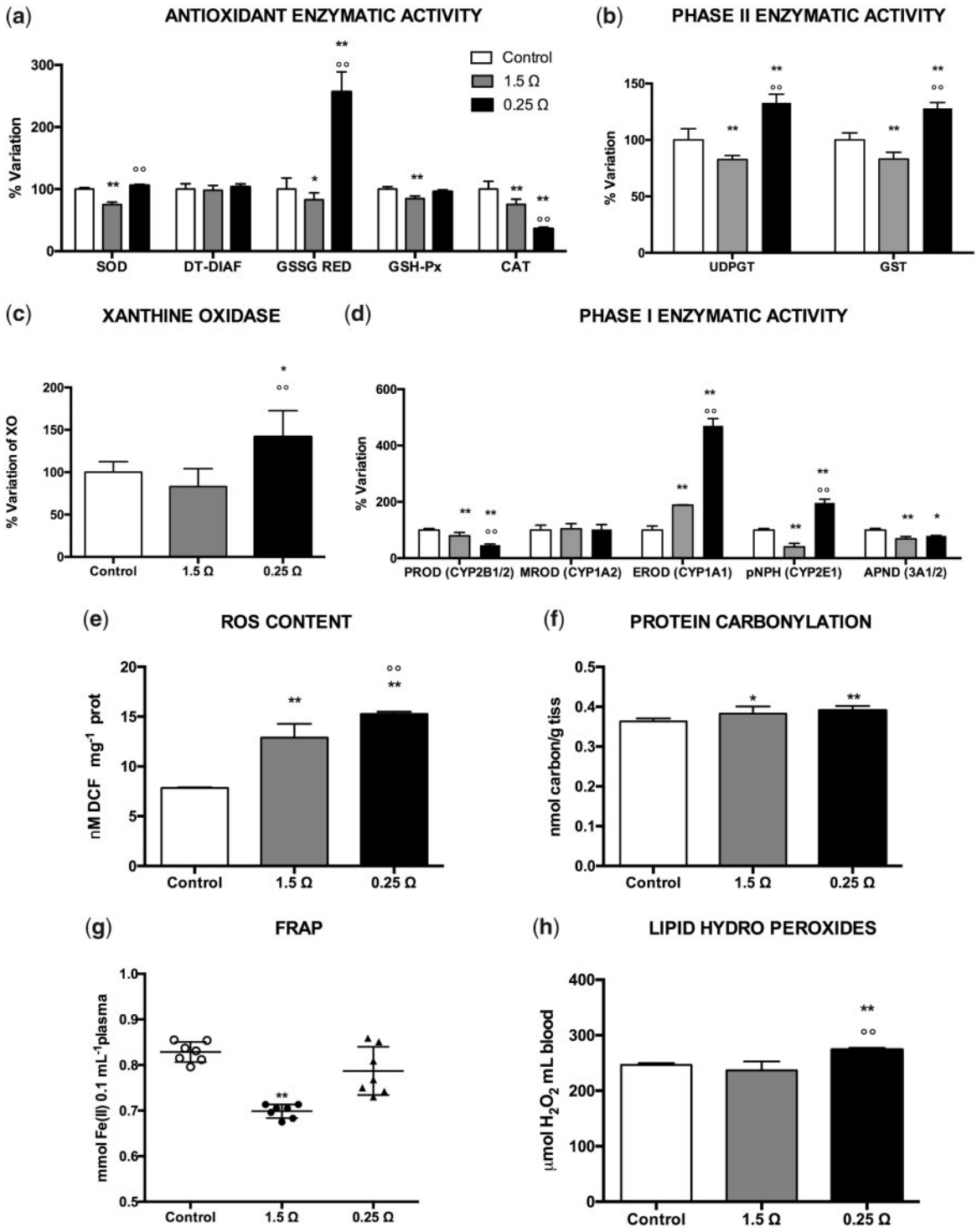

Figure 1. Pro-oxidative effects of vapors generated from electronic cigarette (e-cig) equipped with 1.5 or 0.25 Ω coils. a, Pulmonary antioxidant enzymatic activity. b, Phase II enzymatic activity in lung. c, Xanthine oxidase activity in lung. d, Enzymatic activity of cytochrome P450 (CYP450) isoforms in lung. e, Reactive oxygen species (ROS) levels in lung revealed by using 2′,7′-dichlorofluorescein (DCFH) fluorescent dye. f, Protein carbonylation in lung. g, Ferric reductive antioxidant power (FRAP) in plasma. h, Lipid peroxidation of erythrocytes. (a, b, c, d) Data expressed as percentage variation (mean ± SD of 6 independent replicates from 10 rats) compared with control group arbitrarily set at 100%. (e, f, g, h) Data expressed as mean ± SD of 6 independent replicates. Results were analyzed by means of one-way ANOVA, followed by Tukey's multiple comparison test. $^{*}p < .05$; $^{**}p < .01$ significant results between 1.5 and 0.25 Ω groups and control group. $^{\circ\circ}p < .01$ significant results between 0.25 and 1.5 Ω group.

e-cig vapors were confirmed by structural analysis in lung and bronchoalveolar lavage fluid (Panel 1, 2, Supplementary materials). Finally, due to the critical role of ALDH3A1 in the oxidation of reactive aldehydes and in the cytotoxicity and genotoxicity of cigarette smoke (Jang *et al.*, 2014), we analyzed its expression in rat lung tissue exposed to e-cig vapors. No significant variation in ALDH3A1 expression was observed neither in 1.5 Ω nor in 0.25 Ω group (Figure 4g).

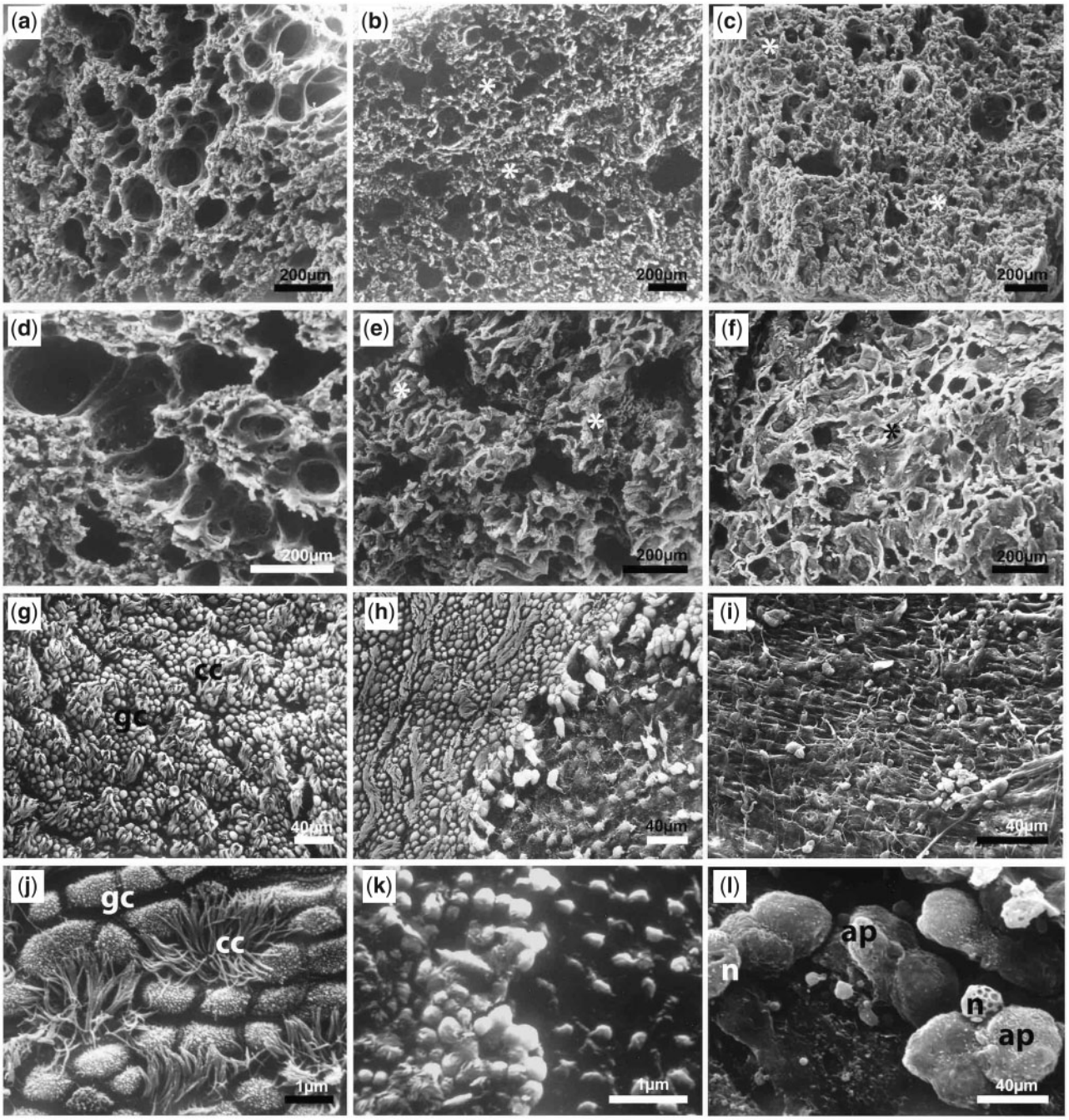

Figure 2. Scanning electron microscopy (SEM) morphologic alterations of lung and trachea tissue in rats exposed to the vapors generated from electronic cigarette (e-cig) equipped with 1.5 or 0.25 Ω coils. First and second lines report images from lung of control group (a, d), 1.5 Ω group (b, e), and 0.25 Ω group (c, f). Third and fourth lines report images from trachea of control group (g, j) in which both ciliated cells (cc) and goblet cells (gc) are appreciable; 1.5 Ω group (h, k) and 0.25 Ω group (i, l) show large areas without epithelium. (*) represents areas of alveoli collapse; n, necrotic cells; ap, apoptotic cells. Samples from 5 rats of each group were analyzed.

Hematological Profile

The hematocrit and hemoglobin (Hb) levels, as well as the total RBC and reticulocyte (RC) count, were significantly higher in the 0.25 Ω group compared with those observed in the control (Figs. 5a–d). Our model evidenced nonsignificant changes in the 1.5 Ω group, but the variations resulted more marked when the resistance was decreased to 0.25 Ω. Lymphocytes count (Figure 5e) showed a dramatic drop in 0.25 Ω group but a nonsignificant decrease in 1.5 Ω group if compared with control. Finally, a change in leucocytes profile is reported in Figure 5f, which indicates that the number of circulating neutrophils was about 8-fold higher in 0.25 Ω group ($p < .01$) compared with control. The alterations of monocytes, eosinophils, and basophils followed an increasing but not significant trend in 0.25 Ω group and a nonsignificant decreasing trend in 1.5 Ω group.

DISCUSSION

Besides the e-liquid, e-cig users can arbitrarily adjust voltage and resistance values of the device. However, due to the

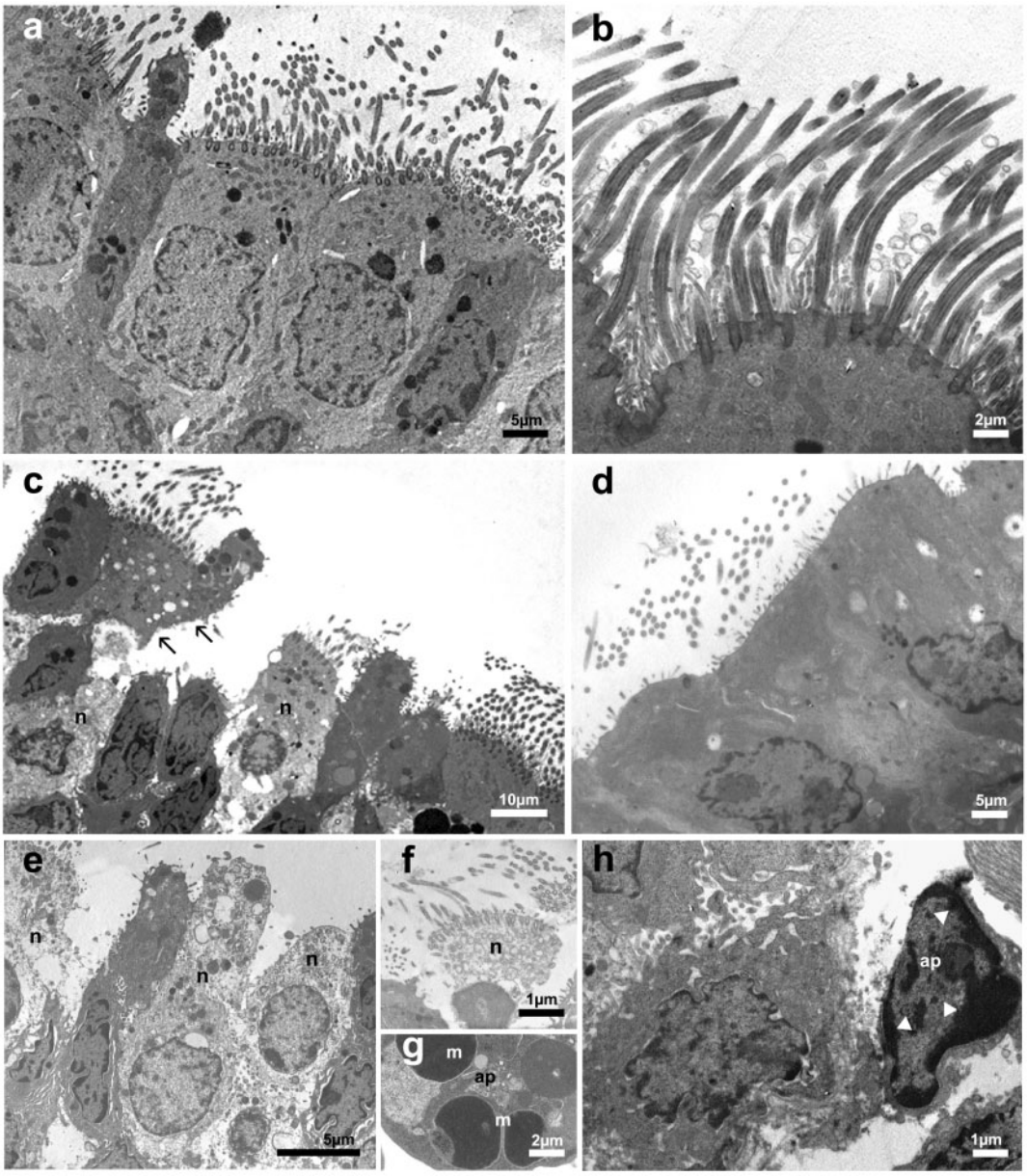

Figure 3. Transmission electron microscopy (TEM) ultrastructural alterations of trachea tissue in rats exposed to the vapors generated from electronic cigarette (e-cig) equipped with 1.5 or 0.25 Ω coils. First line reports images from trachea epithelium of control group (a, b). Second line described 1.5 Ω group (c), and 0.25 Ω group (d) showing a detachment (arrow) of epithelium correlated, in both conditions to the presence of necrotic (e, f) and apoptotic (g, h) cells. n, necrotic cells; ap, apoptotic cells; m, micronuclei; triangle, marginated chromatin. Samples from 5 rats of each group were analyzed.

thermal degradation of the e-liquid components, the inverse relationship between the electric potential difference and the resistance of the e-cig heating filament is responsible for the generation of vapors with different intensity and composition. Here, the device voltage was set at the traditional value of 3.5 V and the effects of low (0.25 Ω) and medium (1.5 Ω) resistances applied to e-cig were investigated.

We found that the amount of selected carbonyls increased as the resistance was reduced. These results are consistent with previous studies that demonstrated the influence of the e-cig total power on the aldehydes production (Geiss *et al.*, 2016). Thus, the customization of the device can seriously influence the exposure levels to vapor-derived carcinogens. The inhalation of so elaborated vapors can compromise the antioxidant machinery and the physiological homeostasis, enhancing the susceptibility to chronic and degenerative diseases.

In our model, we found an imbalance in the enzymatic antioxidant responses. Lung GSSG-red activity was significantly higher in 0.25 Ω group compared with 1.5 Ω and control, in agreement with data referred to heavy smokers, where high levels of GSH are necessary for the detoxification process (Solak *et al.*, 2005). Rats subjected to the vapor from the 1.5 Ω device showed a modest but significant impairment of the detoxifying enzymes, whereas, lowering down Ohms, the deeper changes reflected a general enzymatic up-regulation, due to the higher levels of reactive carbonyl species.

It is known how the induction of CYP superfamily can strongly contribute to ROS overproduction and, at the same time, plays a key role in the bioactivation of premutagens and

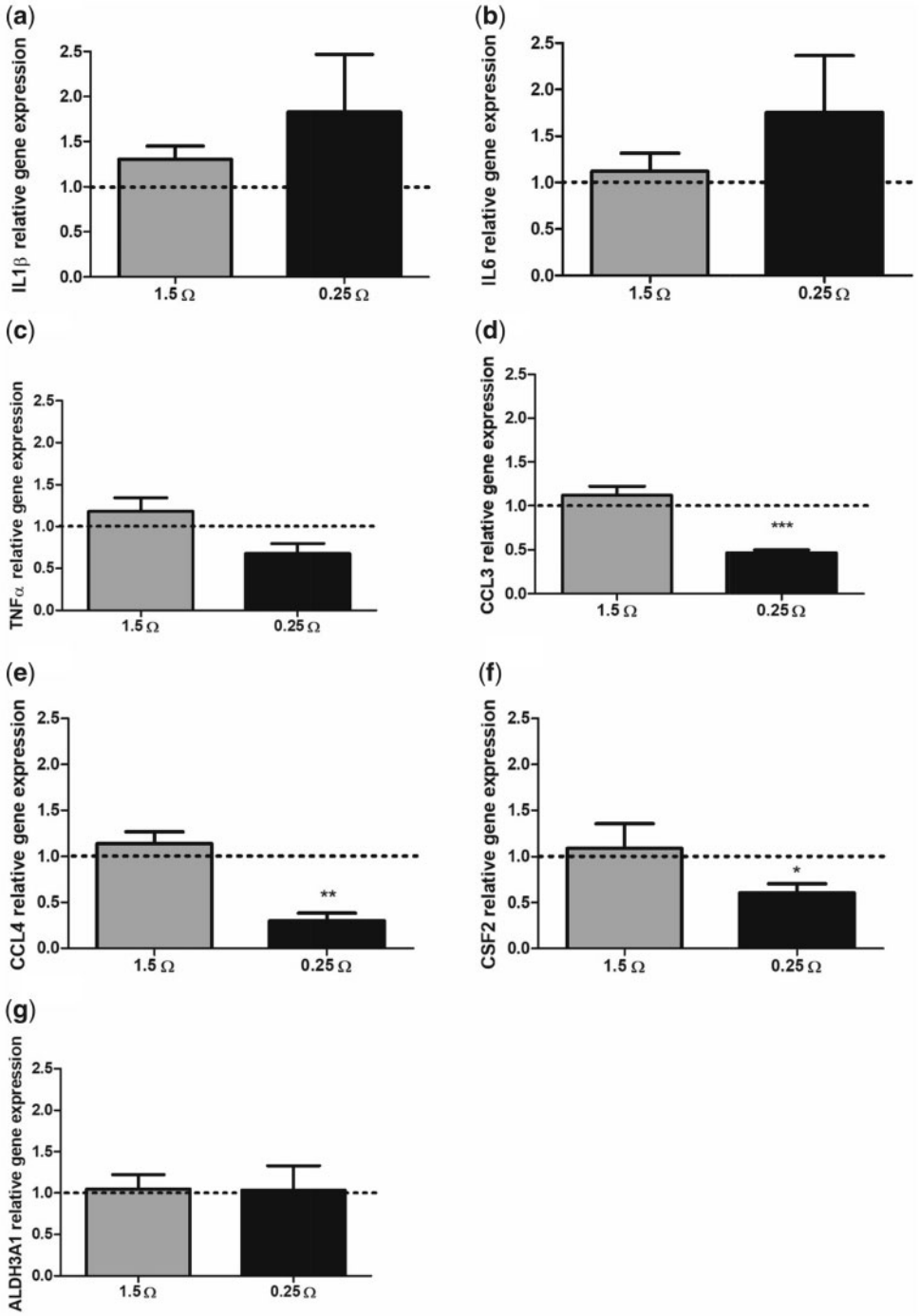

Figure 4. Effects of vapors generate from electronic cigarettes (e-cigs) equipped with 1.5 or 0.25 Ω coils on the pulmonary inflammatory pattern. Relative gene expression of IL1β (a), IL6 (b), TNF-α (c), CCL3 (d), CCL4 (e), CSF2 (f), and ALDH3A1 (g). GAPDH and actin were used as endogenous controls. Data are expressed as mean ± SEM of at least 4 independent replicates. Results were analyzed by means of one-way ANOVA followed by Dunnett's test. $^{*}p < .05$; $^{**}p < .01$; $^{***}p < .001$ significant results versus control (dashed line). The gene expression analysis was conducted on 7 rats in the control group, 7 rats in the 1.5 Ω group, and 4 rats in the 0.25 Ω group.

precarcinogens (Sapone *et al.*, 2012; Vivarelli *et al.*, 2016). In this study, various CYP-supported monooxygenase isoforms increased in the 0.25 Ω group compared with 1.5 Ω and control. In 0.25 Ω group, we found the strongest CYP1A1 induction, an isoform that bioactivates arylamines, dioxins, aromatic amines, and polycyclic aromatic hydrocarbons, and might culminate in DNA adducts that are known to increase lung cancer risk (Vázquez-Gómez *et al.*, 2018). Likewise, CYP2E1 isoform, markedly boosted in our model, catalyzes the metabolism of a wide variety of xenobiotics, including glycerol, acetaldehyde, aromatic compounds, and nitrosamines (Cederbaum, 2014). These data are of particular interest considering that changes in CYP-linked monooxygenases occurred despite the use of nicotine-free e-liquid.

In parallel, pulmonary XO levels were significantly higher in the 0.25 Ω group than in 1.5 Ω and control. Elevated XO was

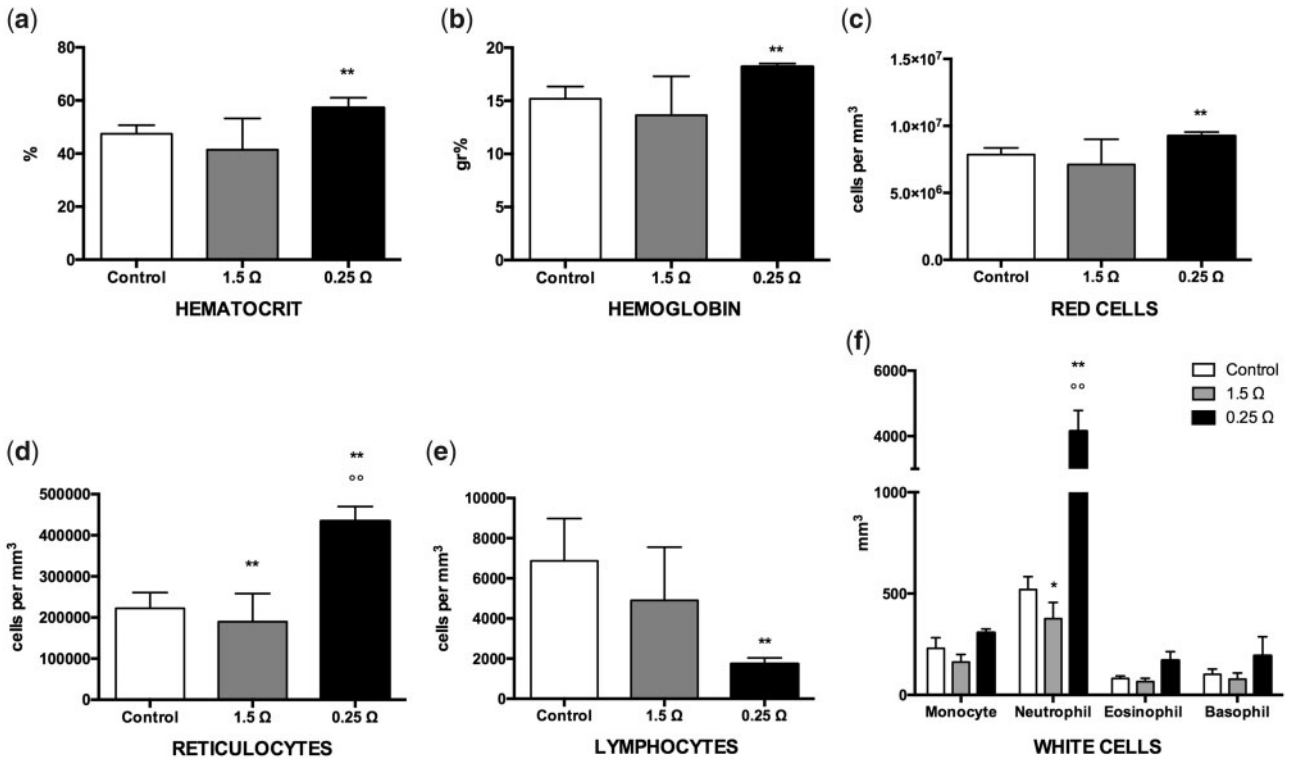

Figure 5. Effects of vapors generate from electronic cigarettes (e-cigs) equipped with 1.5 or 0.25 Ω coils on the hematological profile. Hematocrit (a); haemoglobin (b); red cells (c); reticulocytes (d); lymphocytes(e); white cells (f). Data expressed as mean ± SD of 6 independent replicates from 10 rats. Results were analyzed by means of one-way ANOVA, followed by Tukey's multiple comparison test. $^{*}p < .05$; $^{**}p < .01$ significant results between 1.5 and 0.25 Ω groups and control group. $^{\circ\circ}p < .01$ significant results between 0.25 and 1.5 Ω group.

previously found in patients with COPD compared with control subjects (Ichinose *et al.*, 2003), in an animal model of asthma (Sugiura *et al.*, 1999), and in lungs of animals exposed to cigarette smoke (Kim *et al.*, 2013). Because both XO and CYP catalytic cycle are important sources of the superoxide radical, we measured ROS content in the lung tissue. Exposed rats presented significantly higher ROS levels compared with controls, suggesting that e-cig vapors produced an OSS. The redox imbalance at systemic level was manifested through the significant reduction of plasma antioxidant capacity (FRAP) in the exposed animals. Consistently, data from 0.25 Ω group showed higher levels of hydroperoxides in erythrocyte membranes. Lipid peroxidation induces alteration of fine structures, fluidity, and permeability and modifies low-density lipoprotein to proatherogenic and proinflammatory forms (Greenberg *et al.*, 2008) and generates potentially toxic products with mutagenic and carcinogenic activity (West and Marnett, 2006).

Several non-P450 enzyme systems participate in aldehydes metabolism and one of the most important is the aldehyde dehydrogenase (ALDH). The ALDH3A1 isoform is often upregulated in smoker lung tissue: its enforced mRNA expression is involved in tumorigenesis and it was shown to attenuate cytotoxicity and DNA damage induced by cigarette smoke in human bronchial epithelial cells (Jang *et al.*, 2014; Sullivan *et al.*, 2010). Here, the lack of significant variation in ALDH3A1 gene expression in the tested experimental conditions, may suggest that the aldehydes we selected in e-cig vapor, were not oxidized by the ALDH3A1 isoform (Marchitti *et al.*, 2008). Moreover, the lack of ALDH3A1 overexpression let us assume that the protection from the genotoxicity of e-cig was deficient (Canistro *et al.*, 2017).

The OSS level, the impairment of the antioxidant machinery and the macromolecule damages we found, reflected in the morphological alterations at airway level. A loss of the typical organization in bronchioles and alveoli was evident in the 1.5 Ω group, and more conspicuous in the 0.25 Ω one. In particular, e-cig exposed animals reported alveolar destruction and bronchial epithelium disorganization. A demarcation line between a well-organized tissue and a loss of structure area was also revealed in trachea form from the 1.5 Ω group. More evidently, in 0.25 Ω rats, the number of ciliated cells was dramatically reduced and both apoptotic and necrotic cells were present. These alterations are similar to those reported by smokers and COPD patients (Macnee, 2009), and it was recently shown how e-cig aerosol exposure is associated with inflammation along with the loss of epithelial barrier function in lung cells (Gerloff *et al.*, 2017). To further investigate the inflammatory response to e-cig exposure in our experimental settings, we measured a panel of cytokine and chemokine gene expression: only 2 genes (ie, CCL3 and CCL4) were significantly changed compared with controls and they were all down regulated. The increasing trend of IL1β and IL6 expression in 0.25 Ω group suggests that the more powerful setting may induce a stronger inflammatory status. Widely recognized as modulator of innate immune defenses, IL1β was often found enhanced in COPD patients and may have played a prominent role in its pathophysiology (Botelho *et al.*, 2011), whereas the release of IL6 from cells exposed to e-cig vapor occurred in a dose-dependent manner in response to the aerosol exposures (Lerner *et al.*, 2015). Smoking impacts both innate and adaptive immunity (Qiu *et al.*, 2017), usually decreasing interferon-γ and TNF-α (Strzelak *et al.*, 2018). In our model, we recorded a similar trend for TNF in 0.25 Ω

group, supporting the hypothesis that also e-cig vapors may induce an immune response. Furthermore, the expression of CCL3, CCL4, and CSF2 is in line with the reduced expression of TNF-α. Even though these data are in contrast with the increased number of white blood cells in 0.25 Ω group, they could be explained in light of the findings by Meuronen and colleagues, that suggested how the inflammatory cells are incapable of producing chemokine mRNA in the lower airways in smokers (Meuronen *et al.*, 2008). Because the protein expression of the significantly dysregulated genes was not analyzed in the present research, further studies need to be carried out to confirm the expression level of studied gene at protein level.

As the influence of OSS and inflammatory processes on the hematological parameters in smokers has been found (Strzelak *et al.*, 2018), we investigated the putative changes of hematocrit, Hb levels, RBC, and RC count, and we observed that they were significantly higher in the 0.25 Ω group than in control. These data are in agreement with the hematological profile of patients with a smoking history (Anandha Lakshmi *et al.*, 2014; Kalahasthi and Barman, 2016; Malenica *et al.*, 2017; Ugbebor *et al.*, 2011). Interestingly, as hematological alterations enhanced with the smoking intensity (Anandha Lakshmi *et al.*, 2014; Whitehead *et al.*, 1995), our model showed the most marked changes in the 0.25 Ω group. These observations concur in our hypothesis that vaping at low resistances leads to a more intense exposure. Existing data concerning the influence of smoking on lymphocyte profile are affected by numerous confounding factors of subpopulations (Andreoli *et al.*, 2015; Stämpfli and Anderson, 2009). However, the drop in lymphocyte count from 1.5 to 0.25 Ω group is in line with the inversely relation between the lymphocyte count in smokers and the increasing number of tobacco cigarette per day revealed by Sherke *et al.* (2016). Noteworthy, similar results were also obtained in a cross-sectional study conducted on children with the history of indoor exposure to tobacco smoke (El-Hodhod *et al.*, 2011). Changes in leukocyte profile are in accordance with those emerged from clinical trials showing an increment of the neutrophils moving from light- to heavy-smokers, as well as in patients with COPD (Anandha Lakshmi *et al.*, 2014; Jaroenpool *et al.*, 2016). In particular, the high number of circulating neutrophils herein recorded in the 0.25 Ω group has been previously observed in smokers (Andreoli *et al.*, 2015; Calapai *et al.*, 2009).

In conclusion, the customization of the vaping experience results in a plethora of "personalized toxicological effects," whose repercussions on health is unpredictable. Our study shows how 2 identically settled e-cigs (battery output, temperature, and atomizer setting), loaded with the same liquid (PG/VG ratio, nicotine concentration, and flavors), could generate different amounts of toxic aldehydes, as a mere effect of the value of the heating element.

We therefore suggest e-cig consumers to be cautious assuming that low-voltages may be synonymous of "safer" devices (Thomson and Lewis, 2015). In light of the findings here presented and until robust evidence from epidemiological studies on the putative public health repercussions is provided, the promotion of e-cig by scientific and public health agencies as smoking cessation aid should be considered with extreme caution.

DECLARATION OF CONFLICTING INTERESTS

The authors declared no potential conflicts of interest with respect to the research, authorship, and/or publication of this article.

SUPPLEMENTARY DATA

Supplementary data are available at *Toxicological Sciences* online.

FUNDING

All sources of financial and material support were provided by a grant from the Italian Ministry of Education, University and Research. S.C. PhD fellowship grant was awarded from the Italian Ministry of Education, University and Research. F.V. postdoctoral fellowship grant was cofounded by D.C., M.P., and the Department of Pharmacy and Biotechnology, University of Bologna.

REFERENCES

Anandha Lakshmi, S., Lakshmanan, A., Ganesh Kumar, P., and Saravanan, A. (2014). Effect of intensity of cigarette smoking on haematological and lipid parameters. *J. Clin. Diagn. Res.* **8**, BC11–BC13.

Andreoli, C., Bassi, A., Gregg, E. O., Nunziata, A., Puntoni, R., and Corsini, E. (2015). Effects of cigarette smoking on circulating leukocytes and plasma cytokines in monozygotic twins. *Clin. Chem. Lab. Med.* **53**, 57–64.

Benzie, I. F., and Strain, J. J. (1996). The ferric reducing ability of plasma (FRAP) as a measure of "antioxidant power": The FRAP assay. *Anal. Biochem.* **239**, 70–76.

Bitzer, Z. T., Goel, R., Reilly, S. M., Bhangu, G., Trushin, N., Foulds, J., Muscat, J., and Richie, J. P. (2019). Emissions of free radicals, carbonyls, and nicotine from the NIDA Standardized Research Electronic Cigarette and comparison to similar commercial devices. *Chem. Res. Toxicol.* **32**, 130–138.

Bitzer, Z. T., Goel, R., Reilly, S. M., Elias, R. J., Silakov, A., Foulds, J., Muscat, J., and Richie, J. P. (2018). Effect of flavoring chemicals on free radical formation in electronic cigarette aerosols. *Free Radic. Biol. Med.* **120**, 72–79.

Bonamassa, B., Canistro, D., Sapone, A., Vivarelli, F., Vornoli, A., Longo, V., and Paolini, M. (2016). Harmful effects behind the daily supplementation of a fixed vegetarian blend in the rat model. *Food Chem. Toxicol.* **97**, 367–374.

Botelho, F. M., Bauer, C. M. T., Finch, D., Nikota, J. K., Zavitz, C. C. J., Kelly, A., Lambert, K. N., Piper, S., Foster, M. L., Goldring, J. J. P., *et al.* (2011). IL-1alpha/IL-1R1 expression in chronic obstructive pulmonary disease and mechanistic relevance to smoke-induced neutrophilia in mice. *PLoS One* **6**, e28457.

Burattini, S., Battistelli, M., Codenotti, S., Falcieri, E., Fanzani, A., and Salucci, S. (2016). Melatonin action in tumor skeletal muscle cells: An ultrastructural study. *Acta Histochem.* **118**, 278–285.

Calapai, G., Caputi, A. P., Mannucci, C., Gregg, E. O., Pieratti, A., Aurora Russo, G., Chaudhary, N., Puntoni, R., Lowe, F., McEwan, M., *et al.* (2009). A cross-sectional investigation of biomarkers of risk after a decade of smoking. *Inhal. Toxicol.* **21**, 1138–1143.

Canistro, D., Barillari, J., Melega, S., Sapone, A., Iori, R., Speroni, E., and Paolini, M. (2012). Black cabbage seed extract affects rat Cyp-mediated biotransformation: Organ and sex related differences. *Food Chem. Toxicol.* **50**, 2612–2621.

Canistro, D., Vivarelli, F., Cirillo, S., Babot Marquillas, C., Buschini, A., Lazzaretti, M., Marchi, L., Cardenia, V., Rodriguez-Estrada, M. T., Lodovici, M., *et al.* (2017). E-cigarettes induce toxicological effects that can raise the cancer risk. *Sci. Rep.* **7**, 2028.

Cardenia, V., Vivarelli, F., Cirillo, S., Paolini, M., Canistro, D., and Rodriguez-Estrada, M. T. (2018). The effect of electronic-cigarettes aerosol on rat brain lipid profile. *Biochimie* **153**, 99–108.

Cederbaum, A. I. (2014). Methodology to assay CYP2E1 mixed function oxidase catalytic activity and its induction. *Redox Biol.* **2**, 1048–1054.

Chaumont, M., de Becker, B., Zaher, W., Culié, A., Deprez, G., Mélot, C., Reyé, F., Van Antwerpen, P., Delporte, C., and Debbas, N. (2018). Differential effects of e-cigarette on microvascular endothelial function, arterial stiffness and oxidative stress: A randomized crossover trial. *Sci. Rep.* **8**, 10378.

Chausse, P., Naughton, G., and Dutheil, F. (2015). Electronic cigarettes resistance value of the heating filament could be the key to lung toxicity. *Chest* **148**, e29–e30.

Cirillo, S., Canistro, D., Vivarelli, F., and Paolini, M. (2016). Effects of chlorinated drinking water on the xenobiotic metabolism in *Cyprinus carpio* treated with samples from two Italian municipal networks. *Environ. Sci. Pollut. Res. Int.* **23**, 18777–18788.

El-Hodhod, M. A., Hamdy, A. M., Ahmed, M. B., Youssef, S. R., and Aly, S. M. (2011). Effect of passive smoking on blood lymphocyte apoptosis in children. *Eur. J. Clin. Invest.* **41**, 387–392.

Franks, A. S., Sando, K., and McBane, S. (2018). Do electronic cigarettes have a role in tobacco cessation? *Pharmacotherapy* **38**, 555–568.

Fu, J-J., McDonald, V. M., Baines, K. J., and Gibson, P. G. (2015). Airway IL-1beta and systemic inflammation as predictors of future exacerbation risk in asthma and COPD. *Chest* **148**, 618–629.

Geiss, O., Bianchi, I., and Barrero-Moreno, J. (2016). Correlation of volatile carbonyl yields emitted by e-cigarettes with the temperature of the heating coil and the perceived sensorial quality of the generated vapours. *Int. J. Hyg. Environ. Health* **219**, 268–277.

Gerloff, J., Sundar, I. K., Freter, R., Sekera, E. R., Friedman, A. E., Robinson, R., Pagano, T., and Rahman, I. (2017). Inflammatory response and barrier dysfunction by different e-cigarette flavoring chemicals identified by gas chromatography-mass spectrometry in e-liquids and e-vapors on human lung epithelial cells and fibroblasts. *Appl. In Vitro Toxicol.* **3**, 28–40.

Goel, R., Durand, E., Trushin, N., Prokopczyk, B., Foulds, J., Elias, R. J., and Richie, J. P. (2015). Highly reactive free radicals in electronic cigarette aerosols. *Chem. Res. Toxicol.* **28**, 1675–1677.

Goniewicz, M. L., Knysak, J., Gawron, M., Kosmider, L., Sobczak, A., Kurek, J., Prokopowicz, A., Jablonska-Czapla, M., Rosik-Dulewska, C., Havel, C., *et al.* (2014). Levels of selected carcinogens and toxicants in vapor from electronic cigarettes. *Tob. Control* **23**, 133–139.

Greenberg, M. E., Li, X. M., Gugiu, B. G., Gu, X., Qin, J., Salomon, R. G., and Hazen, S. L. (2008). The lipid whisker model of the structure of oxidized cell membranes. *J. Biol. Chem.* **283**, 2385–2396.

Hawkins, C. L., Morgan, P. E., and Davies, M. J. (2009). Quantification of protein modification by oxidants. *Free Radic. Biol. Med.* **46**, 965–988.

Ichinose, M., Sugiura, H., Yamagata, S., Koarai, A., Tomaki, M., Ogawa, H., Komaki, Y., Barnes, P. J., Shirato, K., and Hattori, T. (2003). Xanthine oxidase inhibition reduces reactive nitrogen species production in COPD airways. *Eur. Respir. J.* **22**, 457–461.

International Agency for Research on Cancer (IARC) (1999). *Agents Classified by the IARC Monographs*, Vols. 1–105. Geneva, Switzerland. Available at: http://monographs.iarc.fr/ENG/Classification/index.php. Accessed March 21, 2019.

International Agency for Research on Cancer (IARC) (2012). *Agents Classified by the IARC Monographs*, Vols. 1–105. Geneva, Switzerland. Available at: http://monographs.iarc.fr/ENG/Classification/index.php. Accessed March 21, 2019.

Jang, J., Bruse, S., Liu, Y., Duffy, V., Zhang, C., Oyamada, N., Randell, S., Matsumoto, A., Thompson, D., Lin, Y., *et al.* (2014). Aldehyde dehydrogenase3A1 protects airway epithelial cells from cigarette smoke-induced DNA damage and cytotoxicity. *Free Radic. Biol. Med.* **68**, 80–86.

Jaroenpool, J., Pattanapanyasat, K., Noonin, N., and Prachongsai, I. (2016). Aberrant neutrophil function among heavy smokers and chronic obstructive pulmonary disease patients. *Asian Pac. J. Allergy Immunol.* **34**, 278–283.

Jensen, R. P., Luo, W., Pankow, J. F., Strongin, R. M., and Peyton, D. H. (2015). Hidden formaldehyde in e-cigarette aerosols. *N. Engl. J. Med.* **372**, 392–394.

Jiang, Z. Y., Hunt, J. V., and Wolff, S. P. (1992). Ferrous ion oxidation in the presence of xylenol orange for detection of lipid hydroperoxide in low density lipoprotein. *Anal. Biochem.* **202**, 384–389.

Kalahasthi, R., and Barman, T. (2016). Effect of lead exposure on the status of reticulocyte count indices among workers from lead battery manufacturing plant. *Toxicol. Res.* **32**, 281–287.

Kang, C. H., Molagoda, I. M. N., Choi, Y. H., Park, C., Moon, D. O., and Kim, G. Y. (2018). Apigenin promotes TRAIL-mediated apoptosis regardless of ROS generation. *Food Chem. Toxicol.* **111**, 623–630.

Kim, B. S., Serebreni, L., Hamdan, O., Wang, L., Parniani, A., Sussan, T., Scott Stephens, R., Boyer, L., Damarla, M., Hassoun, P. M., *et al.* (2013). Xanthine oxidoreductase is a critical mediator of cigarette smoke-induced endothelial cell DNA damage and apoptosis. *Free Radic. Biol. Med.* **60**, 336–346.

Lee, H. W., Park, S. H., Weng, M. W., Wang, H. T., Huang, W. C., Lepor, H., Wu, X. R., Chen, L. C., and Tang, M. S. (2018). E-cigarette smoke damages DNA and reduces repair activity in mouse lung, heart, and bladder as well as in human lung and bladder cells. *Proc. Natl. Acad. Sci. U.S.A.* **115**, e1560–e1569.

Lerner, C. A., Sundar, I. K., Yao, H., Gerloff, J., Ossip, D. J., McIntosh, S., Robinson, R., and Rahman, I. (2015). Vapors produced by electronic cigarettes and e-juices with flavorings induce toxicity, oxidative stress, and inflammatory response in lung epithelial cells and in mouse lung. *PLoS One* **10**, e0116732.

Lestari, K. S., Humairo, M. V., and Agustina, U. (2018). Formaldehyde vapor concentration in electronic cigarettes and health complaints of electronic cigarettes smokers in Indonesia. *J. Environ. Public Health* **2018**, 1.

Levine, R. L., Williams, J. A., Stadtman, E. R., and Shacter, E. (1994). Carbonyl assays for determination of oxidatively modified proteins. *Methods Enzymol.* **233**, 346–357.

Livak, K. J., and Schmittgen, T. D. (2001). Analysis of relative gene expression data using real-time quantitative PCR and the 2(-Delta Delta C(T)) method. *Methods* **25**, 402–408.

Lowry, O. H., Rosebrough, N. J., Farr, A. L., and Randall, R. J. (1951). Protein measurement with the folin phenol reagent. *J. Biol. Chem.* **193**, 265–275.

Macnee, W. (2009). Accelerated lung aging: a novel pathogenic mechanism of chronic obstructive pulmonary disease (COPD). *Biochem Soc Trans.* **37**, 819–823.

Malenica, M., Prnjavorac, B., Bego, T., Dujic, T., Semiz, S., Skrbo, S., Gusic, A., Hadzic, A., and Causevic, A. (2017). Effect of

cigarette smoking on haematological parameters in healthy population. *Med. Arch.* **71**, 132–136.

Marchitti, S. A., Brocker, C., Stagos, D., and Vasiliou, V. (2008). Non-P450 aldehyde oxidizing enzymes: The aldehyde dehydrogenase superfamily. *Expert Opin. Drug Metab. Toxicol.* **4**, 697–720.

McConnell, R., Barrington-Trimis, J. L., Wang, K., Urman, R., Hong, H., Unger, J., Samet, J., Leventhal, A., and Berhane, K. (2017). Electronic cigarette use and respiratory symptoms in adolescents. *Am. J. Respir. Crit. Care Med.* **195**, 1043–1049.

Melega, S., Canistro, D., Pagnotta, E., Iori, R., Sapone, A., and Paolini, M. (2013). Effect of sprout extract from Tuscan black cabbage on xenobiotic-metabolizing and antioxidant enzymes in rat liver. *Mutat. Res.* **751**, 45–51.

Meuronen, A., Majuri, M. L., Alenius, H., Mäntylä, T., Wolff, H., Piirilä, P., and Laitinen, A. (2008). Decreased cytokine and chemokine mRNA expression in bronchoalveolar lavage in asymptomatic smoking subjects. *Respiration* **75**, 450–458.

Muthumalage, T., Prinz, M., Ansah, K. O., Gerloff, J., Sundar, I. K., and Rahman, I. (2018). Inflammatory and oxidative responses induced by exposure to commonly used e-cigarette flavoring chemicals and flavored e-liquids without nicotine. *Front. Physiol.* **8**, 1130.

Qiu, F., Liang, C. L., Liu, H., Zeng, Y. Q., Hou, S., Huang, S., Lai, X., and Dai, Z. (2017). Impacts of cigarette smoking on immune responsiveness: Up and down or upside down? *Oncotarget* **8**, 268–284.

Rodrigues Siqueira, I., Fochesatto, C., da Silva Torres, I. L., Dalmaz, C., and Alexandre Netto, C. (2005). Alexandre Netto aging affects oxidative state in hippocampus, hypothalamus and adrenal glands of Wistar rats. *Life Sci.* **78**, 271–278.

Salucci, S., Battistelli, M., Baldassarri, V., Burini, D., Falcieri, E., and Burattini, S. (2017). Melatonin prevents mitochondrial dysfunctions and death in differentiated skeletal muscle cells. *Microsc. Res. Tech.* **80**, 1174–1181.

Sapey, E., Ahmad, A., Bayley, D., Newbold, P., Snell, N., Rugman, P., and Stockley, R. A. (2009). Imbalances between interleukin-1 and tumor necrosis factor agonists and antagonists in stable COPD. *J. Clin. Immunol.* **29**, 508–516.

Sapone, A., Canistro, D., Melega, S., Moles, R., Vivarelli, F., and Paolini, M. (2012). On enzyme-based anticancer molecular dietary manipulations. *J. Biomed. Biotechnol.* **2012**, 1.

Sapone, A., Canistro, D., Vivarelli, F., and Paolini, M. (2016). Perturbation of xenobiotic metabolism in *Dreissena polymorpha* model exposed in situ to surface water (Lake Trasimene) purified with various disinfectants. *Chemosphere* **144**, 548–554.

Scheffler, S., Dieken, H., Krischenowski, O., and Aufderheide, M. (2015). Cytotoxic evaluation of e-liquid aerosol using different lung-derived cell models. *Int. J. Environ. Res. Public Health* **12**, 12466–12474.

Scott, A., Lugg, S. T., Aldridge, K., Lewis, K. E., Bowden, A., Mahida, R. Y., Grudzinska, F. S., Dosanjh, D., Parekh, D., Foronjy, R., *et al.* (2018). Pro-inflammatory effects of e-cigarette vapour condensate on human alveolar macrophages. *Thorax.* **73**, 1161–1169.

Sherke, A. B., Vadapalli, K., Bhargava, D. V., Sherke, A. R., and Reddy Gopireddy, M. M. (2016). Effect of number of cigarettes smoked per day on red blood cell, leucocyte and platelet count in adult Indian male smokers—A case control study. *Int. J. Med. Res. Health Sci.* **5**, 13–17.

Shintani, H. (2013). Determination of xanthine oxidase. *Pharm. Anal. Acta* **S7**, 004.

Smets, J., Baeyens, F., Chaumont, M., Adriaens, K., and Van Gucht, D. (2019). When less is more: Vaping low-nicotine vs. high-nicotine e-liquid is compensated by increased wattage and higher liquid consumption. *Int. J. Environ. Res. Public Health* **16**, 723–741.

Solak, Z. A., Kabaroğlu, C., Çok, G., Parıldar, Z., Bayındır, Ü., Özmen, D., and Bayındır, O. (2005). Effect of different levels of cigarette smoking on lipid peroxidation, glutathione enzymes and paraoxonase 1 activity in healthy people. *Clin. Exp. Med.* **5**, 99–105.

Stämpfli, M. R., and Anderson, G. P. (2009). How cigarette smoke skews immune responses to promote infection, lung disease and cancer. *Nat. Rev. Immunol.* **9**, 377–384.

Strzelak, A., Ratajczak, A., Adamiec, A., and Feleszko, W. (2018). Tobacco smoke induces and alters immune responses in the lung triggering inflammation, allergy, asthma and other lung diseases: A mechanistic review. *Int. J. Environ. Res. Public Health* **15**, 1033.

Sugiura, H., Ichinose, M., Oyake, T., Mashito, Y., Ohuchi, Y., Endoh, N., Miura, M., Yamagata, S., Koarai, A., Akaike, T., *et al.* (1999). Role of peroxynitrite in airway microvascular hyperpermeability during late allergic phase in guinea pigs. *Am. J. Respir. Crit. Care Med.* **160**, 663–671.

Sullivan, J. P., Spinola, M., Dodge, M., Raso, M. G., Behrens, C., Gao, B., Schuster, K., Shao, C., Larsen, J. E., Sullivan, L. A., *et al.* (2010). Aldehyde dehydrogenase activity selects for lung adenocarcinoma stem cells dependent on notch signaling. *Cancer Res.* **70**, 9937–9948.

Sussan, T. E., Gajghate, S., Thimmulappa, R. K., Ma, J., Kim, J. H., Sudini, K., Consolini, N., Cormier, S. A., Lomnicki, S., Hasan, F., *et al.* (2015). Exposure to electronic cigarettes impairs pulmonary anti-bacterial and anti-viral defenses in a mouse model. *PLoS One* **10**, e0116861.

Thomson, R. H., and Lewis, P. M. (2015). More on hidden formaldehyde in e-cigarette aerosols. *N. Engl. J. Med.* **372**, 1575–1576.

U.S. Environmental Protection Agency (2003). Technology Transfer Network – Air Toxics Web Site. Available at: http://epa.gov/airtoxics/188polls.html. Accessed March 21, 2019.

Ugbebor, O. U., Oseni, B. A., Arinolas, O. G., Osazuwa, F., and Zabayo, O. J. (2011). Red blood cell susceptibility to oxidants in chronic cigarette smokers. *Res. J. Pharm. Biol. Chem. Sci.* **2**, 380–388.

Vasanthi Bathrinarayanan, P., Brown, J. E. P., Marshall, L. J., and Leslie, L. J. (2018). An investigation into e-cigarette cytotoxicity in-vitro using a novel 3D differentiated co-culture model of human airways. *Toxicol. In Vitro* **52**, 255–264.

Vázquez-Gómez, G., Rocha-Zavaleta, L., Rodríguez-Sosa, M., Petrosyan, P., and Rubio-Lightbourn, J. (2018). Benzo[a]pyrene activates an AhR/Src/ERK axis that contributes to CYP1A1 induction and stable DNA adducts formation in lung cells. *Toxicol. Lett.* **289**, 54–62.

Vivarelli, F., Canistro, D., Babot Marquillas, C., Cirillo, S., De Nicola, G. R., Iori, R., Biagi, G., Pinna, C., Gentilini, F., Pozzo, L., *et al.* (2018). The combined effect of Sango sprout juice and caloric restriction on metabolic disorders and gut microbiota composition in an obesity model. *Int. J. Food Sci. Nutr.* **69**, 192–204.

Vivarelli, F., Canistro, D., Cirillo, S., Cardenia, V., Rodriguez-Estrada, M. T., and Paolini, M. (2019). Impairment of testicular function in electronic cigarette (e-cig, e-cigs) exposed rats under low-voltage and nicotine-free conditions. *Life Sci.* **3205**, 30327–30333.

Vivarelli, F., Canistro, D., Franchi, P., Sapone, A., Vornoli, A., Della Croce, C., Longo, V., Lucarini, M., and Paolini, M. (2016). Disruption of redox homeostasis and carcinogen metabolizing enzymes changes by administration of vitamin E to rats. *Life Sci.* **145**, 166–173.

Vivarelli, F., Canistro, D., Sapone, A., De Nicola, G. R., Babot Marquillas, C., Iori, R., Antonazzo, I. C., Gentilini, F., and Paolini, M. (2016). *Raphanus sativus* cv. Sango sprout juice decreases diet-induced obesity in Sprague Dawley rats and ameliorates related disorders. *PLoS One* **11**, e0150913.

Wang, P., Chen, W., Liao, J., Matsuo, T., Ito, K., Fowles, J., Shusterman, D., Mendell, M., and Kumagai, K. (2017). A device-independent evaluation of carbonyl emissions from heated electronic cigarette solvents. *PLoS One* **12**, e0169811.

West, J. D., and Marnett, L. J. (2006). Endogenous reactive intermediates as modulators of cell signaling and cell death. *Chem. Res. Toxicol.* **19**, 173–194.

Whitehead, T. P., Robinson, D., Allaway, S. L., and Hale, A. C. (1995). The effects of cigarette smoking and alcohol consumption on blood haemoglobin, erythrocytes and leucocytes: A dose related study on male subjects. *Clin. Lab. Haematol.* **17**, 131–138.

Zhang, Z., Kleinstreuer, C., and Feng, Y. (2012). Vapor deposition during cigarette smoke inhalation in a subject-specific human airway model. *J. Aerosol. Sci.* **53**, 40–60.